Supporting Information

Barium Alginate Gel Beads: A Homochiral Porous Material from Brown Algae for Heterogeneous Asymmetric Catalysis

Pietro Pecchini,[†] Daniel Antonio Aguilera,[†‡‖] Alberto Soccio,[†] Alessio Lombardi,[†] Fátima Sanz Azcona,[†] Nicolò Santarelli,[†] Mariafrancesca Fochi,[†] Pierrick Gaudin,[‡] Nathalie Tanchoux,[‡] and Luca Bernardi[†]**

† Department of Industrial Chemistry "Toso Montanari", Center for Chemical Catalysis – C^3, and INSTM RU Bologna, Alma Mater Studiorum – University of Bologna, V. Gobetti 85, 40129 Bologna (Italy). E-mail: luca.bernardi2@unibo.it

‡ ICGM, University of Montpellier, CNRS, ENSCM, 1919 route de Mende, 34293, Montpellier Cedex 5 (France). E-mail: nathalie.tanchoux@enscm.fr

‖ Laboratoire de Physicochimie des Polymères et des Interfaces (LPPI), CY Cergy Paris Université, CY Tech, 5 Mail Gay Lussac, Neuville sur Oise, 95031 Cergy-Pontoise Cedex (France).

Table of Contents

Methods and Materials……S1

Selected optimization results……S2

Screening of different metal alginates in the Friedel-Crafts reaction between nitroalkene **1a** and indole **2a**……S2

Screening of alginates with different M/G ratios……S3

Screening of solvents……S4

Screening of oxygenated solvents……S6

Additional screening of alginates with different M/G ratios……S8

Screening of drying agents and reaction temperature……S8

Catalyst loading……S10

Robustness of the reaction and optimized reaction protocol……S10

Catalyst heterogeneity – Sheldon test……S12

Catalyst preparation, alginate composition and surface areas……S14

Reaction limitations……S16

Mechanistic considerations……S17

Interactions between catalyst and substrates……S17

Origin of enantioinduction……S19

Catalyst recovery and reuse……S22

Preparation and characterization of barium alginate gel beads……S23

Representative procedure for the catalytic reaction……S28

Procedure for catalyst recovery and reuse……S29

Results of the catalytic reactions and characterization of products **3**……S30

References……S76

Methods and Materials

The ^{1}H, ^{13}C and ^{19}F NMR spectra were recorded on a Varian Mercury 400 spectrometer. Chemical shifts (δ) are reported in ppm relative to residual $CHCl_3$ signals for ^{1}H (7.26 ppm) and $CDCl_3$ for ^{13}C (77.0 ppm) NMR, and using $CF_3C_6H_5$ as external reference calibrated at -63.72 ppm for ^{19}F NMR. Chromatographic separations were carried out using 70 – 230 mesh silica. High Resolution Mass Spectra (HRMS) were recorded on a Waters Xevo Q-TOF spectrometer. Specific optical rotations were measured on a Perkin-Elmer 241 Polarimeter equipped with a sodium lamp and are reported as follows: $[\alpha]_{\lambda}^{T\,^{\circ}C}$ (c = g/100 mL in solvent). The enantiomeric excess (ee) of the products was determined by HPLC equipped with chiral stationary phase columns, with a UV detector operating at 254 nm. Infrared (ATR) spectra were recorded on a Bruker Alpha II spectrometer equipped with an ATR probe. Microwave Plasma Atomic Emission Spectroscopy (MP AES) analysis was performed with a MP-AES Agilent 4210 instrument, building a calibration curve with 0.02 mg/L, 0.10 mg/L, 0.50 mg/L, 1.00 mg/L and 2.00 mg/L Ba^{2+} solutions obtained by dillution of a standard solution (Sigma-Aldrich, catalogue number: 206970). Ethanol **SG-Ba** beads were converted to aerogel **AeG-Ba** by using a Polaron 3100 apparatus or a Leica EM CPD300 Automated Critical Point Dryer. Thermogravimetric analyses (TGA) were measured with a Perkin-Elmer STA6000 system. Surface areas were calculated by the BET method using a Micrometrics TriStar or a BELSORP-mini II machine (BEL Japan, Inc.) apparatus on aerogel (**AeG**) samples, after degassing at 50 °C for >6 h. The absolute configuration of products **3** was assigned by comparison with literature data or by analogy. Analytical grade solvents and commercially available reagents were used as received, unless otherwise stated. Dry THF was obtained by distillation from Na/benzophenone before use. Non-commercially available nitroalkenes **1** were prepared following literature procedures.[1] Commercial sodium alginate salts with different α-L-guluronate (G) and β-D-mannuronate (M) ratios were provided by FMC Biopolymer [Protanal 200S (M/G = 3:7, viscosity of 1% w/w solution: 306 cP), Protanal 200DL (M/G = 4:6, viscosity of 1% w/w solution: 254 cP), and Protanal 240D (M/G = 7:3, viscosity of 1% w/w solution: 115 cP)] or purchased from Sigma-Aldrich [catalogue number 180947, M/G ca. 7/3,[2] viscosity of 1% w/w solution: 5-25 cP]. 3,4 and 5 Å Molecular sieves (pellets, 2-4 mm) were purchased from AlfaAesar and activated before use by heating with a heatgun under vacuum for a few minutes in a Schlenk tube, cooled under vacuum, and placed under a nitrogen atmosphere. Racemic samples (references for HPLC analyses) were obtained using Schreiner's thiourea (1,3-bis(3,5-bis(trifluoromethyl)phenyl)thiourea) catalyst, and performing the reactions in CH_2Cl_2 (0.5-1 M) at RT for 48-72 h.

Selected optimization results

Screening of different metal alginates in the Friedel-Crafts reaction between nitroalkene 1a and indole 2a

At the outset, the reaction between **1a** and **2a** was studied using alginate gel beads based on different metals, and alginic acid, all derived from a guluronic-rich alginate (Protanal 200S, D-mannuronic(M)/L-gluronic(G) ratio = 3/7). Aerogels (**AeG**), obtained by $scCO_2$ drying, or solvogels (**SG** in ethanol) were used depending on the availability. A solvent exchange from ethanol to dichloromethane was carried out before using the **SG** catalysts in the reactions. Catalyst loading was set to reach about 20 mol% value based on metal. With the exception of alginic acid, the approximate amount of metal in each bead was calculated by weighing 10 dry beads, and by applying the equation:

$$mmol\ (M) = \frac{weight\ of\ 1\ bead\ in\ mg}{[350.232 + atomic\ weight\ of\ M](\frac{mg}{mmol})}$$

wherein 350.232 corresponds to the molecular weight of two uronate monomers, (G or M) complexing one cation. This turned out to be a good approximation of the amount of metal, when compared with the experimentally determined amount (TGA), at least in the case of the **AeG-Ba** catalyst (see section: preparation and characterization of barium alginate gel beads). In practice, having at hand beads weighing between 0.7 and 0.9 mg, this translated to the requirement of using five beads to reach ca. 20 mol% loading in all cases (0.05 mmol scale reaction). Table S1 shows the results of a preliminary screening using different alginate metals. It is possible to conclude that the activity of the catalysts strongly depends on the metal, since copper, calcium, strontium and barium alginates could drive the reaction to completion in less than one day (entries 1-4), while cobalt, nickel and zinc alginate provided much slower reactions (entries 5-7). Alginic acid does not seem efficient in catalyzing this reaction (entry 8). As far as the enantioselectivity is concerned, copper, barium and nickel could provide a small, yet measurable and reproducible, enantioinduction in this reaction (entries 1, 4, 6). Interestingly, the sense of enantioinduction offered by barium alginate is opposite to the one given by copper and nickel alginates.

Table S1. Preliminary screening of metal alginates.[a]

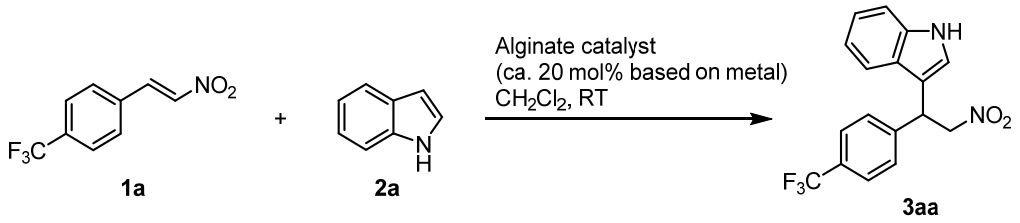

Entry	Catalyst	Time [h]	Conversion[b] [%]	ee[c] [%]
1	**AeG-Cu**	<18	>95	21 (*R*)
2	**AeG-Ca**	<18	>95	<5
3	**SG-Sr**	<18	>95	<5
4	**SG-Ba**	<18	>95	24 (*S*)
5	**SG-Co**	88	67	<5
6	**AeG-Ni**	70	74	8 (*R*)
7	**SG-Zn**	88	>95	<5
8	**AeG-H**[d]	190	53	<5

[a] Conditions: **1a** (0.05 mmol), **2a** (0.075 mmol), 5 gel beads (corresponding to ca. 20 mol% loading based on metal), CH_2Cl_2 (150 µL), RT. [b] Determined by ^{19}F NMR on a reaction sample. [c] Determined by CSP HPLC analysis of the crude mixture. [d] 40 mol% loading based on carboxylic acid.

Screening of alginates with different M/G ratios

The most promising metal alginates from the previous screening were further investigated by preparing and testing aerogels derived from commercial sodium alginates (FMC Biopolymer) with different M/G ratios. It is known that the M/G ratio influences the properties of the gel materials especially in terms of stiffness, which increases with the G content.[3] Furthermore, reactions were more carefully followed in order to assess the reaction time and give a better evaluation of the activity displayed by the catalysts. As shown in Table S2, the higher activity of barium and copper alginates compared to their nickel counterparts was confirmed. Remarkably, the reactions with barium alginates went to completion in less than two hours. As far as the enantioselectivity is concerned, a barium aerogel catalyst gave the same performances of the previously employed solvogel (compare entry 4 of Table S2 with entry 4 of Table S1), while guluronic rich, thus stiffer, gels gave in general better enantioinduction. The better enantioinducing power of copper and barium catalysts compared to the nickel ones was confirmed too. Thus, copper and barium alginates, derived from G-rich alginate 200S, were selected for further studies.

Table S2. Screening of alginates with varying M/G ratios.[a]

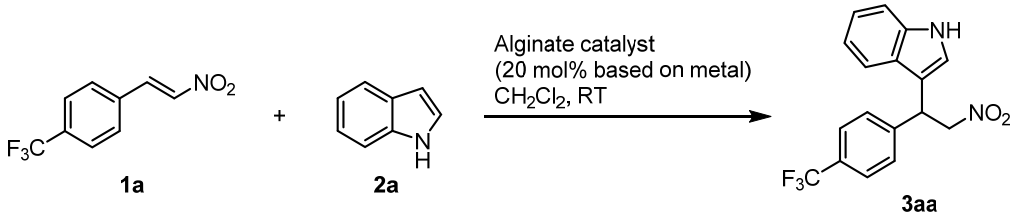

Entry	Alginate (commercial name)	M/G ratio	Catalyst	Time [h]	Conversion[b] [%]	ee[c] [%]
1	Protanal 200S	3/7	**AeG-Cu**	4	91	21 (*R*)
2	Protanal 200DL	4/6	**AeG-Cu**	4	93	21 (*R*)
3	Protanal 240D	7/3	**AeG-Cu**	19	92	15 (*R*)
4	Protanal 200S	3/7	**AeG-Ba**	2	>95	24 (*S*)
5	Protanal 200DL	4/6	**AeG-Ba**	2	>95	18 (*S*)
6	Protanal 240D	7/3	**AeG-Ba**	2	>95	8 (*S*)
7	Protanal 200S	3/7	**AeG-Ni**	70	74	8 (*R*)
8	Protanal 200DL	4/6	**AeG-Ni**	70	95	4 (*R*)
9	Protanal 240D	7/3	**AeG-Ni**	70	>95	<5

[a] Conditions: **1a** (0.05 mmol), **2a** (0.075 mmol), 5 gel beads (corresponding to ca. 20 mol% loading based on metal), CH_2Cl_2 (150 µL), RT. [b] Determined by ^{19}F NMR on a reaction sample. [c] Determined by CSP HPLC analysis of the crude mixture.

Screening of solvents

AeG-Cu and **AeG-Ba** derived from G-rich alginate were then tested in a range of solvents (Table S3). Alcoholic solvents do not seem suitable for the reaction (entries 5,6 and 12,13), since they gave a dirty reaction profile in contrast to the other reactions performed so far. Furthermore, while the enantioinducing properties of barium alginate were maintained in these solvents, its copper counterpart gave the product in essentially racemic form. A more hindered alcohol such as isopropanol restored a clean reaction profile with barium alginate, accompanied by an enantioselectivity comparable to the reaction performed in dichloromethane (entries 10 and 14). The solvent polarity influences negatively the performances of the copper alginate catalyst in this reaction. Both activity and enantioselectivity sharply decreased in moving from toluene or dichloromethane to more polar solvents such as acetonitrile, THF, or TBME (entries 1-3, and 7,8). Also chloroform gave a worse result than dichloromethane with this catalyst (entry 3). In contrast, the barium alginate catalyst benefits, in part, from the use of solvents of higher polarity and/or coordinating properties than dichloromethane or toluene (entries 9-11, 14-17). While the reactivity decreased, best enantioselectivities were achieved using THF or EtOAc in the reaction (entries 15 and 17). Attempts to combine the higher activity displayed in dichloromethane with the higher

enantioselectivity offered by more polar or coordinating solvents, thus using solvent mixtures, were not particularly successful (entries 18-21).

Table S3. Screening of different solvents using **AeG-Cu** and **AeG-Ba** catalysts.[a]

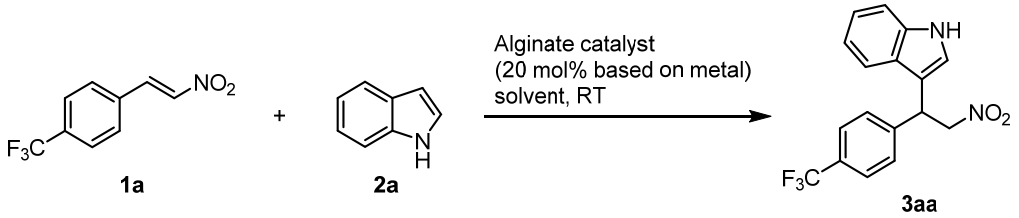

Entry	Catalyst	Solvent	Time [h]	Conversion[b] [%]	*ee*[c] [%]
1	**AeG-Cu**	Toluene	19	>95	17 (*R*)
2	**AeG-Cu**	CH_2Cl_2	19	>95	21 (*R*)
3	**AeG-Cu**	$CHCl_3$	64	82	13 (*R*)
4	**AeG-Cu**	CH_3CN	96	13	n.d.
5	**AeG-Cu**	EtOH	264	Multiple products	<5
6	**AeG-Cu**	MeOH	64	Multiple products	n.d.
7	**AeG-Cu**	THF	64	<5	n.d.
8	**AeG-Cu**	TBME	64	55	8 (*R*)
9	**AeG-Ba**	Toluene	1.5	>95	19 (*S*)
10	**AeG-Ba**	CH_2Cl_2	2	>95	24 (*S*)
11	**AeG-Ba**	CH_3CN	51	>95	30 (*S*)
12	**AeG-Ba**	EtOH	24	Multiple products	50 (*S*)
13	**AeG-Ba**	MeOH	52	Multiple products	23 (*S*)
14	**AeG-Ba**	i-PrOH	24	>95	30 (*S*)
15	**AeG-Ba**	THF	48	70	60 (*S*)
16	**AeG-Ba**	TBME	2	>95	38 (*S*)
17	**AeG-Ba**	EtOAc	24	91	56 (*S*)
18	**AeG-Ba**	CH_2Cl_2/EtOH 2:1	24	93	46 (*S*)
19	**AeG-Ba**	CH_2Cl_2/THF 2:1	6	>95	43 (*S*)
20	**AeG-Ba**	CH_2Cl_2/EtOAc 2:1	4	>95	37 (*S*)
21	**AeG-Ba**	CH_2Cl_2/DMF 14:1	52	92	19 (*S*)

[a] Conditions: **1a** (0.05 mmol), **2a** (0.075 mmol), 5 gel beads (corresponding to ca. 20 mol% loading based on metal), solvent (150 µL), RT. [b] Determined by ^{19}F NMR on a reaction sample. [c] Determined by CSP HPLC analysis of the crude mixture.

Screening of oxygenated solvents

Considering the promising results obtained with THF and EtOAc, an extended screening of different oxygenated solvents was carried out. Solvogel catalyst **SG-Ba**, stored in EtOH, was used in these experiments, swapping the solvent from EtOH to the reaction medium by at least five washings of 15 minutes each, prior to the catalytic reactions. The results are collected in Table S4. Ethereal solvents seems to give better conversions compared to esters or ketone ones, with the exception of EtOAc (compare entries 1,3-8 with 2,9,10). More polar solvents like DMC (dimethylcarbonate) or DMSO shut down catalyst activity (entries 11,12). As far as the enantioselectivity is concerned, most ether solvents tested gave results similar to THF (Et_2O, CPME, 2-MeTHF, 1,4-dioxane, entries 1,3,4,7,8), with some exceptions (*i*-Pr_2O, anisole, entries 5,6). In contrast, *i*-PrOAc and acetone gave worse results than EtOAc in the reaction (entries 9,10 *vs* 2). In summary, this screening confirmed that the **SG-Ba** performs best in ether solvents, in terms of enantioselectivity for the addition of **2a** to **1a**. Amongst the different ether solvents, THF surpasses slightly its counterparts. The effect of water in the reaction was then shortly investigated. The results reported in entries 13-15 show that water has a negative influence on catalyst activity, even in relatively small amounts. Considering that untreated, thus containing traces of water, THF had been used in all previous experiments, these results called for the careful control of this parameter in the reaction mixture (*vide infra*). An attempt to use directly the EtOH solvogel **SG-Ba** in the reaction, thus avoiding the solvent exchange process which soaks the beads with THF, indicated that the catalyst does not tolerate EtOH neither, since very low conversion was observed for this reaction (entry 16).

Table S4. Screening of oxygenated solvents using **SG-Ba** catalyst in the reaction.[a]

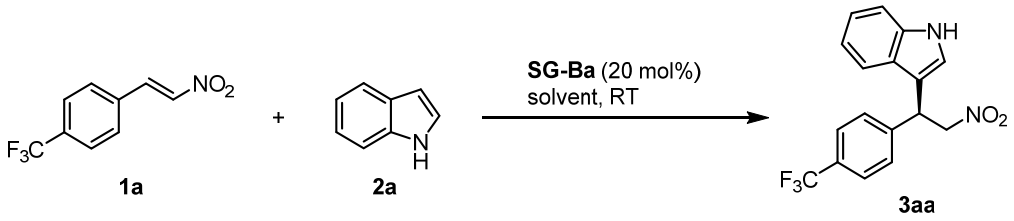

Entry	Solvent	Time [h]	Conversion[b] [%]	ee[c] [%]
1	THF	48	70	60
2	EtOAc	24	91	56
3	Et_2O	3.5	>95	51
4	CPME	22	>95	55
5	*i*-Pr_2O	4	>95	26
6	Anisole	21	>95	27
7	2-MeTHF	45	87	52
8	1,4-dioxane	21	>95	55
9	*i*-PrOAc	72	44	20
10	Acetone	72	52	40
11	DMC	72	28	<5
12	DMSO	72	<5	-
13	THF/H_2O 9:1	42	<5	-
14	THF/H_2O (95:5)	22	<5	-
15	THF/H_2O (97:3)	22	12	n.d.
16[d]	THF	48	11	n.d.

[a] Conditions: **1a** (0.05 mmol), **2a** (0.075 mmol), 5 **SG-Ba** beads (corresponding to ca. 20 mol% loading based on barium), solvent (150 µL), RT. [b] Determined by ^{19}F NMR on a reaction sample. [c] Determined by CSP HPLC analysis of the crude mixture. [d] **SG-Ba** in EtOH was used. N.d.: not determined.

Additional screening of alginates with different M/G ratios

The behaviour of catalysts derived from alginates with different M/G ratios was further inspected using some ethereal solvents. As shown in Table S5, a worsening of catalytic activity and enantioselectivity was observed using the mannuronic-rich alginate Protanal 240D in the three solvents tested (entries 3,6,9), compared to the other alginates. Conversely, materials derived from Protanal 200S and Protanal 200DL gave more similar results (compare entries 1 and 2, 4 and 5, 7 and 8), although the gel derived from the guluronic-rich Protanal 200S confirmed to be the most competent material.

Table S5. Screening of **SG-Ba** catalysts derived from alginates with different M/G ratios.[a]

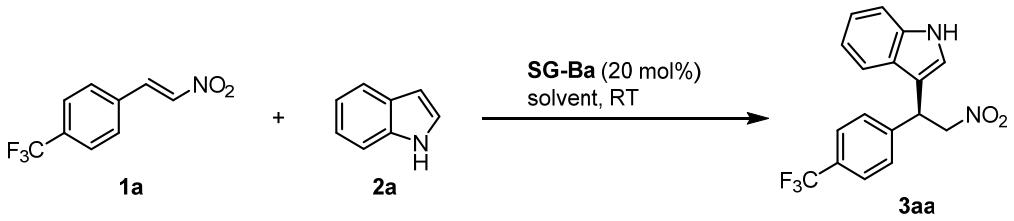

Entry	Alginate (commercial name)	M/G ratio	Solvent	Time [h]	Conversion[b] [%]	ee[c] [%]
1	Protanal 200S	3/7	THF	48	70	60
2	Protanal 200DL	4/6	THF	70	67	60
3	Protanal 240D	7/3	THF	70	42	35
4	Protanal 200S	3/7	CPME	22	>95	55
5	Protanal 200DL	4/6	CPME	22	>95	42
6	Protanal 240D	7/3	CPME	44	87	19
7	Protanal 200S	3/7	Et_2O	3.5	>95	51
8	Protanal 200DL	4/6	Et_2O	3	>95	47
9	Protanal 240D	7/3	Et_2O	21	>95	15

[a] Conditions: **1a** (0.05 mmol), **2a** (0.075 mmol), 5 gel beads (corresponding to ca. 20 mol% loading based on metal), solvent (150 µL), RT. [b] Determined by ^{19}F NMR on a reaction sample. [c] Determined by CSP HPLC analysis of the crude mixture.

Screening of drying agents and reaction temperature

Given the negative influence of water in the reaction outcome, untreated THF was replaced by freshly distilled one (from sodium/benzophenone) in the solvent exchange giving the THF containing **SG-Ba**, and in the catalytic reaction. This experiment, reported in Table S6, entry 2, did not lead to any improvement compared to the previously employed protocol (entry 1). Reasoning that distilled THF might still contain traces of water, the use of activated molecular sieves as drying agents was considered. Thus, molecular sieves of different sizes (3,4 and 5 Å), in pellets, were activated by heating with a heatgun under high vacuum, cooled under vacuum, placed under nitrogen and then

used in the reaction. No precautions were taken to exclude moisture from the reaction set up. As shown in Table S6, entries 3-5, these drying agents had a remarkably positive effect on the reaction outcome, leading not only to a full conversion of nitroalkene **1a** within a shorter timeframe (<24 h), but also to an improved enantiomeric excess of about 80% for product **3aa** (entries 3-5). Reducing the reaction temperature to 0 °C provided an additional improvement, while further reduction to -20 °C was not feasible (entries 6,7). Testing the three molecular sieves at 0 °C indicated that all three drying agents give similar beneficial effect to the reaction outcome (entries 6,8,9). Additional experiments (not shown) indicated that, i) the use of molecular sieves during the solvent exchange process of **SG-Ag** from EtOH to THF does not bring any additional benefit; ii) a reaction under a nitrogen atmosphere using Schlenk techniques provides the same results as a reaction performed in a test tube without specific precautions to exclude moisture or air; iii) the amount of solvent in the reaction does not have an appreciable influence on reaction outcome, provided that there is enough solvent to soak and cover well the solid materials of the mixture (**SG-Ba** beads and MS); iv) stirring is not necessary, it is sufficient to incubate the mixture at the appropriate temperature for the given time.

Table S6. Utilization of drying agents in the reaction and screening of temperatures.[a]

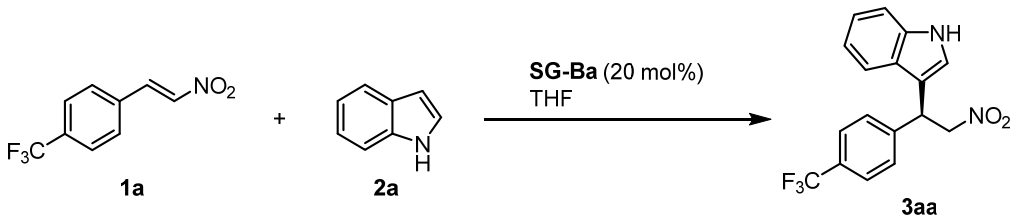

Entry	Solvent	Drying agent	T [°C]	Time [h]	Conversion[b] [%]	ee[c] [%]
1	Untreated THF	-	RT	48	70	60
2	Dry THF	-	RT	48	59	60
3	Dry THF	MS 3 Å[d]	RT	24	93	82
4	Dry THF	MS 4 Å[d]	RT	24	>95	80
5	Dry THF	MS 5 Å[d]	RT	24	89	80
6	Dry THF	MS 4 Å[d]	0	26	92	85
7	Dry THF	MS 4 Å[d]	-20	28	25	n.d.
8	Dry THF	MS 3 Å[d]	0	48	>95	85
9	Dry THF	MS 5 Å[d]	0	48	>95	84

[a] Conditions: **1a** (0.05 mmol), **2a** (0.075 mmol), 5 **SG-Ba** beads (corresponding to ca. 20 mol% loading based on barium), solvent (150 µL). [b] Determined by ^{19}F NMR on a reaction sample. [c] Determined by CSP HPLC analysis of the crude mixture. [d] ca. 30 mg of activated MS (pellets) were used. N.d.: not determined.

Catalyst loading

The amount of catalyst had been set to 20 mol% so far, based on the approximate metal content of the alginate catalyst. The approximate amount of barium in the beads, which was calculated as 0.00205 mmol/mg, or 28.2% w/w, according to this equation

$$mmol\ (Ba) = \frac{weight\ of\ 1\ bead\ in\ mg}{[350.232 + 137.327](\frac{mg}{mmol})}$$

is a good approximation of the amount experimentally determined by TGA analysis (26.6%), confirming that the reactions were set up using 20 mol% of loading. Applying the newly found conditions, it was tested if a lower catalyst loading could be used in the reaction. The results reported in Table S7 show that the enantioselectivity of the reaction is maintained up to 10 mol%, with a minor reduction when 5 mol% loading was used. Conversely, the reaction reached an acceptable conversion level up to 10 mol% loading, with a more obvious lowering at a lower 5 mol%. It was also verified that the reaction in the absence of catalyst does not proceed at all (entry 5).

Table S7. Reaction performed at different catalyst loadings.[a]

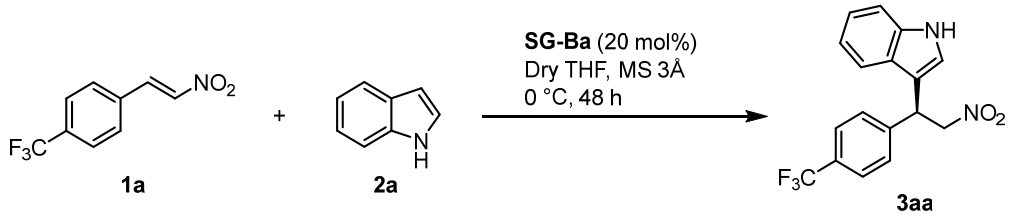

Entry	Catalyst loading[b] [mol%]	Conversion[c] [%]	ee[d] [%]
1	20	>95	85
2	15	89	85
3	10	82	85
4	5	67	83
5	0	<5	-

[a] Conditions: **1a** (0.05 mmol), **2a** (0.075 mmol, 1.5 equiv), x **SG-Ba** beads, solvent (150-200 µL), ca. 30 mg of activated MS 3Å. [b] Approximate loading, based on barium. [c] Determined by ^{19}F NMR on a reaction sample. [d] Determined by CSP HPLC analysis of the crude mixture.

Robustness of the reaction and optimized reaction protocol

The influence of the presence of adventitious moisture in the mixture was inspected by using untreated THF during both the solvent exchange of **SG-Ag** from EtOH to THF, and during the catalytic reaction. The data reported in the entries 1 and 2 of Table S8 show that essentially the same results were obtained. Thus, the reaction is not sensitive to minor amounts of water, if

performed in the presence of molecular sieves. However, when the less electron-poor nitroalkene **1b** was employed, only a moderate conversion in the product **3ba** was achieved (entry 3). Fortunately, the enantiomeric excess of **3ba** was found to be very good. In order to improve the conversion in this reaction, it turned out to be sufficient to use a larger amount of molecular sieves, combined with a larger excess of indole **2a** (2.5 equiv instead of 1.5 equiv), in the reaction (entry 4). Such modification allowed the obtainment of fully satisfactory results with **1b**, and was verified to be readily applicable to the previously employed **1a** (entry 5). These conditions were considered as the optimal ones for the reaction.

Table S8. Robustness of the reaction and optimized reaction protocol.[a]

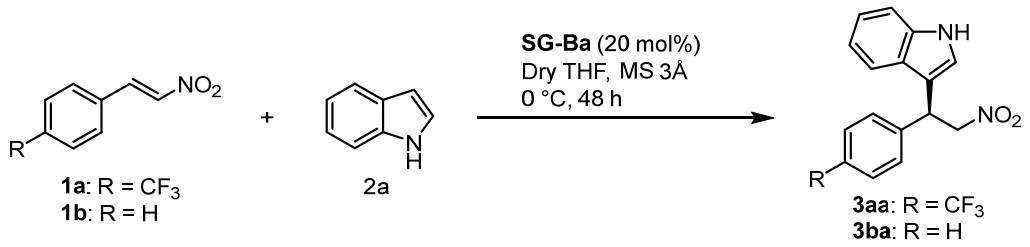

Entry	**1**	equiv **2a**	MS 3 Å[b] [mg]	**3**	Conversion[c] [%]	ee[d] [%]
1	**1a**	1.5	30	**3aa**	>95	85
2[e]	**1a**	1.5	30	**3aa**	>95	85
3	**1b**	1.5	30	**3ba**	52	89
4	**1b**	2.5	90	**3ba**	95%	89
5	**1a**	2.5	90	**3aa**	>95	87

[a] Conditions: **1** (0.05 mmol), **2a** (y mmol), 5 **SG-Ba** beads, THF (150-200 µL), activated MS 3 Å. [b] Approximate amount of MS 3 Å, pellets. [c] Determined by ^{19}F NMR on a reaction sample (**3aa**), or by ^{1}H NMR after evaporation (**3ba**). [d] Determined by CSP HPLC analysis of the crude mixture. [e] Untreated THF was used as solvent.

Catalyst heterogeneity – Sheldon test

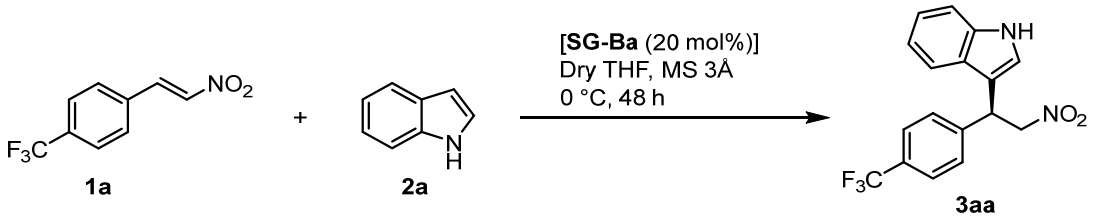

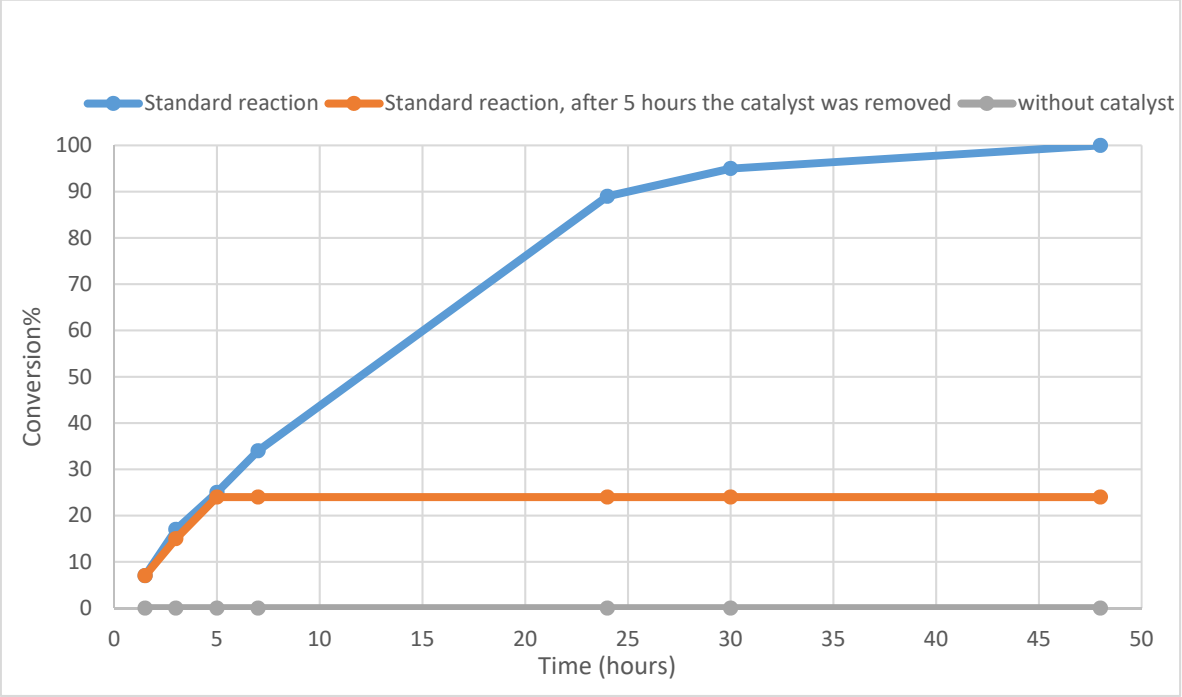

Scheme S1. Sheldon and blank tests. Conversion determined by analysing reaction samples diluted in $CDCl_3$ with ^{19}F NMR.

Sheldon test was performed under the optimised reaction conditions in order to determine the possible leaching of catalytically active species in solution, and to confirm that the catalysis is indeed heterogeneous. The protocol used consists in the parallel set up of three reactions, two standard ones and a blank without catalyst, which were conveniently monitored by analysing samples taken at different times with ^{19}F NMR. The first reaction was allowed to proceed for the standard reaction time (48 h). In the second one, performed under the same conditions, the catalyst beads were removed with a spoon after 5 hours, and then checked for possible residual reactivity of the system. The third reaction can be considered as a check test, because no alginate beads were added to the reaction. As shown in Scheme S1, the Sheldon test gave satisfying results, that is, catalysis is heterogeneous, and there is no leakage of catalytically active material in solution. In fact, TGA analyses of the beads before and after the reaction are essentially superimposable. The lack of barium leaching during the catalytic process was confirmed by a Microwave Plasma Atomic Emission Spectroscopy analysis. In more detail, the beads and the molecular sieves were removed from the

vial after the reaction, the mixture concentrated to dryness and then dissolved in acetone (1 mL) and analyzed by MP-AES. The amount of barium ions in this solution was found to be lower than the detection limit (0.03 ppm, that is, 10 times the standard deviation of the blank analysis). Moreover, the reaction does not proceed without alginate beads catalyst, accounting for the same enantioselectivity measured for the product obtained in the first and in the second reaction (87% ee). Finally, TGA analysis of the beads before and after the reaction provided essentially identical results. Moreover, the reaction was performed using different barium salts as catalysts (BaO, $BaCl_2$, $Ba(OH)_2$, $Ba(NO_3)_2$ and $Ba(OAc)_2$). None of these experiments provided the product, thus highlighting the capability of alginates in providing a competent barium catalyst species in an organic reaction medium.

Catalyst preparation, alginate composition and surface areas

First of all, the protocol for the solvent exchange required to prepare the **SG-Ba** soaked in THF from its EtOH solvogel was studied. The standard protocol involves a direct solvent exchange by washing several times (>5, 15 minutes each) the **SG-Ba** beads with pure THF. Suspecting that such direct washing procedure could induce a modification of the gel structure, a gradual exchange process was tested, that is, the washings were performed using increasing amounts of THF in EtOH (1:9, 3:7, 5:5, 7:3, then 100% THF for five times). The data reported in Table S9, entries 1 and 2, show that the direct and the more cumbersome gradual solvent exchange from EtOH to THF, gave comparable results. Then, direct preparation of **SG-Ba** soaked in THF from its hydrogel **HyG-Ba** form was carried out. Thus **HyG-Ba** beads in water were washed five times (15 min each) with THF, and the resulting **SG-Ba** was used in the reaction, leading to results comparable with the ones obtained from **SG-Ba** in ethanol (entry 3).

Table S9. Effect of different preparation of **SG-Ba** catalyst, of the M/G ratio, and of the formulation, on the reaction.[a]

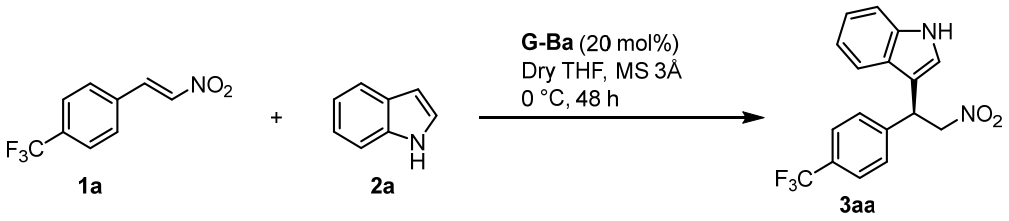

Entry	Alginate (commercial name)	M/G ratio	Pre-Catalyst	wt Ba^{2+}[b] [%]	S_{BET}[c] [m^2g^{-1}]	Conversion[d] [%]	ee[e] [%]
1	Protanal 200S	3/7	**SG-Ba**	26.6	585[f]	>95	87
2	Protanal 200S	3/7	**SG-Ba**[g]	26.6	585[f]	>95	87
3	Protanal 200S	3/7	**HyG-Ba**[h]	26.6	585[f]	>95	87
4	Protanal 200DL	4/6	**SG-Ba**	26.4	542[f]	>95	87
5	Protanal 240D	7/3	**SG-Ba**	25.6	437[f]	56[i]	70
6	Protanal 200S	3/7	**XG-Ba**	26.6	<10	<5	-

[a] Conditions: **1a** (0.14 mmol), **2a** (0.42 mmol), 8 **G-Ba** beads, THF (400 µL), activated MS 3Å (ca. 200 mg), 0 °C, 48 h. [b] Determined by TGA. [c] Determined on the dry material using the BET method by means of N_2 adsorption/desorption measurement at -196 °C. [d] Determined by ^{19}F NMR on a reaction sample. [e] Determined by CSP HPLC analysis of the crude mixture. [f] Determined on the corresponding **AeG-Ba**. [g] **SG-Ba** soaked in THF was prepared by gradual solvent exchange from **SG-Ba** in EtOH. [h] **SG-Ba** soaked in THF was prepared by direct solvent exchange from **HyG-Ba**. [i] 96 h reaction time.

Although preliminary results using catalysts prepared from alginates with lower guluronic content did not give satisfactory results (see Table S5), these materials, all featuring very similar barium contents, were tested again under the optimized reaction conditions (entries 4 and 5). While the

results in terms of enantioselectivity substantiated our assumption that stiffer gels could be more efficient as enantioinducers, the lower activity displayed by the M-rich gel (entry 5) was somehow surprising, since it is not justifiable by differences in surface area. Possibly, it could be ascribed to a different local environment for barium due to different geometric conformations of the M/G blocks.[4] On the other hand, an alginate with a 4/6 ratio between the two monomers gave the same results of its G-rich counterpart (compare entries 1 and 4). This result indicates a certain tolerance in the composition of the biopolymer, ensuring robustness and less strict reliance on specific natural sources.

Moving to study the utilization of dry materials in the reaction, the activity of xerogel **XG-Ba** beads, obtained by direct evaporation, was tested. These beads with very low surface area were not active as catalysts for this reaction (entry 6), highlighting that a disperse material with high surface area is required for an efficient catalysis. In fact, it is well-known and demonstrated in heterogeneous catalysis when using porous catalytic materials, that some of the key-points leading to a high activity are a surface area and pore size, which allow a good accessibility to active sites - not only on the surface of the catalyst but also within the pores – and permit the diffusion of the molecules throughout the pores of the materials. In the present work, we found that the size of the beads does not influence the catalytic properties, suggesting that the catalysis occurs in the whole bulk of the beads, and not on their external surface only.

When comparing the surface area obtained in this work to those of mesoporous silicas used as chiral catalysts supports, surface areas obtained here are in the lowest range of those obtained using ordered mesoporous silicas such as MCM-41, for which surface areas can be as much as 800 m^2g^{-1}.[5] In the case of CMOFs and CCOFs used for asymmetric catalysis, which is a rapidly expanding field, surface areas can range between 1000 and 4000 m^2g^{-1}.[6] Nevertheless, the values obtained here are within the range of "useful" values allowing access of substrates to the active sites within the bulk of the material, as proven by the experiments above, and by our previous work on the use of alginic acid as catalyst for a non-enantioselective Mannich reaction.[7]

Concerning the transfer of chiral information, referring to chiral mesoporous catalysts as silicas is less easy as many parameters come into play, for example the strategy used to immobilize the chiral ligand/metal – by grafting, electrostatic interactions, encapsulation, entrapment – the density of catalytic sites and their position in the porous network, or the effect of pore size which can induce increase or decrease of enantioselectivity, compared to the homogeneous counterpart, due for example to confinement effects or modification of the spatial arrangement of chiral ligands due to grafting.[8] Here the enantioselectivity is induced by the support itself; and more precisely by the spatial arrangement of the polymeric network, and not by a chiral catalyst added to a porous support. Therefore, one can suppose that the extent of the surface area, i.e. the surface potentially in contact with a prochiral substrate is of utmost importance for the transfer of chiral information.

Reaction limitations

During the study of the scope of the reaction, some substrates were found to render poor results. As summarized in Scheme S2, reactions with aliphatic nitroalkenes, even if tested at three different temperatures (RT, 0 °C, -20 °C), did not provide the desired Friedel-Crafts adducts in satisfactory yields. The lower reactivity of these nitroalkenes (*vs* nitrostyrenes), combined with their propensity to undergo dimerization and oligomerization processes by formation of extended nitronate intermediates via deprotonation at their γ-position, rendered these reactions inefficient. However, the formation of these oligomerization products indicate the proficiency of the catalytic system to promote soft-enolization processes, warranting future investigations in this direction.

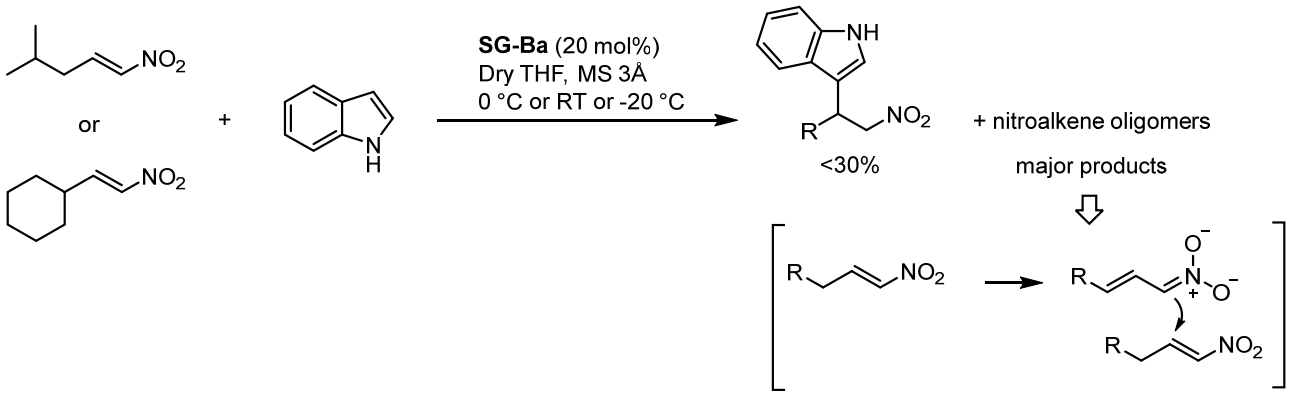

Scheme S2. Unsuccessful reactions with aliphatic nitroalkenes.

As far as the indole reaction partner is concerned (Scheme S3), 2-methylindole and 7-methylindole were found to react well with nitroalkene **1a**, but the corresponding products were obtained with low enantioselectivity values. Conversely, a reaction with N-methyl indole did not afford the addition product. The results with these substrates, where the indole N-H is hindered by vicinal methyl groups or is not present at all, suggest that an interaction between the N-H of the indole partner and the catalyst is operative in this reaction, in line with several reported asymmetric reactions engaging N-H indole substrates (see next section).

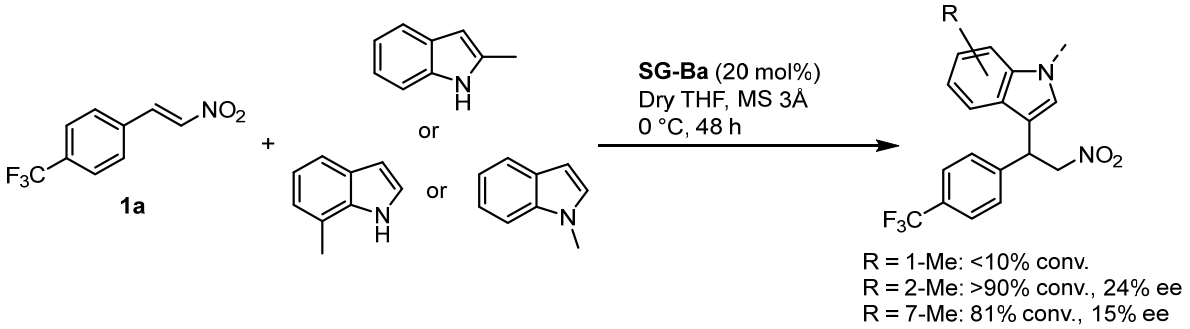

Scheme S3. Unsuccessful reactions with 1-, 2-, and 7-methylindole.

Mechanistic considerations

Interactions between catalyst and substrates

We first tried to rationalize the key interactions between catalyst and substrates, responsible for the catalytic activity of **SG-Ba**.

First of all, it is possible to exclude that **SG-Ba** promotes this reaction by activating the nitroalkene exclusively via hydrogen-bond interactions, given the dramatically poor activity shown by an alginic acid gel (**AeG-H**) in this reaction (Table S1). This suggests that barium acts as a Lewis acid, activating the nitroalkene for the nucleophilic addition of indole. This hypothesis was confirmed by experiments performed using different additives (Table S10), that were compared with results obtained with the optimized protocol (entry 1). Entries 2-4 show that basic additives such as amines and pyridines suppress the catalyst activity, even when used in equimolar amounts with respect to barium, presumably through coordination to the metal ion. On the other hand, even the addition of 50 mol% of a primary alcohol such as MeOH has a negative effect on catalyst performances (entry 5). The importance of the coordinative property of the additives is confirmed by the experiment reported in entry 6, that reports that the more hindered thus less coordinating *t*-BuOH has only a marginal influence on the reaction outcome. To test the effect of water, it was necessary to apply a reaction protocol alternative to the standard one, which involves molecular sieves in the reaction. Thus, the substrates **1a** and **2a** dissolved in THF and the beads soaked in THF were treated separately with activated molecular sieves, to remove adventitious water. The molecular sieves were removed from the substrates solution, which was cooled to 0 °C. Water (ca. 50 mol%) was added, followed by the beads. The reaction was then run as usual. This experiment, reported in entry 7, shows that water has a striking detrimental effect on catalyst activity. On the other hand, performing the same experiment but without adding water showed the importance of the presence of molecular sieves during the catalytic process (entry 8), as already reported in Tables S6 and S8. The striking positive influence of molecular sieves on reaction outcome can be tentatively interpreted considering their role as drying agents, since even traces of water have a profound negative impact on catalyst activity. By removing molecular sieves prior to the reaction, traces of water might be present during the catalytic process, thus resulting in poor catalyst performances. However, the involvement of molecular sieves in proton-transfer processes, although not so likely considering the heterogeneous nature of the catalytic process, cannot be fully excluded, considering evidences on this reaction and related ones when performed under homogeneous acid catalysis conditions.[9] Remarkably, in one literature example, this reaction performed using a Brønsted acid catalyst - a chiral phosphoric acid - did not proceed in the absence of molecular sieves.

Table S10. Experiments using different additives in the reaction.[a]

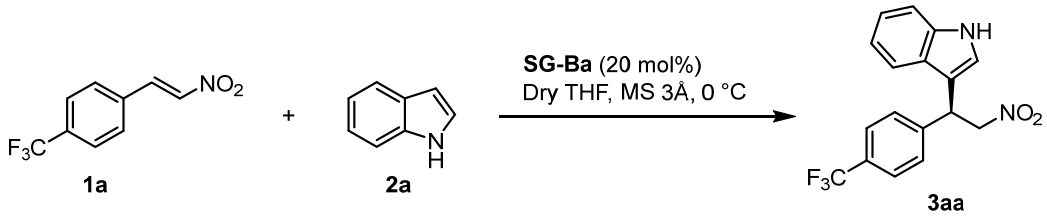

Entry	Additive [mol%]	Time [h]	Conversion[b] [%]	ee[c] [%]
1	-	48	>95	87
2	DMAP [20]	60	7	n.d.
3	Et_3N [20]	60	3	n.d.
4	2,2'-bipyridine [20]	60	17	n.d.
5	MeOH [50]	72	56	68
6	*t*-BuOH [50]	72	>95	80
7[d]	H_2O [50]	144	12	n.d.
8[d]	-	144	32	56

[a] Conditions: **1a** (0.14 mmol), **2a** (0.35 mmol), 10-12 **SG-Ba** beads, THF (400 µL), activated MS 3 Å, 0 °C. [b] Determined by ^{19}F NMR on a reaction sample. [c] Determined by CSP HPLC analysis of the crude mixture. [d] Beads and substrates **1a** and **2a** in THF were treated separately with activated MS, then MS were removed and the beads added to the substrates solution.

On the other hand, the data reported in Scheme S3 indicate that the indole N-H plays a key role in the stereodetermining step of the reaction. Its absence in N-methylindole prevented the reaction proceeding, while 2-methyl and 7-methylindole substrates, wherein the N-H is hindered by neighbouring methyl groups, afforded the products with low enantioselectivities.

In another Friedel-Crafts reaction of N-H indoles, catalysed by a chiral BINOL barium complex under homogeneous conditions, the formation of a genuine barium-indolide intermediate via deprotonation of the indole N-H (pK_a of indole = 21.0 in DMSO)[10] was proposed.[11] However, in the case of the **SG-Ba** catalysed reaction, the basicity of the carboxylates of the material (typical pK_a of aliphatic carboxylic acid ca. 12 in DMSO), does not seem sufficient to form a barium indolide intermediate. In contrast, the role of the indole N-H may be to provide a handle for catalyst anchoring, through a hydrogen bond with some of the Lewis basic functionalities of the biopolymer backbone. Possibly, the negatively charged carboxylates fulfil this role (Scheme S4). It is worth to recall that the interaction between alkaline earth metals and the uronate units in alginates is mainly electrostatic in nature.[12] The H-bond between the carboxylate and the indole N-H assists the barium ion in its Lewis acidic action, facilitating the formation of an ordered transition state, and ultimately the transmission of the chiral information from the biopolymer to the transition state. On the other hand, this type of weak interaction between the N-H of the indole and Lewis basic functionalities of catalysts, facilitating

enantioselective additions via a bifunctional mechanism, is common to many asymmetric additions of indoles to electrophilic substrates such as nitroalkenes.[13]

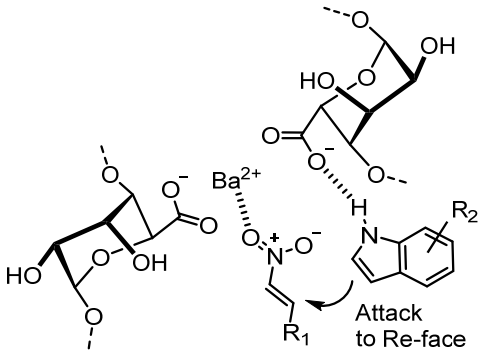

Scheme S4. Bifunctional mechanism of the catalyst in the reaction.

Origin of enantioinduction

It is instead very difficult to predict a plausible geometry of the transition state, which would account for the factors directing the reaction towards the preferential formation of the major enantiomeric product. Such exercise is first hampered by the strong influence of weakly coordinating solvents on reaction outcome. As shown in Tables S3 and S4, THF decreases catalyst activity but boosts enantioselectivity, suggesting that coordination of the solvent to the metal occurs. Considering the capability of barium to accommodate different coordination numbers, it is difficult to envisage the geometry of the Lewis acid centre of the catalyst. Moreover, and more importantly, the biopolymer contains two different uronic monomers: α-L-guluronic (G) and β-D-mannuronic (M) (Scheme S5). Alginates are in fact linear block co-polymers, wherein these monomers are linked in a (1 → 4) fashion and arranged with fixed G($^1C_4$) and M($^4C_1$) conformations. The block co-polymer is constituted by sequences homogeneously constituted by G units (GG-blocks), sequences built by M units (MM-blocks) and alternate mixed sequences (MG-blocks), of various lengths.

α-L-Guluronic acid (G) **β-D-Mannuronic acid (M)**

Scheme S5. The two monomers of alginates.

The different blocks are structurally different, and thus give different properties to the material. The chains containing predominantly GG blocks are characterised by a buckled ribbon-like structure, while the MM blocks generate a flat ribbon-like structure, and the heteropolymeric regions with GM and MG blocks give a helix-like structure. The structure of the G-rich regions of alginate gels with

divalent cations, such as barium, is usually exemplified with the so-called egg-box model, wherein G residues bind cooperatively the cations resulting in well-defined diamond shape holes (Scheme S6). It is worth stressing that, besides the electrostatic interactions between the carboxylate of the uronic units and the metal, the gel structure is characterized by a network of hydrogen bonds and additional interactions between the ions and the oxygen atoms of the backbone, which additionally contribute to define its structure. The cooperative binding of the G resides results in enhanced stiffness and reduced flexibility to the GG-block, compared to the MM-blocks, which in turn are stiffer and less flexible than the GM-blocks.[14] Finally, the structural features of the material can also be influenced by the cross-linking agent.[4]

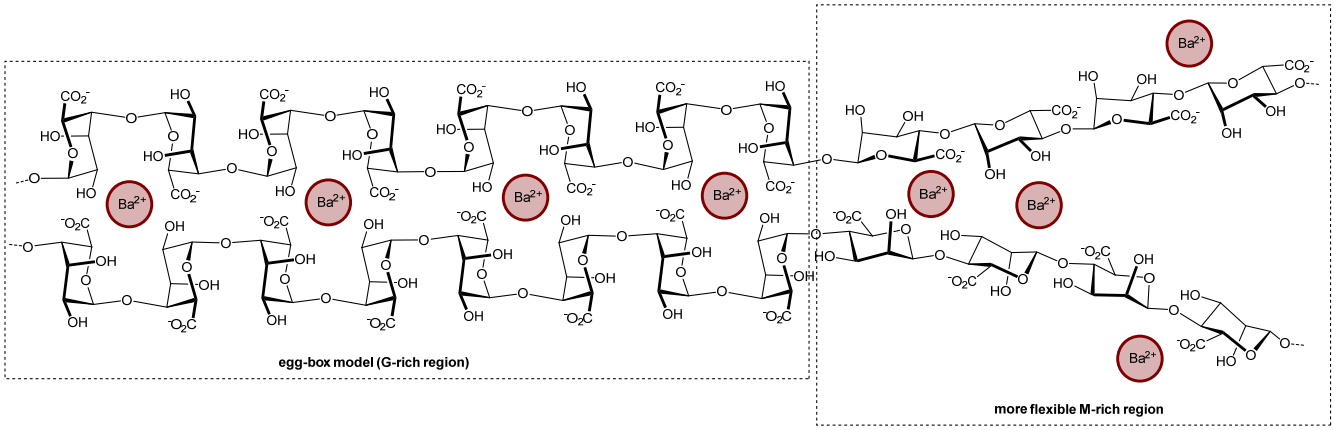

Scheme S6. Simplified model of the structure of barium alginate gels.

As shown in Tables S2, S5 and S9, catalysts richer in guluronic monomers rendered higher enantioselectivities in the reaction. An attempt was done to increase the G-content of the material by gellifying sodium alginate solutions containing also sodium guluronate oligomers (ca. 10 guluronate units, 10-30% of sodium alginate in weight), and using them the reaction between **1a** and **2a**. These attempts were not successful. The resulting materials were found to be poorly active and enantioselective in the reaction. Furthermore, we prepared a barium solvogel derived from a sodium alginate (Sigma-Aldrich catalogue number 180947) with a mannuronic content comparable to the one of Protanal 240D (M/G ca. 7/3), but featuring lower viscosity (1% w/w solution: 5-25 cP vs 115 cP). Even though the material had similar S_{BET} (445 *vs* 437 m^2/g), its activity and enantioinduction were far from the ones obtained with the **SG-Ba** obtained from Protanal 240D. When the newly prepared catalyst was used in the standard reaction, the product **3aa** was obtained with just 42% conversion and 31% ee after 96 h, while the previously employed **SG-Ba** gave 56% conversion and 70% ee after the same reaction time. Finally, we tested if swelling the xerogel **XG-Ba** in water for several hours could restore the catalytic proficiency of the material. The thus obtained gel was used in the standard reaction between **1a** and **2a**, after gradual solvent exchange to EtOH and then to THF, but was found to be much less active and enantioselective (41% conversion after 60 h, 42% ee) than the previously employed solvogel **SG-Ba**.

From this series of experiments, we can conclude that the ratio between the two monomers is only one of factors controlling the enantioinduction. At the current stage, the roles of the different blocks of the biopolymer (GG-, MM-, and MG-) is not clear. In other words, it is not clear if all portions of the polymer are catalytically competent, or some of the blocks have only a structural function. Nevertheless, the experiment performed with the swelled **XG-Ba** suggests that it is the structure of the material as a whole the responsible for the performances of the heterogeneous **SG-Ba** catalyst. The failure of previous attempts to harness the intrinsic chirality of alginates in asymmetric catalysis has been ascribed to poor access to crystalline regions of the gels.[15] It is tempting to hypothesise that, in this catalytic process with **SG-Ba**, the substrates can access highly ordered/crystalline regions of the polymer, and that these regions are effective in both reaction promotion and enantioinduction. The combination of a larger cation such as barium with a solvent weakly coordinating it might be the key to render these less accessible regions available for catalysis.

Catalyst recovery and reuse

These tests were set up in order to check if the activity and selectivity of alginate beads were dropping after one or more reaction cycles. Commercial nitroalkene **1b** was used for convenience in these tests. Preliminary experiments showed the beneficial effect of washing the catalyst beads with EtOH between the reaction cycles, presumably resulting in a more thorough cleaning of the catalyst surface. Thus, after each run, the reaction solvent was removed, the beads were extracted with EtOH (2 times, a few minutes each), the reaction solvent and extracts were combined, filtered on a plug of silica, evaporated and analysed by ^{1}H NMR and HPLC to determine reaction conversion and enantiomeric excess, respectively. Before use in the subsequent run, the EtOH SG-Ba beads were reconditioned as THF SG-Ba beads with five washes with THF of 15 minutes each, with low stirring. As shown in Scheme S7, the catalyst keeps comparable activity and enantioselectivity in the first four runs. An evident drop is instead observed for the fifth run. It is important to note that the beads appeared macroscopically intact even after five runs, although darkened progressively with the reaction cycles.

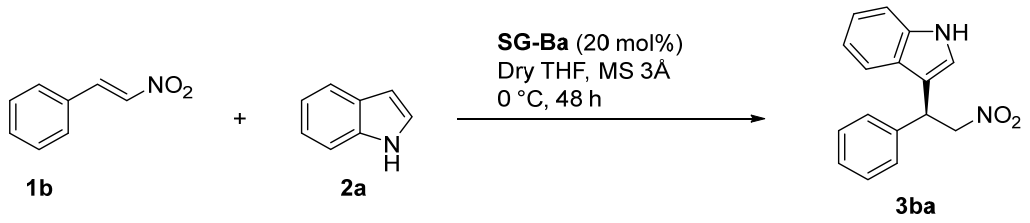

	Run 1	Run 2	Run 3	Run 4	Run 5
Conversion [%]	90	>95	>95	83	51
***ee* [%]**	89	85	87	85	77

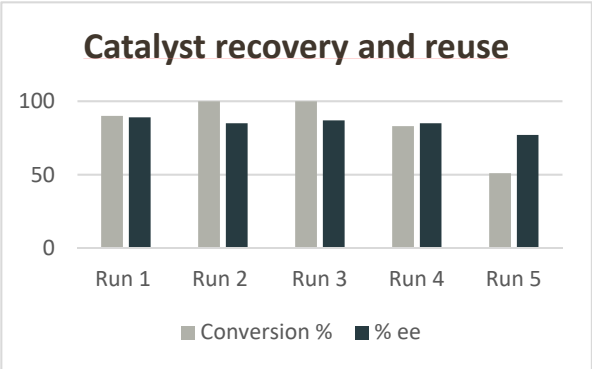

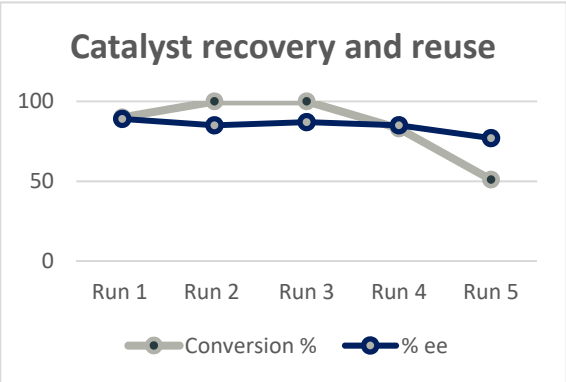

Scheme S7. Catalyst recovery and reuse in the reaction between nitroalkene **1b** and indole **2a**.

Preparation and characterization of barium alginate gel beads.

Preparation of hydrogel HyG-Ba, solvogel (EtOH) SG-Ba, and xerogel XG-Ba beads[16]

A 2% w/w sodium alginate (2 g) solution in deionized water (100 mL) was prepared by magnetically stirring the mixture in an Erlenmeyer flask overnight. The thus obtained viscous solution was transferred to a dropping funnel, and added dropwise to a Beaker containing 200 mL of 0.1 mol/L aqueous solution of $BaCl_2$ (prepared by dissolving 4.885 g of $BaCl_2 \cdot 2H_2O$ in 200 mL of deionized water), kept under magnetic stirring at RT. The amount of $BaCl_2$ corresponds to an excess of barium ions (4 equivalents, considering two uronic units for complexation of an ion). The formation of the hydrogel beads is instantaneous and clearly visible. The resulting beads were stirred gently overnight to allow their maturation, and were then washed carefully with deionized water (5 x ca. 200 mL), affording the hydrogel **HyG-Ba** beads, which soaked in deionized water can be stored in a refrigerator. These beads were then converted to solvogel (EtOH) **SG-Ba** beads, through the immersion of the beads in a series of EtOH/H_2O baths, with increasing EtOH content (10%, 30%, 50%, 70%, 90%, and 100% x 5 EtOH) for 15 minutes each with magnetic stirring. The last EtOH bath containing the beads was treated with activated 3 Å MS, placed in a teabag-like container made of filter paper, for 24-72 h at RT. After removal of the MS, the **SG-Ba** beads, soaked in EtOH, can be stored in a refrigerator. Xerogel **XG-Ba** beads were prepared by direct evaporation of EtOH from **SG-Ba** beads under reduced pressure, until constant weight. A typical preparation using a dropping funnel affords beads of ca. 0.4 cm of diameter and 1.70 mg, corresponding to 0.0035 mmol of barium in each bead.

Figure S1 in the next page reports some pictures of the beads obtained using this procedure.

Alginate gel beads from three commercial sodium alginates, characterized by different M/G ratios (Protanal 200S, M/G = 3:7; Protanal 200DL, M/G = 4:6; Protanal 240D, M/G = 7:3), were prepared successfully using this protocols.

The robustness of the protocol was verified by preparing different **SG-Ba** batches (with Protanal 200S) varying some of the parameters: concentration of the sodium alginate solution (1-3%); concentration of the $BaCl_2$ solution (0.05-2 M) and amount of $BaCl_2$ (2-8 equiv); temperature (0 – 40 °C), size of the dropping device (dropping funnel *vs* a syringe with small gauge giving beads of ca. 0.3 cm of diameter and 0.9 mg) and then applying the resulting **SG-Ba** beads in the catalytic reaction between **1a** and **2a**. None of these variations gave appreciable deviations in the catalytic performances, neither in terms of activity nor of enantioinducing properties. On the other hand, we found that the catalytic performances of aerogel beads **AeG-Ba** tend to worsen with their storage time. We are not sure if this worsening is caused by adsorption of water, or by a minor structural change. Anyhow, this observation prompted to use solvogel beads **SG-Ba** during this study.

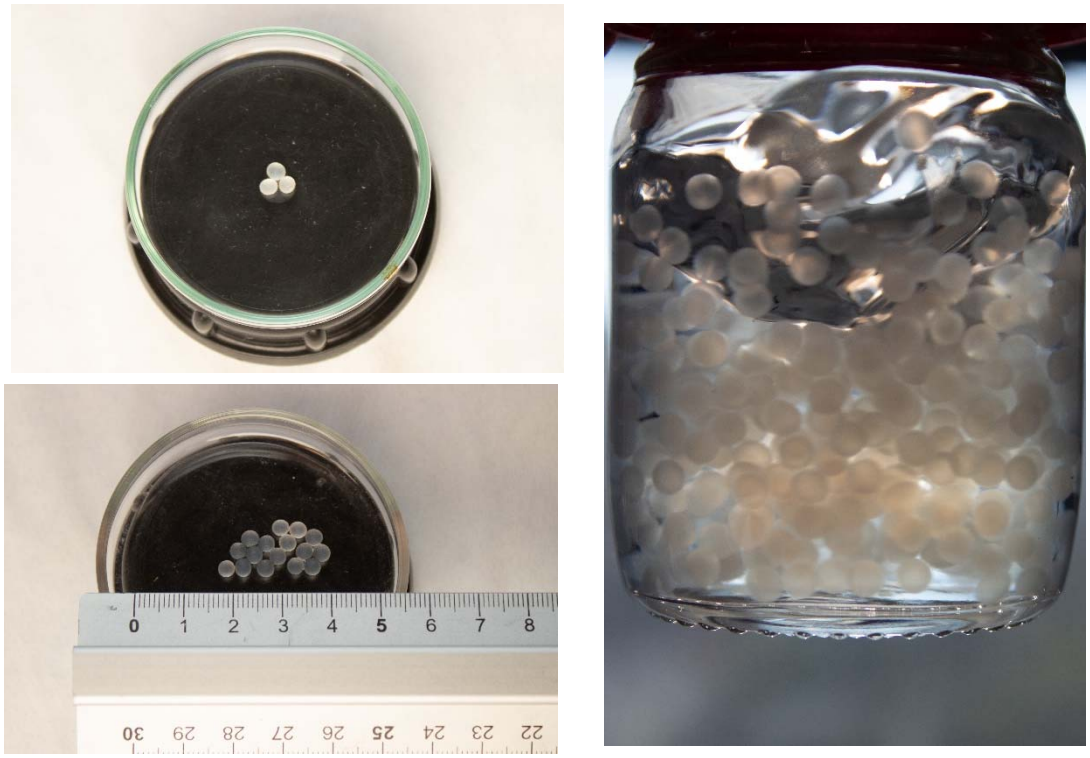

Figure S1. Photos of **SG-Ba** beads. Left: **SG-Ba** beads on a Petri dish. Right: **SG-Ba** beads in EtOH swirling in their storage flask container.

Characterization of the alginate gels

For each of the three **SG-Ba** prepared from different alginates, ATR-IR spectra were acquired by squeezing one bead with the ATR-IR tip thus forming a film. Figure S2 reports the recorded spectra. The three spectra show the characteristic two bands of asymmetric and symmetric stretchings of the carboxylate groups, at ca. 1'600 and 1'400 cm^{-1}, respectively.

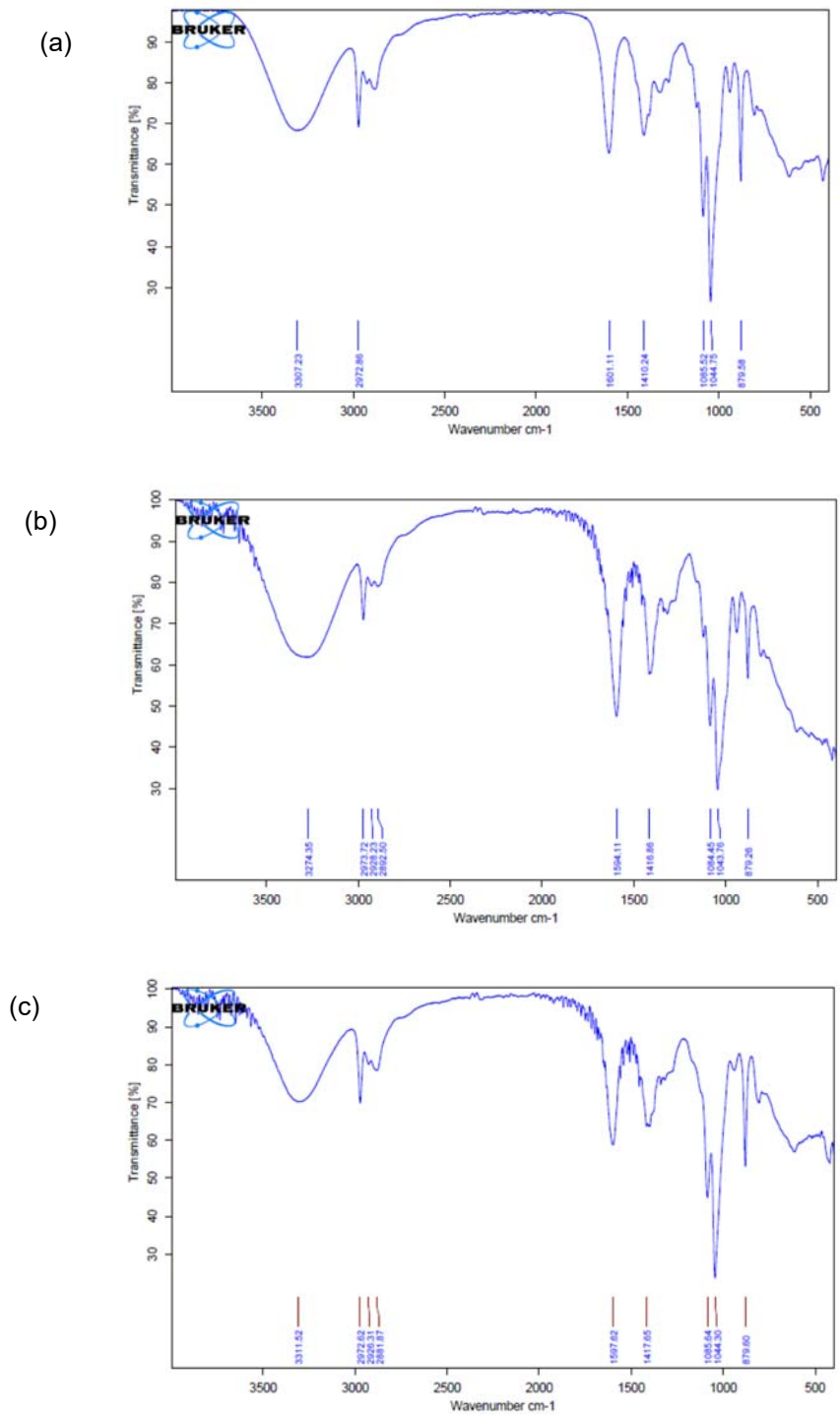

Figure S2. ATR-IR spctra of **SG-Ba** prepared from: (a) Protanal 200S (M/G = 3:7); (b) Protanal 200DL (M/G = 4:6); (c) Protanal 240D (M/G = 7:3).

To determine the surface areas of the materials, the **SG-Ba** were converted to the corresponding aerogels **AeG-Ba** by treatment of the samples with supercritical CO_2.[16a] The TGA profiles, performed under air, showed the typical behavior of the thermal degradation of alginate gels. Three main zones were found (Figure S3). The first zone, between 30 °C and 170 °C, corresponds to the loss of water in the samples. The second zone, between 150 °C and 250 °C, is due to the first step of degradation of the polysaccharide associated to the decomposition of the carboxylic groups. The third zone, between 250 °C and 400 °C, is mostly the further degradation of alginate likely related to the hydroxyl groups.[17] The decrease in the G quantity seems to be detrimental to the thermal stability of the gels. Using the initial mass value of each sample (after water loss), and the residual mass of $BaCO_3$, the weight percentages of barium in the **SG-Ba** were calculated (see Table S10). The values were found to be comparable for the three samples.

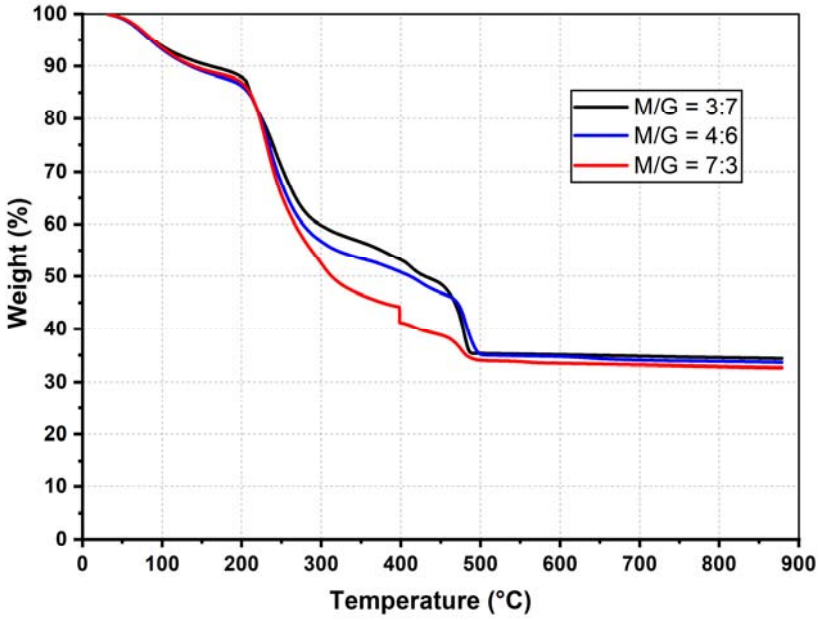

Figure S3. TGA profiles in air at 5 °C min^{-1} for **AeG-Ba** prepared from three alginates with different M/G ratios: Black line: Protanal 200S (M/G = 3:7); Blue line: Protanal 200DL (M/G = 4:6); Red line: Protanal 240D (M/G = 7:3).

The isotherms of adsorption and the specific surface area determination by BET method are shown in the Figure S4 and Table S10, respectively. The BET surface areas for the gels are in the range between 437 and 585 m^2g^{-1}.

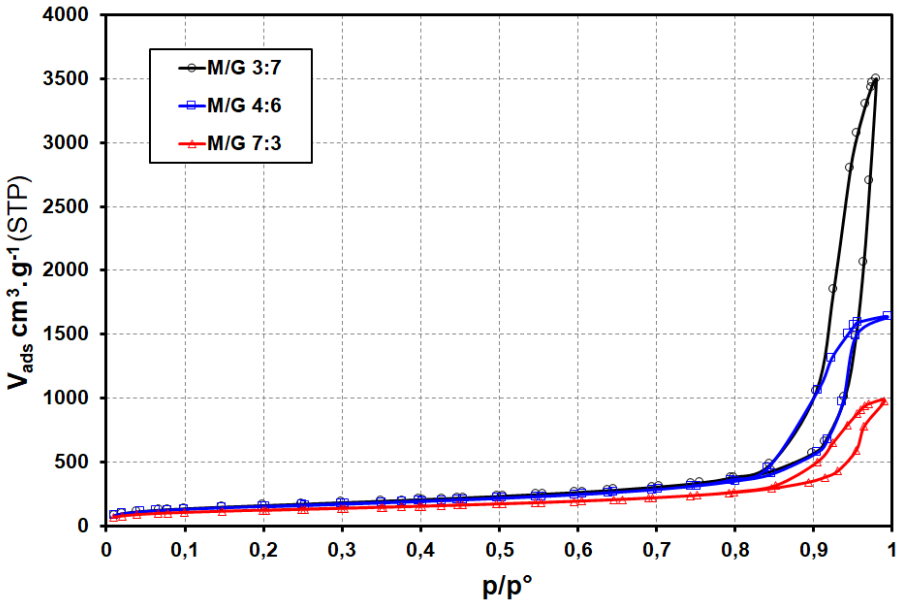

Figure S4. Isotherms of adsorption for **AeG-Ba** prepared from three alginates with different M/G ratios: Black line: Protanal 200S (M/G = 3:7); Blue line: Protanal 200DL (M/G = 4:6); Red line: Protanal 240D (M/G = 7:3).

Table S10. Results of the TGA analysis and BET area for barium alginate gels (**AeG-Ba**) with different M/G ratios.

Entry	Alginate (commercial name)	M/G ratio	Loss[a] [%]	wt Ba^{2+}[b] [%]	S_{BET}[c] [m^2g^{-1}]
1	Protanal 200S	3/7	61.8	26.6	585
2	Protanal 200DL	4/6	62.0	26.4	542
3	Protanal 240D	7/3	63.2	25.6	437

[a] Percentage of mass loss determined by TGA using as initial value the mass of each sample after H_2O loss. [b] Weight percentage of Barium in alginate beads determined by TGA. Residual phase: $BaCO_3$. [c] Determined using the BET method by means of N_2 adsorption/desorption measurement at -196 °C.

Representative procedure for the catalytic reaction

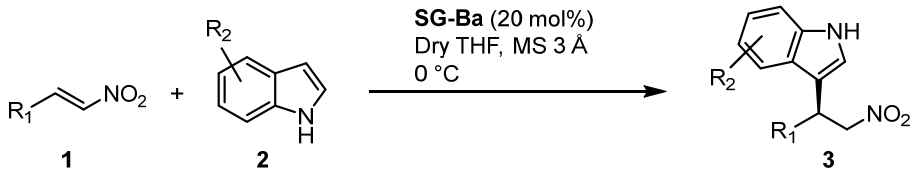

Eight **SG-Ba** beads soaked in EtOH, which correspond to 0.028 mmol of barium, were placed in a vial equipped with a magnetic stirring bar. Dry THF (ca. 3 mL) was then added, the vial capped and the mixture stirred gently for ca. 15 minutes. Excess THF was removed carefully by a Pasteur pipette. This operation was repeated five times, in order to achieve complete solvent exchange (EtOH → THF). Nitroalkene **1** (0.14 mmol), indole **2** (0.35 mmol, 2.5 equiv) were weighed in a test tube, and dissolved in dry THF (0.50 mL). After cooling the solution to 0 °C, the **SG-Ba** beads previously soaked in THF (8 beads, corresponding to 0.028 mmol of barium, 20 mol% catalyst loading) were added by means of a small spoon, followed by activated 3 Å MS (five small pellets, corresponding to ca. 200 mg). The tube was carefully capped and placed in an ice-filled Dewar container, which was placed in a fridge. The reaction was followed by TLC and, after the appropriate time, the tube was removed from the ice bath. The liquids of the mixture were filtered on a plug of silica gel into a flask by means of a Pasteur pipette. EtOAc (1-2 mL) was added to the test tube, and allowed standing with the solids (**SG-Ba** beads and molecular sieves) few minutes, with occasional manual stirring. The liquids were filtered and added to the the previous flask, as above, and the same operation repeated four times. The plug was flushed with EtOAc, and the solvents evaporated. The residue obtained was then purified by chromatography on silica gel (PE/EtOAc mixtures), affording the Friedel-Crafts adduct **3**.

Procedure for catalyst recovery and reuse

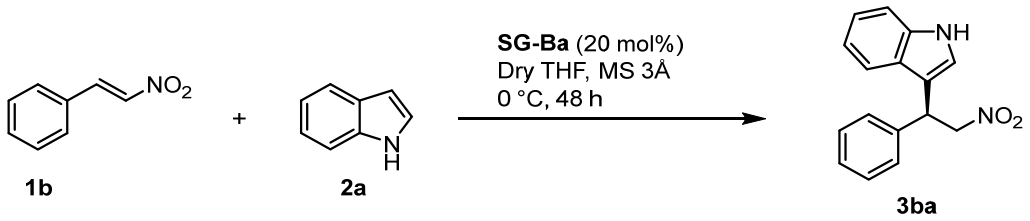

Eight **SG-Ba** beads soaked in EtOH, which correspond to 0.028 mmol of barium, were placed in a vial equipped with a magnetic stirring bar. Dry THF (ca. 3 mL) was then added, the vial capped and the mixture stirred gently for ca. 15 minutes. Excess THF was removed carefully by a Pasteur pipette. This operation was repeated five times, in order to achieve complete solvent exchange (EtOH → THF). Nitroalkene **1b** (20.9 mg, 0.14 mmol), indole **2a** (41.0 mg, 0.35 mmol, 2.5 equiv) were weighed in a test tube, and dissolved in dry THF (0.50 mL). After cooling the solution to 0 °C, the **SG-Ba** beads previously soaked in THF (8 beads, corresponding to 0.028 mmol of barium, 20 mol% catalyst loading) were added by means of a spoon, followed by activated 3 Å MS (five small pellets, corresponding to ca. 200 mg). The tube was carefully capped and placed in an ice-filled Dewar container, which was placed in a fridge. After 48 h, the tube was removed from the ice bath. The liquids of the mixture were filtered on a plug of silica gel into a flask by means of a Pasteur pipette. EtOH (1-2 mL) was added to the test tube, and allowed standing with the solids (**SG-Ba** beads and molecular sieves) few minutes, with occasional manual stirring. The liquids were filtered and added to the previous flask, as above, and the same operation repeated one more time. The plug was flushed with EtOAc, and the solvents evaporated. The residue obtained was analysed by ^{1}H NMR and chiral stationary phase HPLC to determine the conversion and enantiomeric excess, respectively. Molecular sieves were then removed from the test tube, the gel beads were soaked in THF by using the above protocol, and a new reaction cycle was set up using the same procedure of the first cycle.

Results of the catalytic reactions and characterization of products 3

(*S*)-3-(2-Nitro-1-(4-(trifluoromethyl)phenyl)ethyl)-1*H*-indole (3aa)

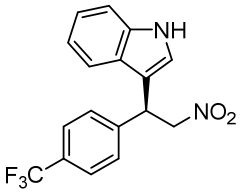

Following the general procedure (48 h reaction time), the title compound was obtained in 79% yield after chromatography on silica gel. The enantiomeric excess of the product was determined by CSP HPLC: ADH column, *n*-hexane/*i*-PrOH 90:10, 0.75 mL/min, t_{maj} = 26.5 min; t_{min} = 21.6 min, 87% ee. Spectral and optical data are in accordance with the literature.[18]

^{1}H NMR ($CDCl_3$, 400 MHz) δ= 8.15 (br s, 1H), 7.59 (d, J = 8.2 Hz, 2H), 7.47 (d, J = 8.4 Hz, 2H), 7.41 (dt, J = 8.1, 0.9 Hz, 1H), 7.38 (dt, J = 8.2, 0.9 Hz, 1H), 7.23 (ddd, J = 8.2, 7.1, 1.2 Hz, 1H), 7.10 (ddd, J = 8.0, 7.1, 1.0 Hz, 1H), 7.04 (dd, J = 2.6, 0.9 Hz, 1H), 5.26 (t, J = 8.0 Hz, 1H), 5.09 (dd, J = 12.7, 7.3 Hz, 1H), 4.97 (dd, J = 12.7, 8.7 Hz, 1H).

^{13}C NMR ($CDCl_3$, 101 MHz) δ= 143.2, 136.5, 129.9 (q, J = 32.6 Hz), 128.1, 125.9 (q, J = 3.8 Hz), 125.8, 124.0 (q, J = 274.6), 122.6, 121.6, 120.2, 118.7, 113.6, 111.5, 79.0, 41.3.

^{19}F NMR ($CDCl_3$, 376 MHz) δ= -62.6 (s, 3F).

$[\alpha]_D^{RT}$ = +1.4 (c = 0.5, $CHCl_3$).

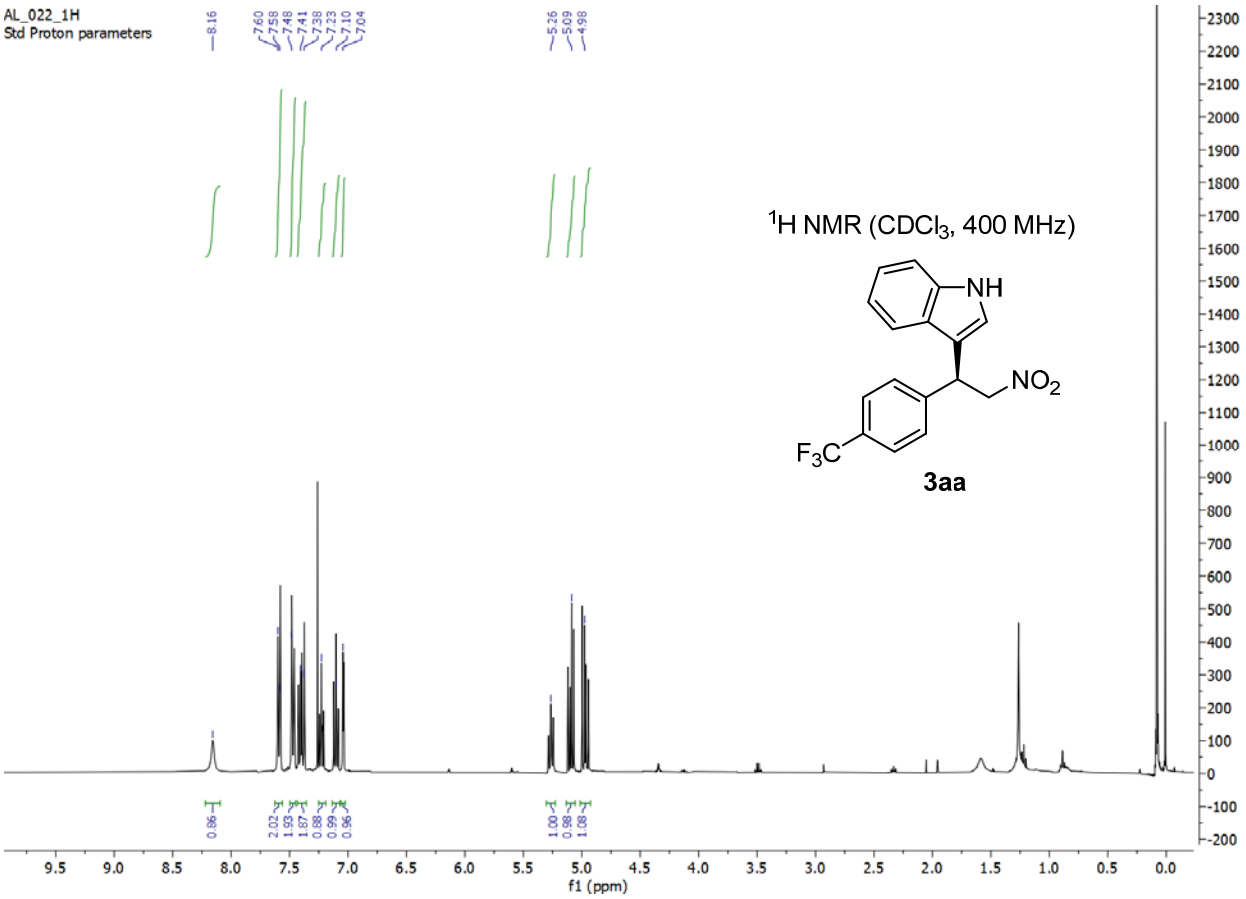
AL_022_1H
Std Proton parameters
^{1}H NMR ($CDCl_3$, 400 MHz)
NH
NO_2
F_3C
3aa
f1 (ppm)

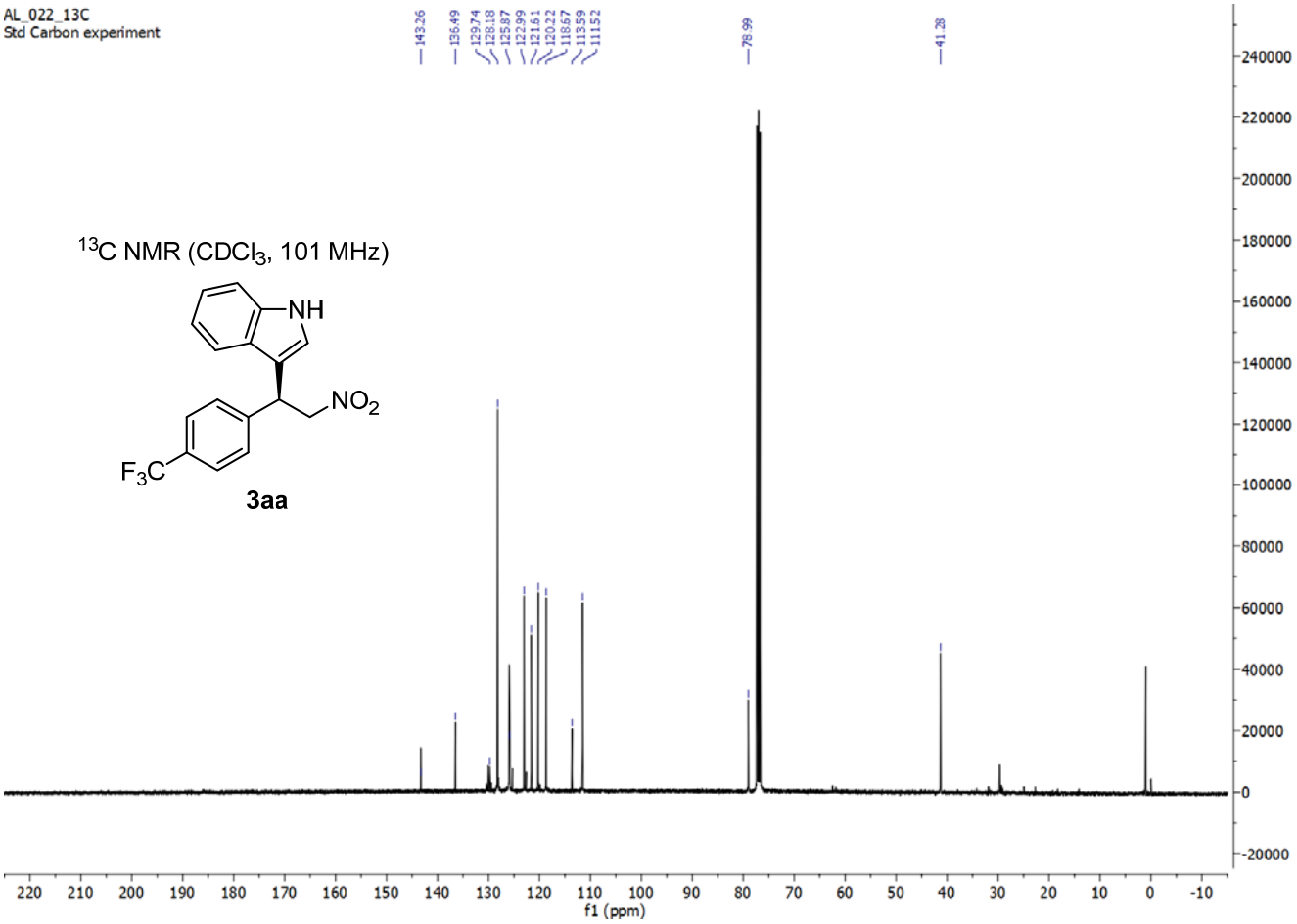
AL_022_13C
Std Carbon experiment
^{13}C NMR ($CDCl_3$, 101 MHz)
NH
NO_2
F_3C
3aa
f1 (ppm)

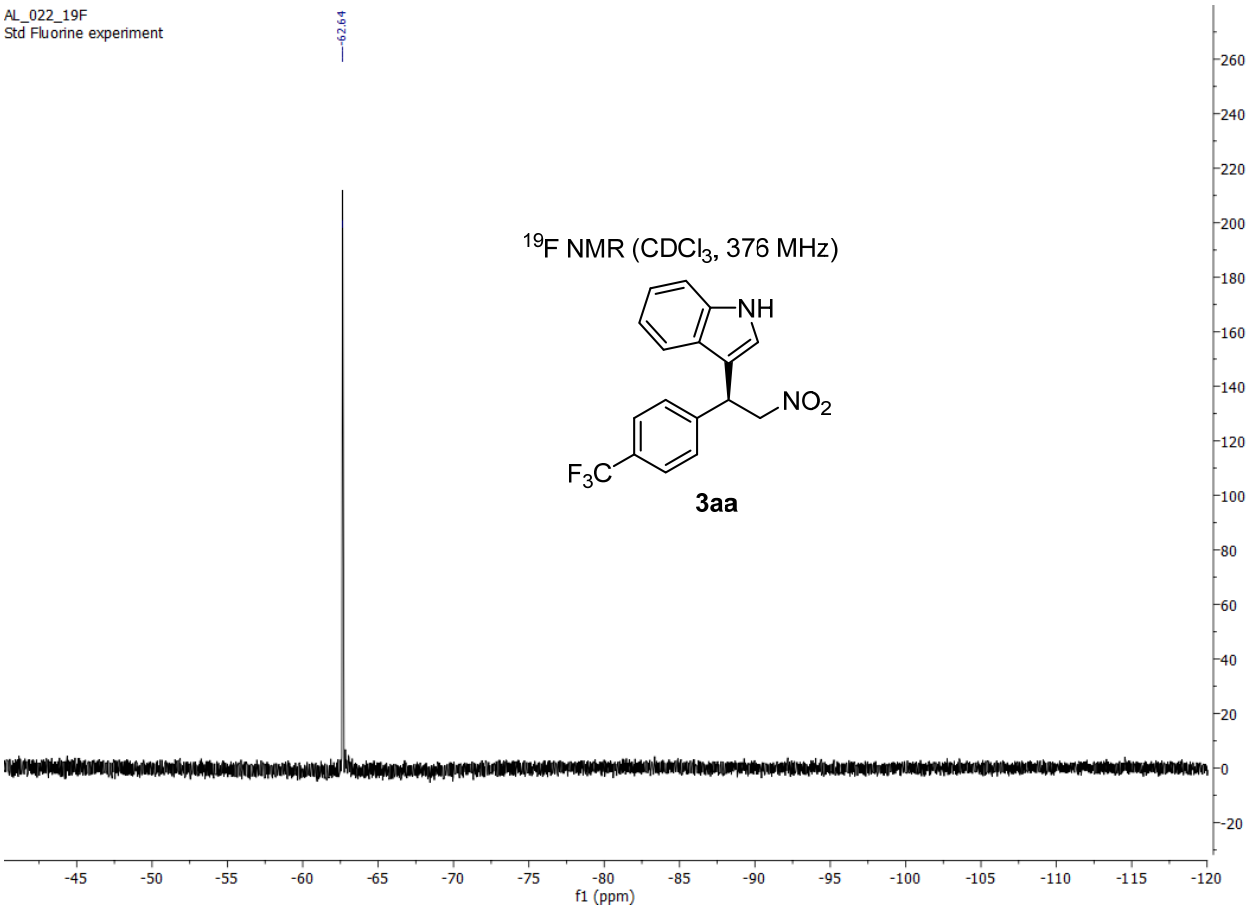
AL_022_19F
Std Fluorine experiment
-62.64
^{19}F NMR ($CDCl_3$, 376 MHz)
NH
NO_2
F_3C
3aa
260
240
220
200
180
160
140
120
100
80
60
40
20
0
-20
-45
-50
-55
-60
-65
-70
-75
-80
-85
-90
-95
-100
-105
-110
-115
-120
f1 (ppm)

HPLC traces of compounds *rac*-3aa and 3aa.

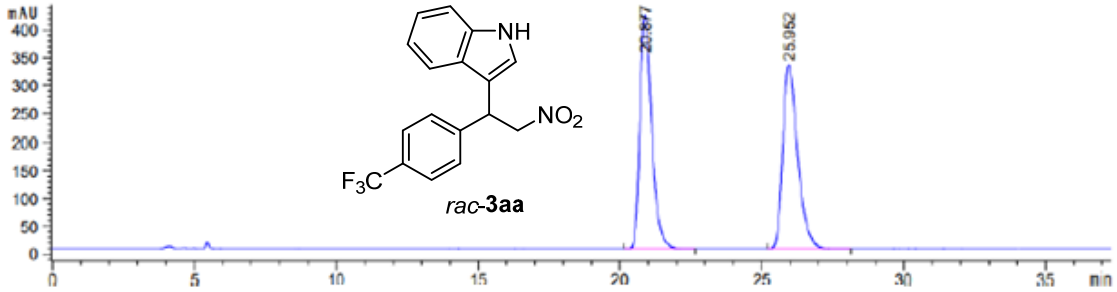

Peak #	RetTime [min]	Type	Width [min]	Area [mAU*s]	Height [mAU]	Area %
1	20.877	BB	0.4401	1.20268e4	415.02301	49.9916
2	25.952	BB	0.5607	1.20309e4	327.42154	50.0084

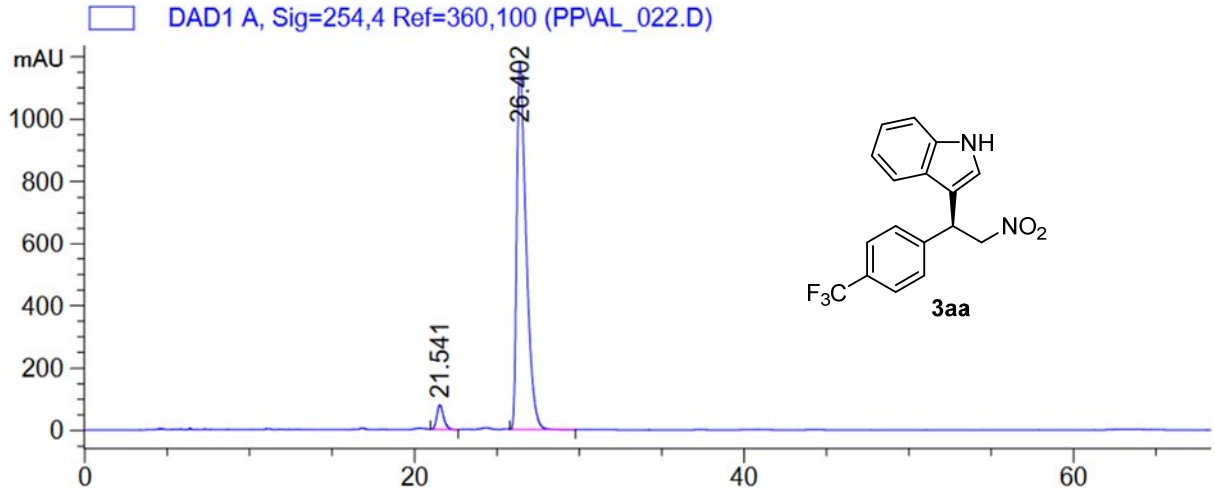

Signal 1: DAD1 A, Sig=254,4 Ref=360,100

Peak #	RetTime [min]	Type	Width [min]	Area [mAU*s]	Height [mAU]	Area %
1	21.541	VB	0.4410	2302.75806	79.70985	6.4968
2	26.397	MM T	0.5347	3.31418e4	1032.93872	93.5032
Totals :				3.54446e4	1112.64857	

(*S*)-5-Methyl-3-(2-nitro-1-(4-(trifluoromethyl)phenyl)ethyl)-1*H*-indole (3ab)

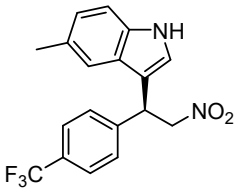

Following the general procedure (72 h reaction time), the title compound was obtained in 50% yield after chromatography on silica gel. The enantiomeric excess of the product was determined by CSP HPLC: ADH column, *n*-hexane/*i*-PrOH 90:10, 0.75 mL/min, t_{maj} = 21.0 min; t_{min} = 15.6 min, 89% ee.

^{1}H NMR ($CDCl_3$, 400 MHz) δ= 8.06 (br s, 1H), 7.60 (d, J = 8.0 Hz, 2H), 7.48 (d, J = 8.4 Hz, 2H), 7.27 (d, J = 8.1 Hz, 1H), 7.22 (m, 1H), 7.06 (dd, J = 8.3, 1.6 Hz, 1H), 6.98 (dd, J = 2.5, 0.9 Hz, 1H), 5.24 (dd, J = 8.8, 7.2 Hz, 1H), 5.08 (dd, J = 12.7, 7.1 Hz, 1H), 4.96 (dd, J = 12.7, 8.9 Hz, 1H), 2.42 (s, 3H).

^{13}C NMR ($CDCl_3$, 101 MHz) δ= 143.3, 134.8, 129.8 (q, J = 33.8 Hz), 129.6, 128.1, 126.0, 125.1 (q, J = 1.3 Hz), 124.6, 123.9 (q, J = 273.0 Hz) , 121.8, 118.2, 113.0, 111.2, 78.9, 41.2, 21.5.

^{19}F NMR ($CDCl_3$, 376 MHz) δ= -62.6 (s, 3F).

$[\alpha]_D^{RT}$ = -12.1 (c = 0.5, CH_2Cl_2).

HRMS (ESI) m/z: [M - H]+ Calculated for $C_{18}H_{15}F_3N_2O_2$ = 347.1007; Found = 347.1019.

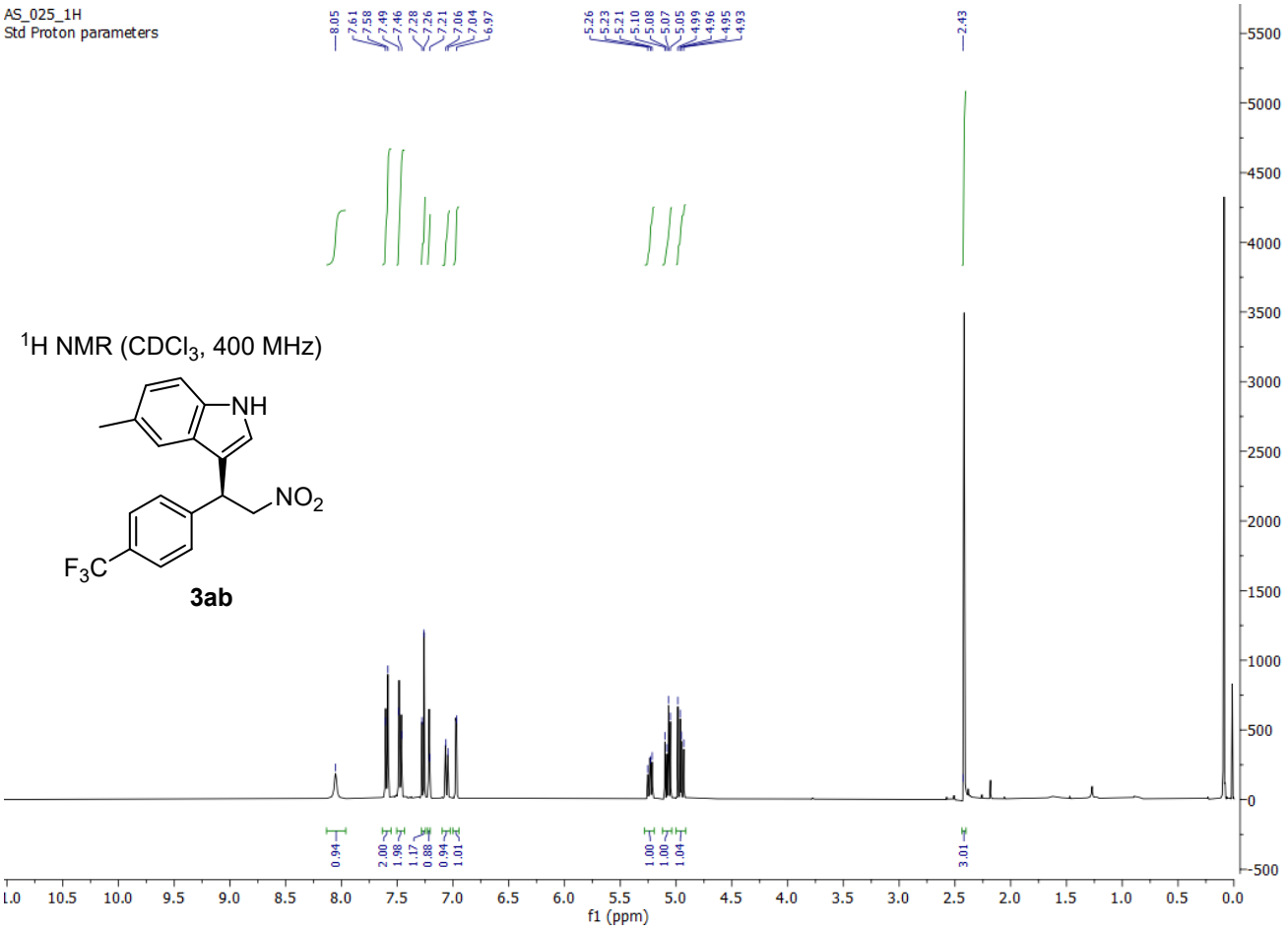

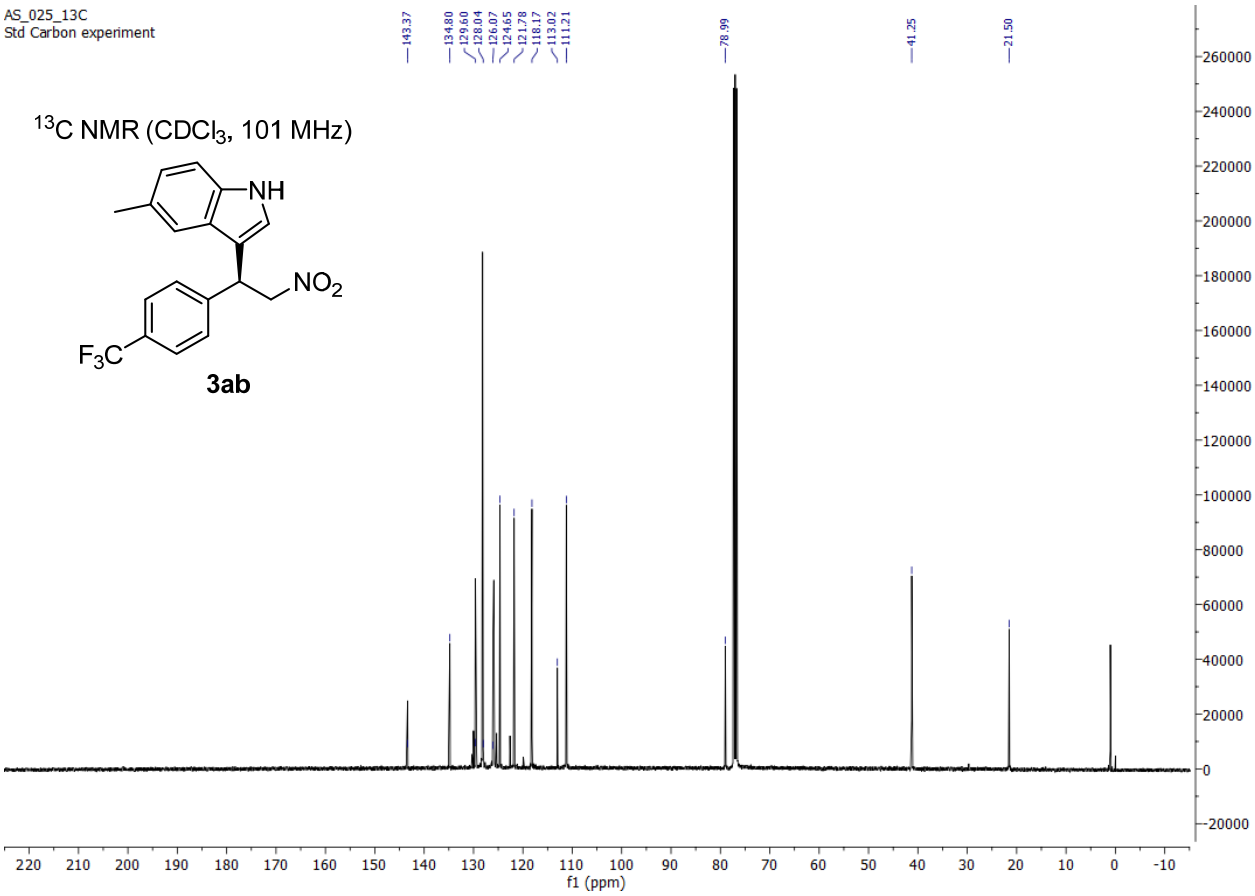

^{13}C NMR ($CDCl_3$, 101 MHz)

3ab

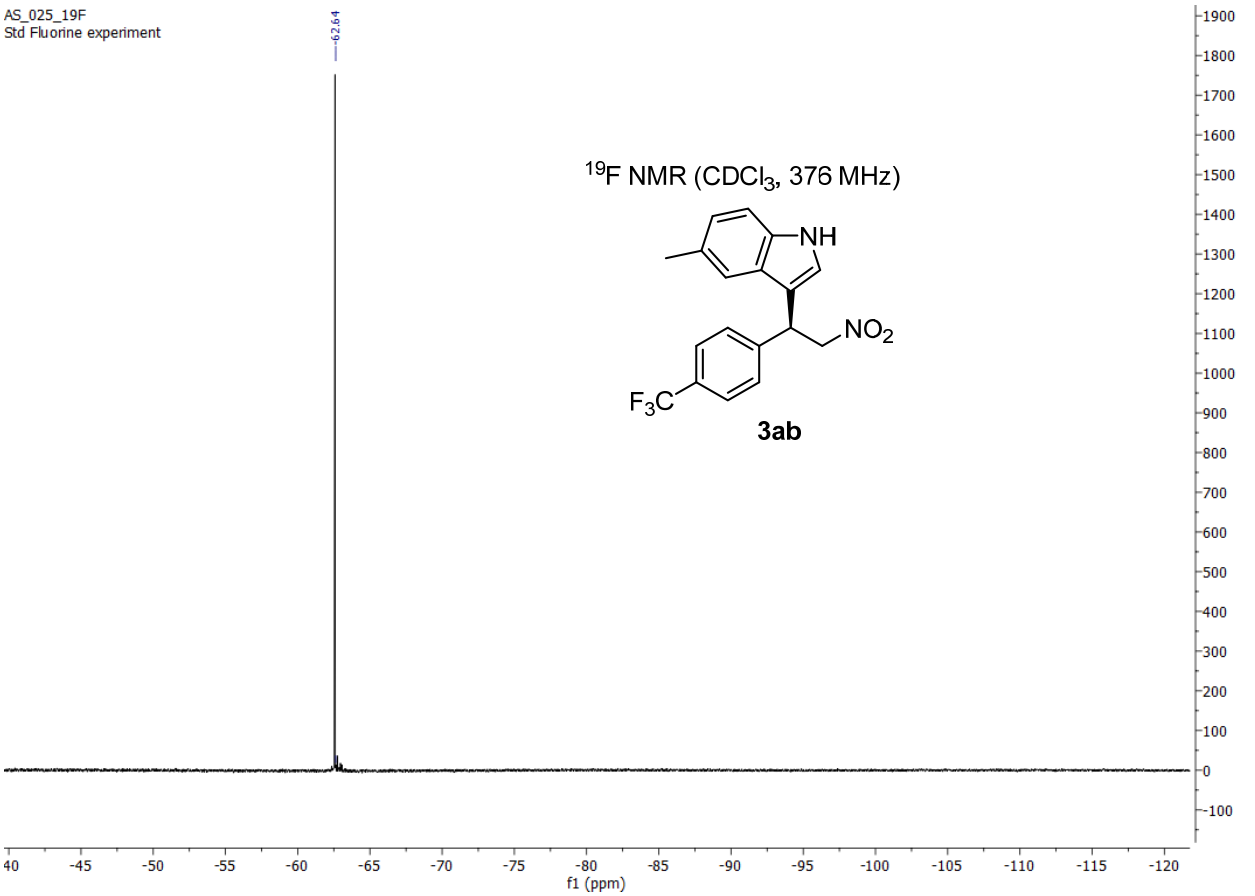

^{19}F NMR ($CDCl_3$, 376 MHz)

3ab

HPLC traces of compounds *rac*-3ab and 3ab.

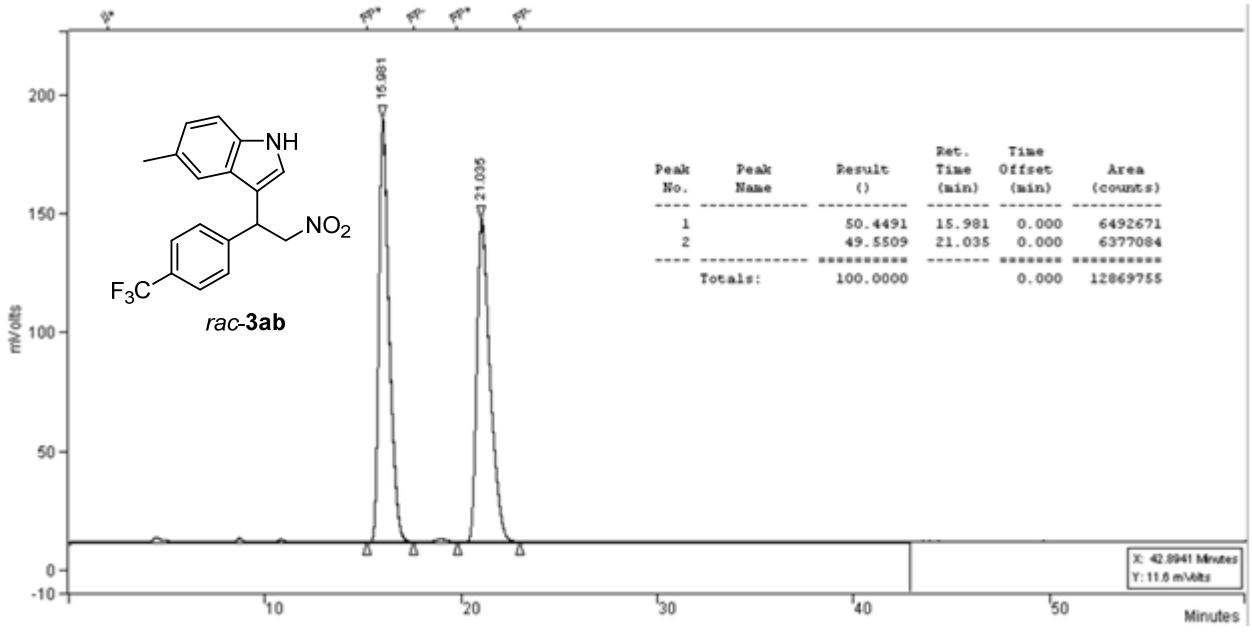

Peak No.	Peak Name	Result ()	Ret. Time (min)	Time Offset (min)	Area (counts)
1		50.4491	15.981	0.000	6492671
2		49.5509	21.035	0.000	6377084
	Totals:	100.0000		0.000	12869755

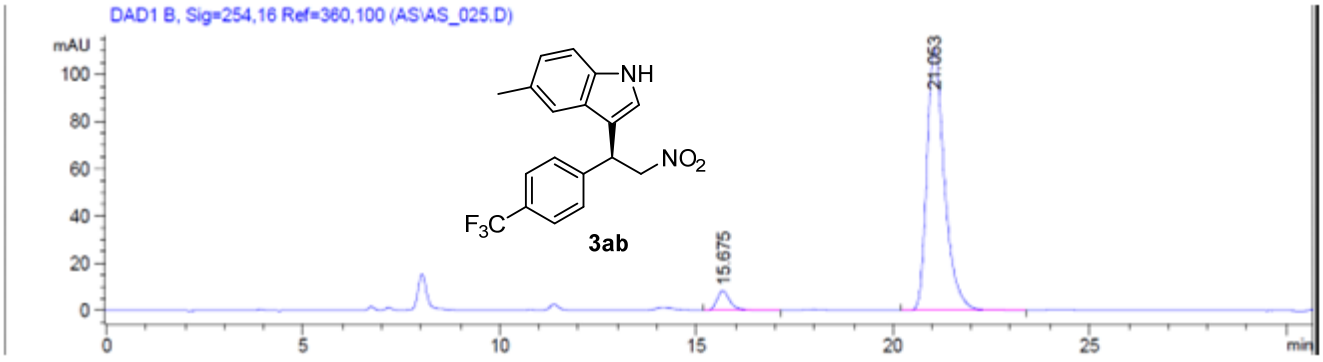

Signal 2: DAD1 B, Sig=254,16 Ref=360,100

Peak #	RetTime [min]	Type	Width [min]	Area [mAU*s]	Height [mAU]	Area %
1	15.675	BB	0.3494	192.80396	8.35000	5.3107
2	21.053	BB	0.4739	3437.68726	110.82967	94.6893
Totals :				3630.49121	119.17968	

(*S*)-5-Methoxy-3-(2-nitro-1-(4-(trifluoromethyl)phenyl)ethyl)-1*H*-indole (3ac)

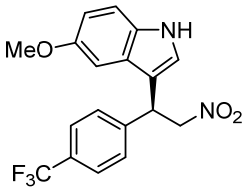

Following the general procedure but using 1.5 equiv of indole **2c** (48 h reaction time), the title compound was obtained in 61% yield after chromatography on silica gel. The enantiomeric excess of the product was determined by CSP HPLC: ADH column, *n*-hexane/*i*-PrOH 80:20, 0.75 mL/min, t_{maj} = 14.4 min; t_{min} = 10.9 min, 82% ee.

^{1}H NMR ($CDCl_3$, 400 MHz) δ= 8.06 (br s, 1H), 7.59 (d, J = 9.1 Hz, 2H), 7.47 (d, J = 9.1 Hz, 2H), 7.26 (d, J = 8.9 Hz, 1H), 7.00 (d, J = 3.0 Hz, 1H), 6.88 (dd, J = 8.8, 2.4 Hz, 1H), 6.80 (d, J = 2.4 Hz, 1H), 5.21 (t, J = 7.9 Hz, 1H), 5.07 (dd, J = 12.7, 7.2 Hz, 1H), 4.95 (dd, J = 12.7, 8.7 Hz, 1H), 3.78 (s, 3H).

^{13}C NMR ($CDCl_3$, 101 MHz) δ= 154.4, 143.3, 131.6, 129.9 (q, J = 32.5 Hz), 128.8, 126.3, 125.9 (q, J = 4.0 Hz), 124.0 (q, J = 272.7 Hz), 122.3, 113.2, 113.0, 112.2, 100.6, 79.0, 55.8, 41.3.

^{19}F NMR ($CDCl_3$, 376 MHz) δ= -62.6 (s, 3F).

$[\alpha]_D^{RT}$ = -25.6 (c = 0.5, CH_2Cl_2).

HRMS (ESI) m/z: [M - H]+ Calculated for $C_{18}H_{14}F_3N_2O_3$= 363.0957; Found=363.0966.

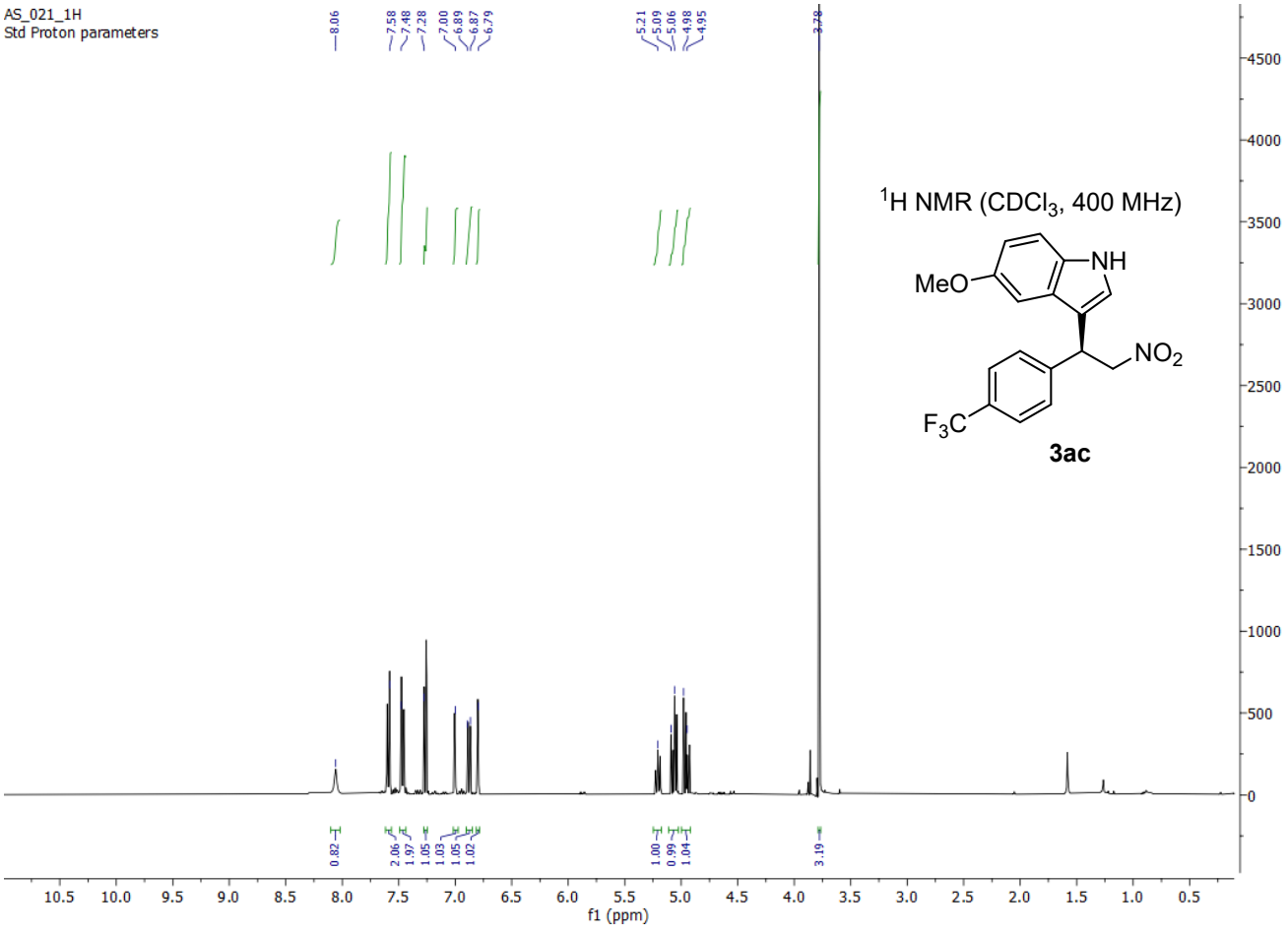

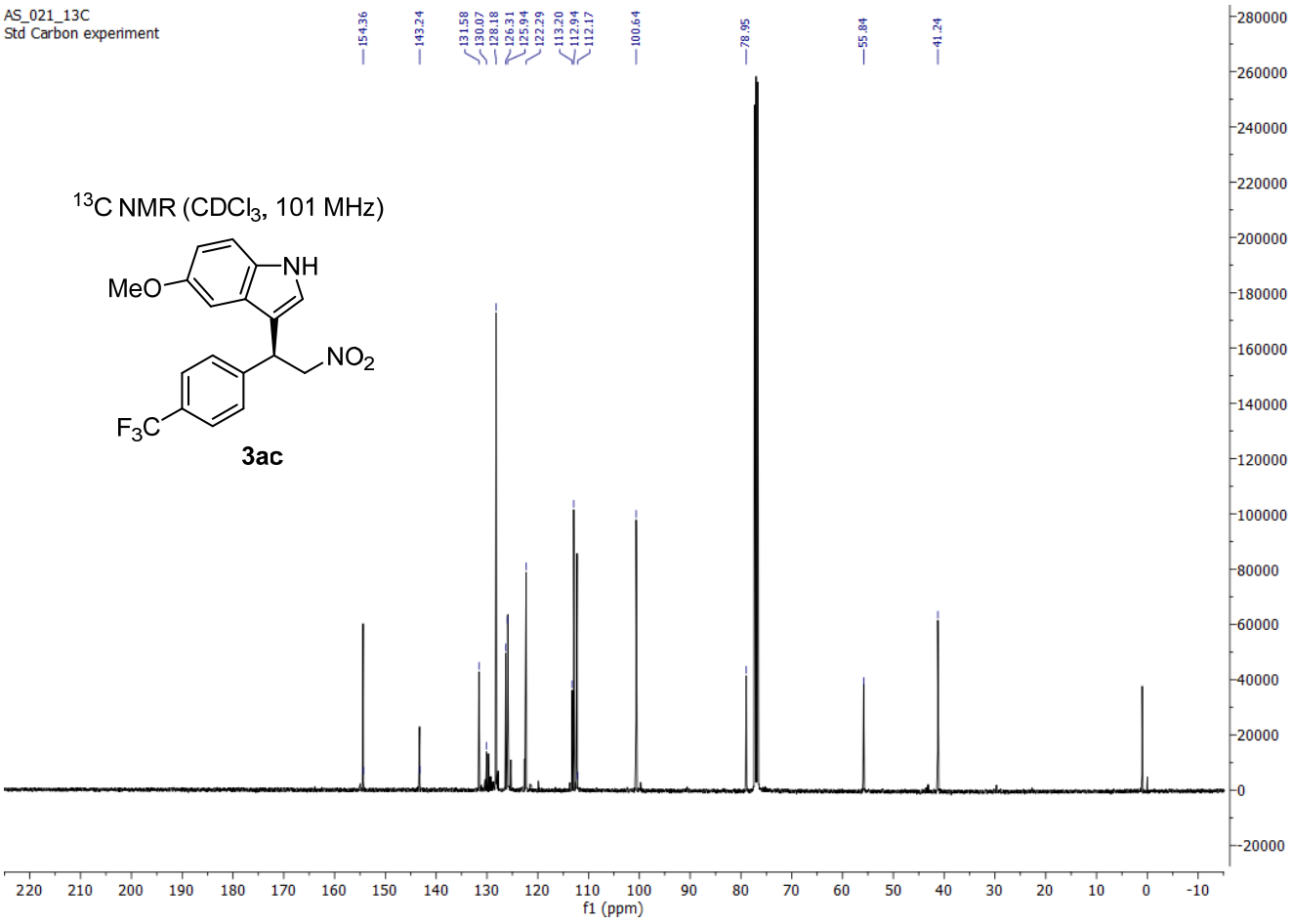
AS_021_13C
Std Carbon experiment
154.36
143.24
131.58
130.07
128.18
126.31
125.94
122.29
113.20
112.94
112.17
100.64
78.95
55.84
41.24
^{13}C NMR ($CDCl_3$, 101 MHz)
MeO
NH
NO_2
F_3C
3ac
f1 (ppm)

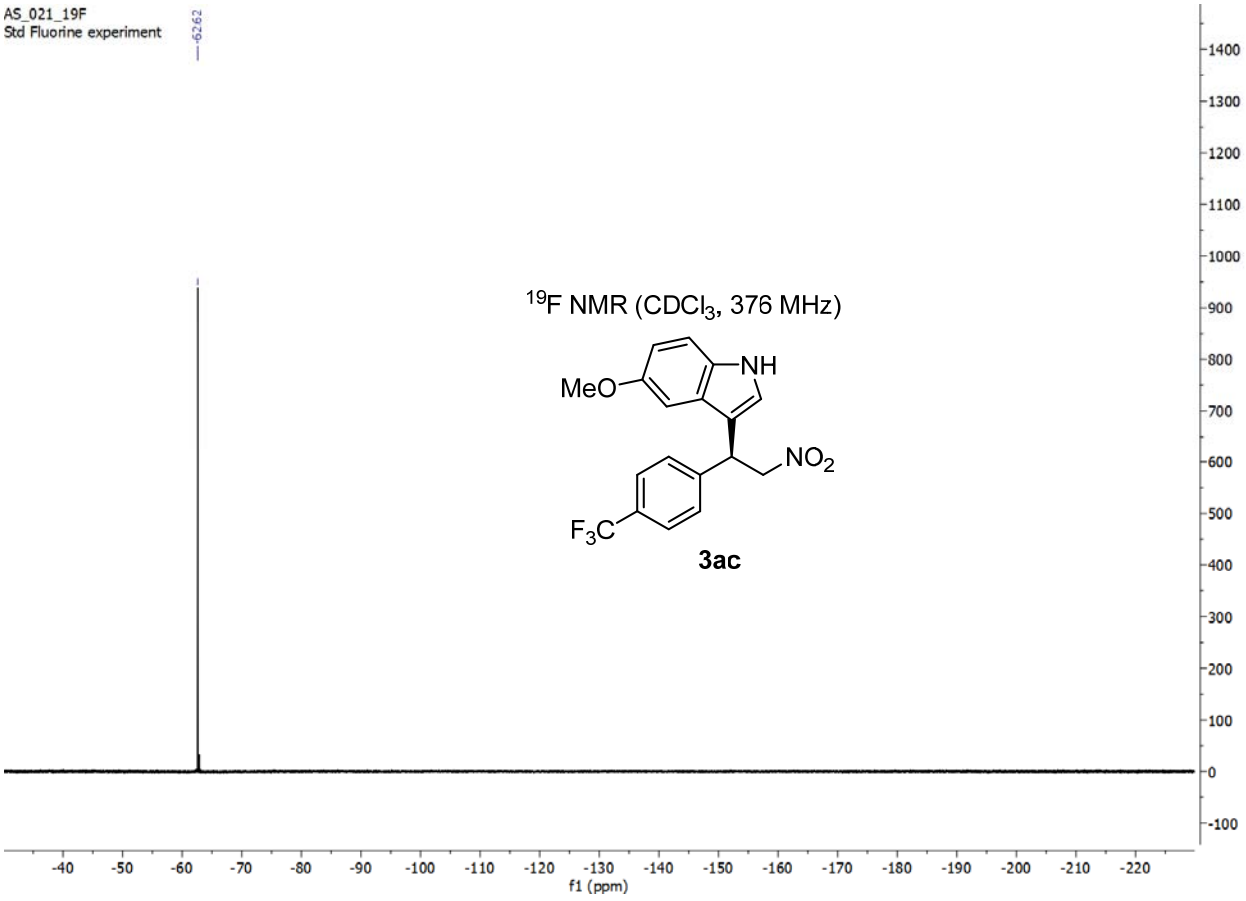
AS_021_19F
Std Fluorine experiment
-62.62
^{19}F NMR ($CDCl_3$, 376 MHz)
MeO
NH
NO_2
F_3C
3ac
f1 (ppm)

HPLC traces of compounds *rac*-3ac and 3ac.

Sample Info : SC_005, hex.iso 80-20; 0.75 ml/min AD-H

Additional Info : Peak(s) manually integrated

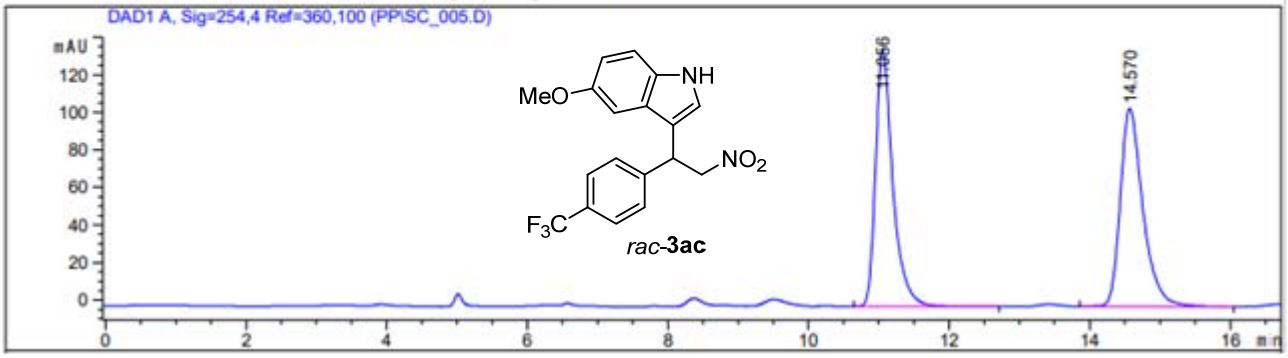

Signal 1: DAD1 A, Sig=254,4 Ref=360,100

Peak #	RetTime [min]	Type	Width [min]	Area [mAU*s]	Height [mAU]	Area %
1	11.056	BB	0.2596	2338.34326	136.66438	49.8124
2	14.570	BB	0.3368	2355.95459	105.41183	50.1876
Totals :				4694.29785	242.07621	

Sample Info : AS_021_80-20, 0,75 mL/min, 80:20 hex:ipr, 25°C, AD-H

Additional Info : Peak(s) manually integrated

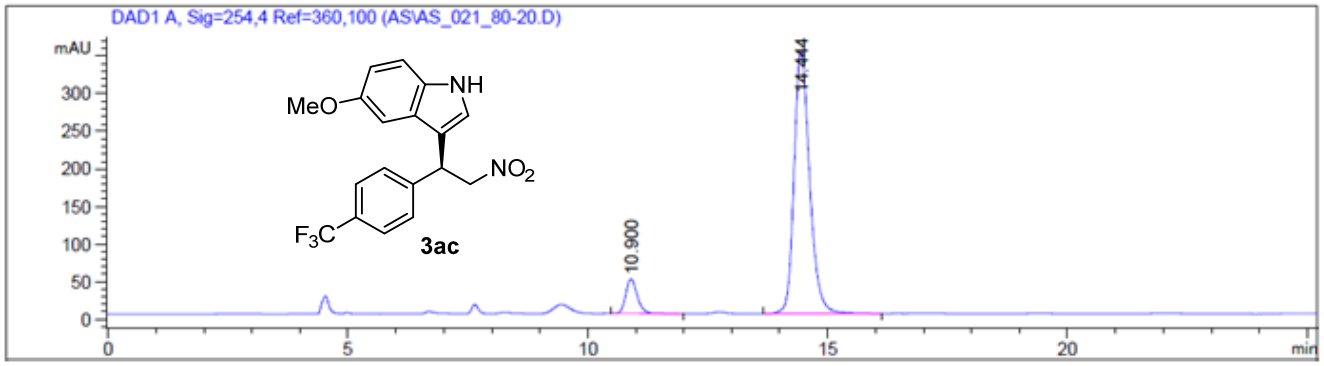

Signal 1: DAD1 A, Sig=254,4 Ref=360,100

Peak #	RetTime [min]	Type	Width [min]	Area [mAU*s]	Height [mAU]	Area %
1	10.900	BB	0.2545	771.70526	46.28243	8.8800
2	14.444	BB	0.3456	7918.64502	350.48914	91.1200
Totals :				8690.35028	396.77156	

(*S*)-5-Chloro-3-(2-nitro-1-(4-(trifluoromethyl)phenyl)ethyl)-1*H*-indole (3ad)

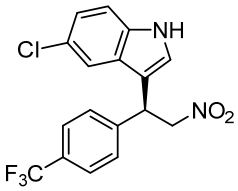

Following the general procedure (72 h reaction time), the title compound was obtained in 45% yield after chromatography on silica gel. The enantiomeric excess oft he product was determined by CSP HPLC: ADH column, *n*-hexane/*i*-PrOH 80:20, 0.75 mL/min, t_{maj} = 22.4 min; t_{min} = 17.8 min, 85% ee.

^{1}H NMR ($CDCl_3$, 400 MHz) δ= 8.21 (br s, 1H), 7.58 (d, J = 8.3 Hz, 2H), 7.42 (d, J = 8.6 Hz, 2H), 7.35 (dt, J = 1.9, 0.7 Hz, 1H), 7.29 – 7.22 (m, 1H), 7.15 (ddd, J = 8.5, 2.0, 0.4 Hz, 1H), 7.07 (dd, J = 2.6, 0.9 Hz, 1H), 5.18 (t, J = 8.0 Hz, 1H), 5.03 (dd, J = 12.7, 7.7 Hz, 1H), 4.92 (dd, J = 12.7, 8.3 Hz, 1H).

^{13}C NMR ($CDCl_3$, 101 MHz) δ= 142.8, 134.8, 133.4, 130.1 (q, J = 32.7 Hz), 128.1, 126.9, 126.1 (q, J = 3.7 Hz), 125.2 (q, J = 271.1 Hz), 123.4, 122.9, 118.1, 113.3, 112.6, 78.6, 41.0.

^{19}F NMR ($CDCl_3$, 376 MHz) δ= -62.6 (s, 3F).

$[\alpha]_D^{RT}$ = -4.0 (c = 0.5, CH_2Cl_2).

HRMS (ESI) m/z: [M - H]+ Calculated for $C_{17}H_{11}ClF_3N_2O_2$= 367.0461; Found=367.0476.

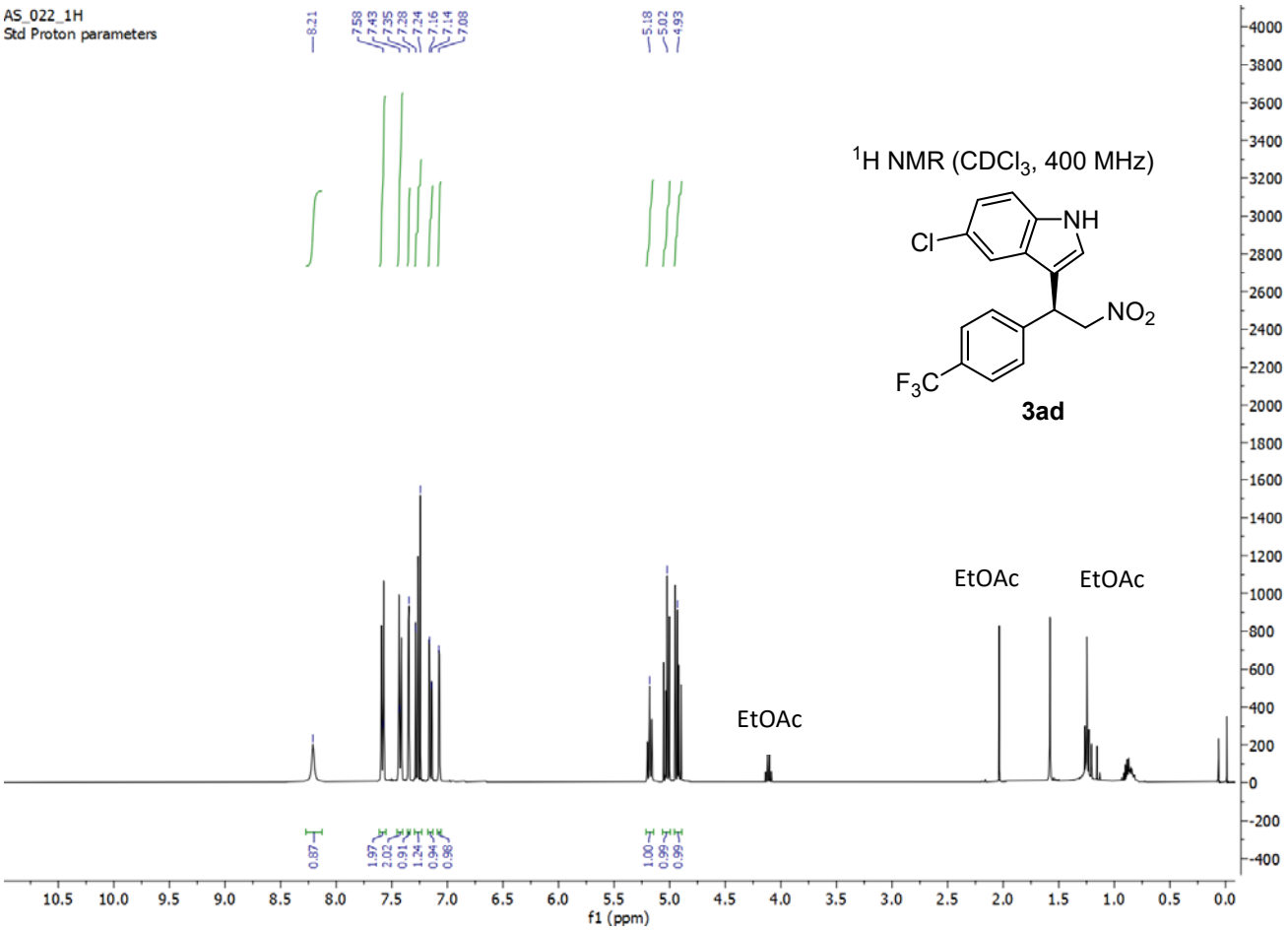

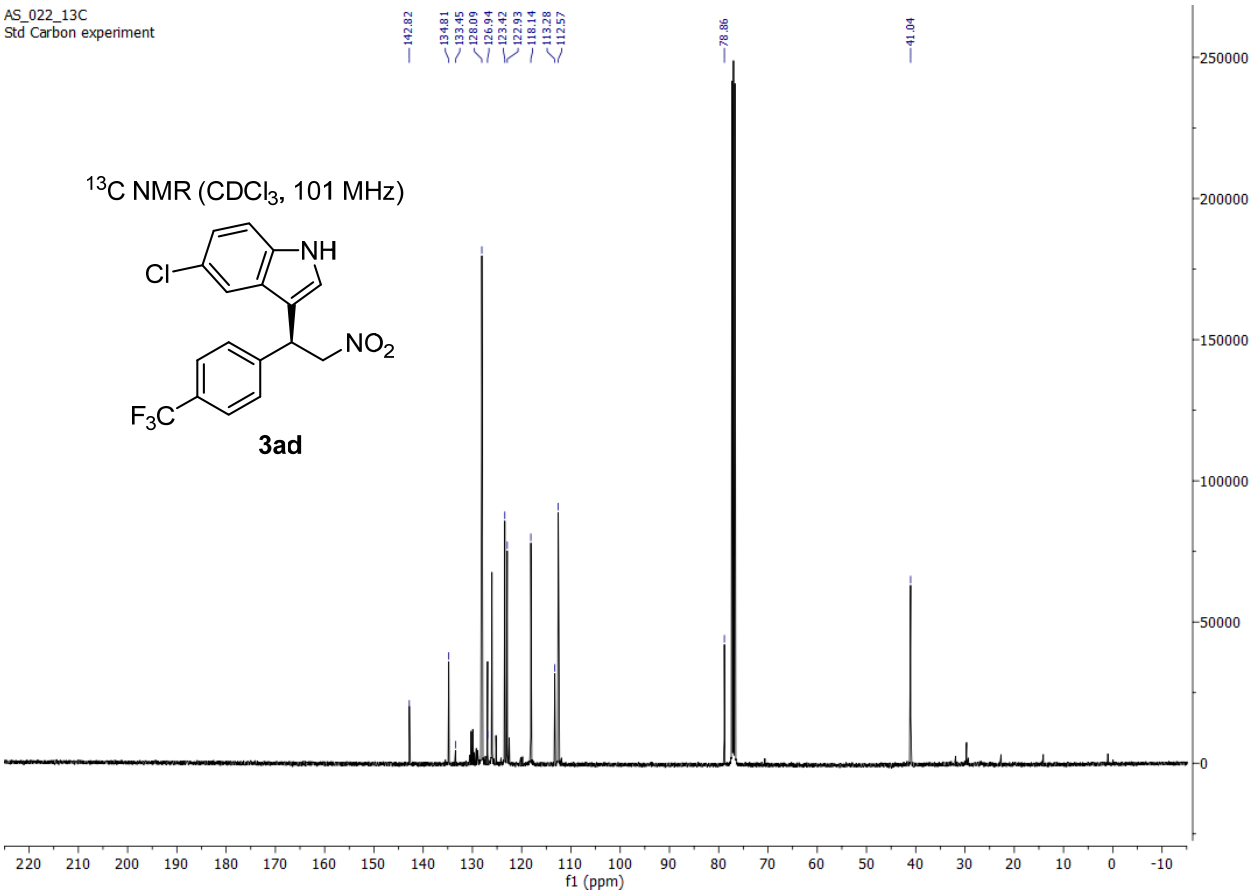

^{13}C NMR ($CDCl_3$, 101 MHz)

3ad

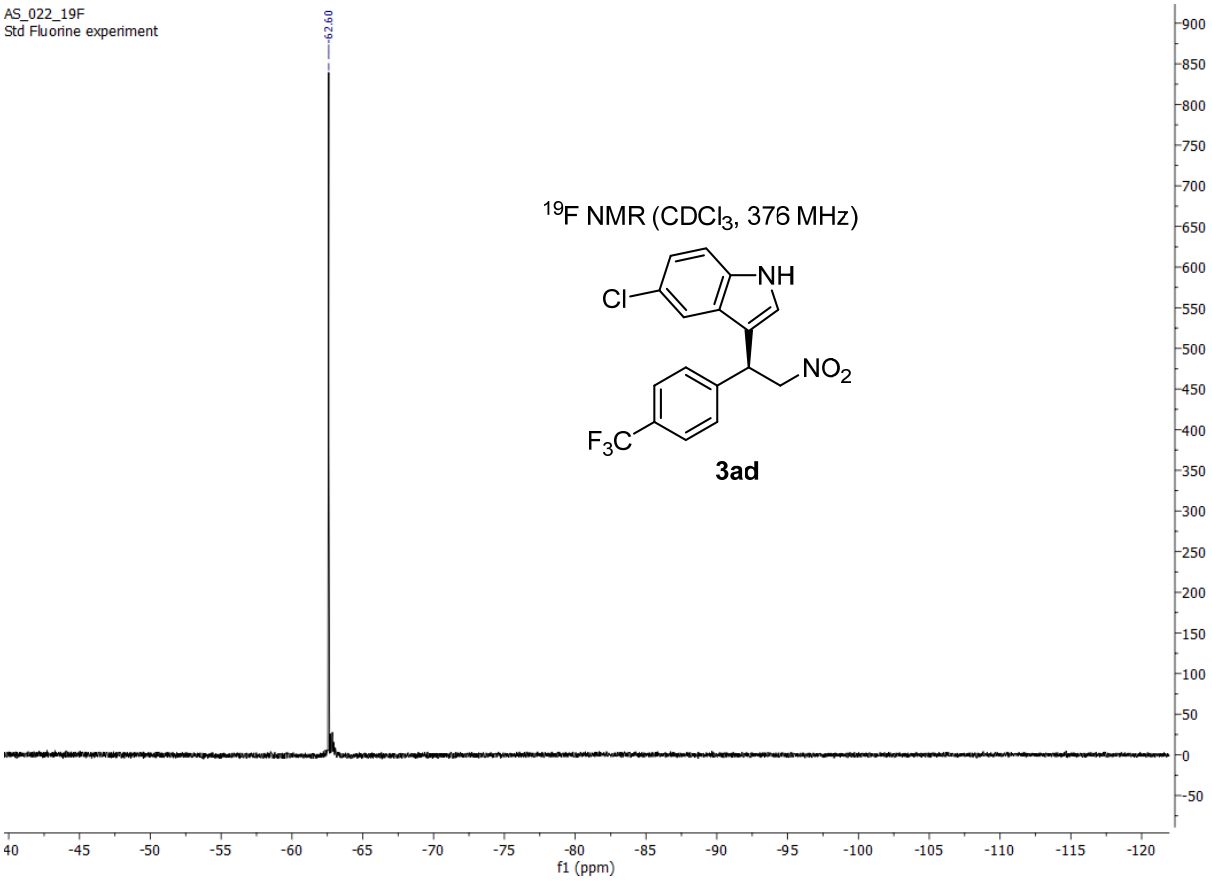

^{19}F NMR ($CDCl_3$, 376 MHz)

3ad

HPLC traces of compounds *rac*-3ad and 3ad.

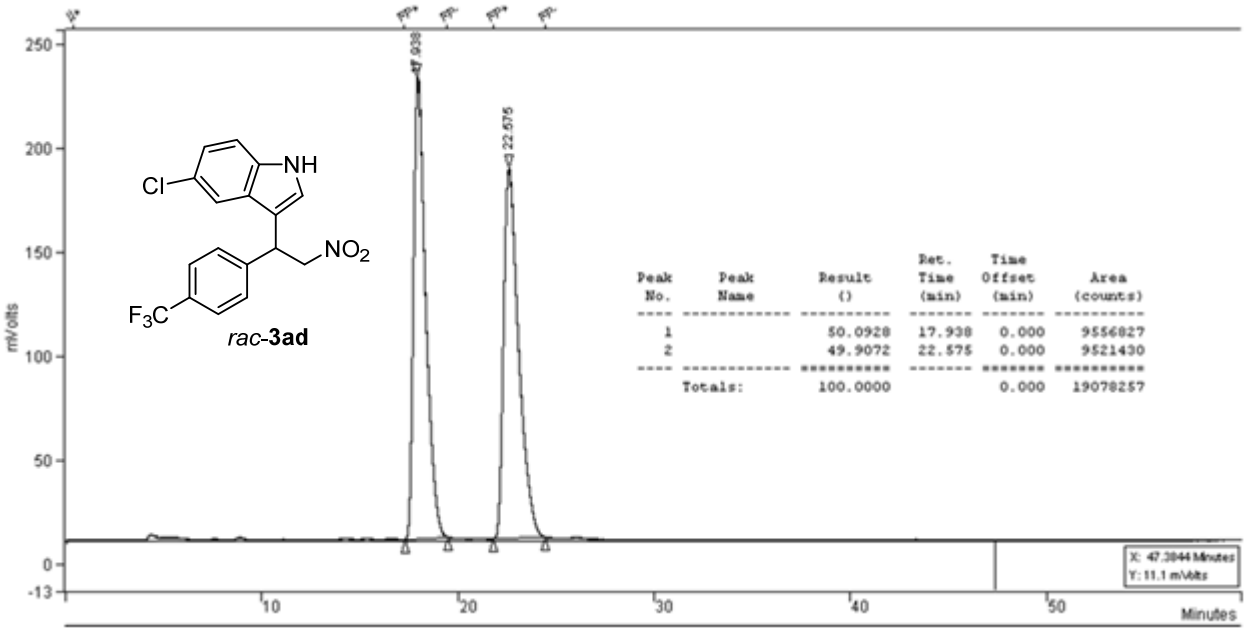

Peak No.	Peak Name	Result ()	Ret. Time (min)	Time Offset (min)	Area (counts)
1		50.0928	17.938	0.000	9556827
2		49.9072	22.575	0.000	9521430
Totals:		100.0000		0.000	19078257

Sample Info : AS_032, 0,750 mL/min, 90:10 hex:ipr, 25°C, AD-H

Additional Info : Peak(s) manually integrated

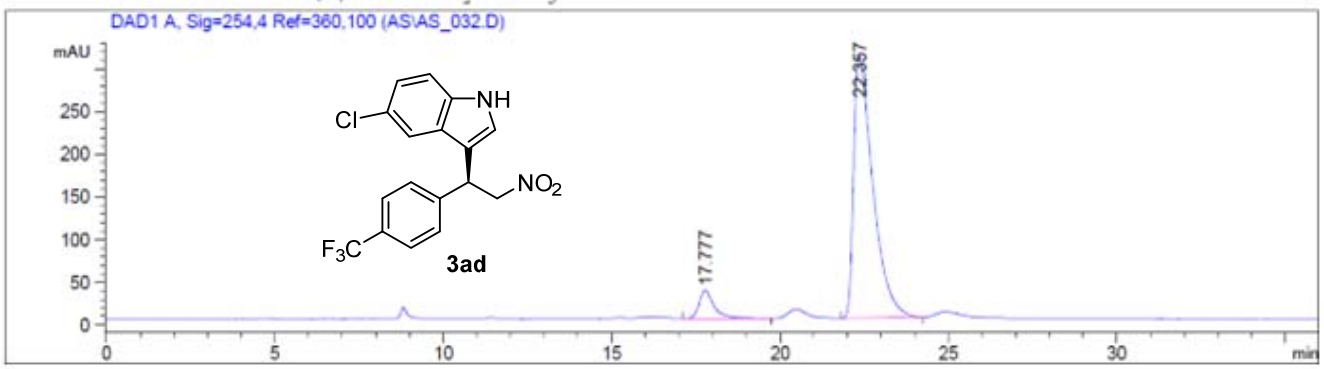

Signal 1: DAD1 A, Sig=254,4 Ref=360,100

Peak #	RetTime [min]	Type	Width [min]	Area [mAU*s]	Height [mAU]	Area %
1	17.777	BB	0.4583	1019.33942	32.82515	7.7142
2	22.357	BB	0.5878	1.21944e4	308.07144	92.2858
Totals :				1.32138e4	340.89659	

(*S*)-4-Methyl-3-(2-nitro-1-(4-(trifluoromethyl)phenyl)ethyl)-1*H*-indole (3ae)

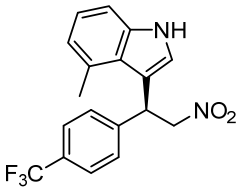

Following the general procedure (72 h reaction time), the title compound was obtained in 55% yield after chromatography on silica gel. The enantiomeric excess of the product was determined by CSP HPLC: ADH column, *n*-hexane/*i*-PrOH 90:10, 0.75 mL/min, t_{maj} = 19.4 min; t_{min} = 17.1 min, 85% ee.

^{1}H NMR ($CDCl_3$, 400 MHz) δ= 8.19 (br s, 1H), 7.58 (d, J = 9.5 Hz, 2H), 7.40 (d, J = 8.4 Hz, 2H), 7.23 (d, J = 8.2 Hz, 1H), 7.14 – 7.06 (m, 2H), 6.83 (d, J = 7.1 Hz, 1H), 5.62 (t, J = 8.1 Hz, 1H), 5.00 (dd, J = 12.8, 8.1 Hz, 1H), 4.87 (dd, J = 12.8, 8.0 Hz, 1H), 2.55 (s, 3H).

^{13}C NMR ($CDCl_3$, 101 MHz) δ= 144.3, 136.9, 130.4, 129.8 (q, J = 32.4 Hz), 128.5, 126.0 (q, J = 3.8 Hz), 124.8, 123.9 (q, J = 271.5 Hz), 123.1, 122.1, 121.6, 113.9, 109.4, 79.9, 41.9, 20.5.

^{19}F NMR ($CDCl_3$, 376 MHz) δ= -62.6 (s, 3F)

$[\alpha]_D^{RT}$ = +51.0 (c = 0.5, CH_2Cl_2).

HRMS (ESI) m/z: [M - H]+ Calculated for $C_{18}H_{15}F_3N_2O_2$= 347.1007; Found=347.1023

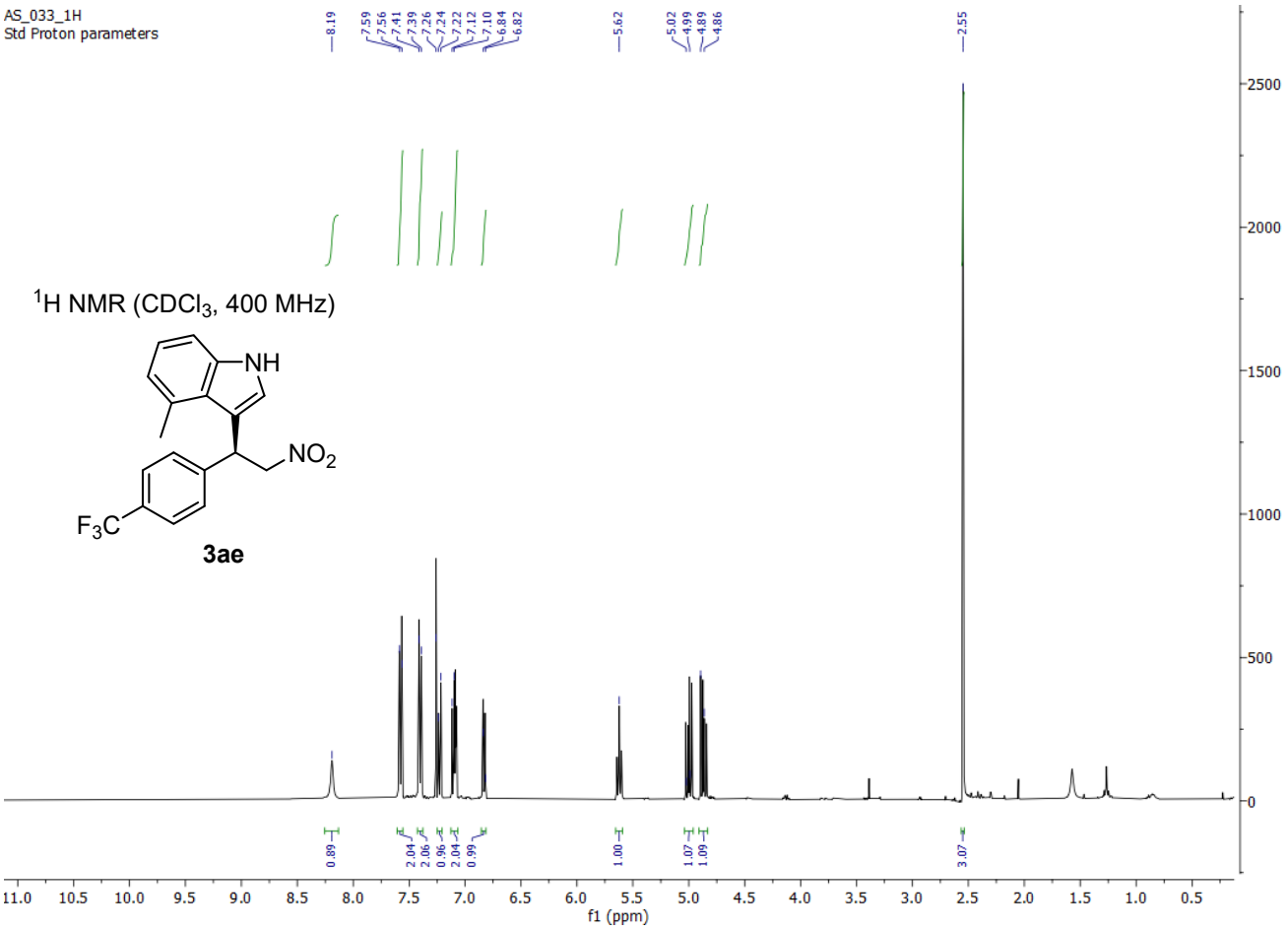

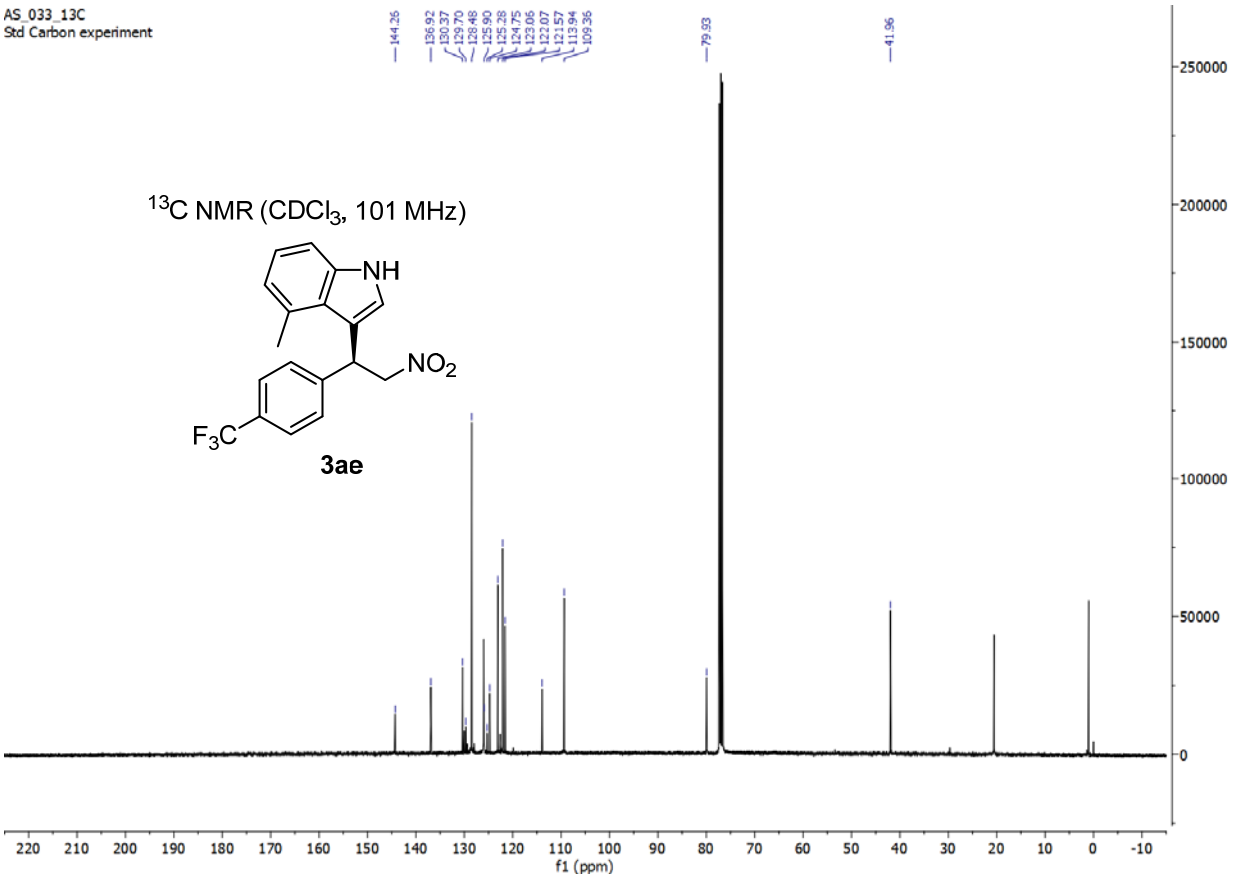
AS_033_13C
Std Carbon experiment
144.26
136.92
130.37
129.70
128.48
125.90
125.28
124.75
123.06
122.07
121.57
113.94
109.36
79.93
41.96
250000
200000
150000
100000
50000
0
220 210 200 190 180 170 160 150 140 130 120 110 100 90 80 70 60 50 40 30 20 10 0 -10
f1 (ppm)
13C NMR (CDCl3, 101 MHz)
NH
NO2
F3C
3ae

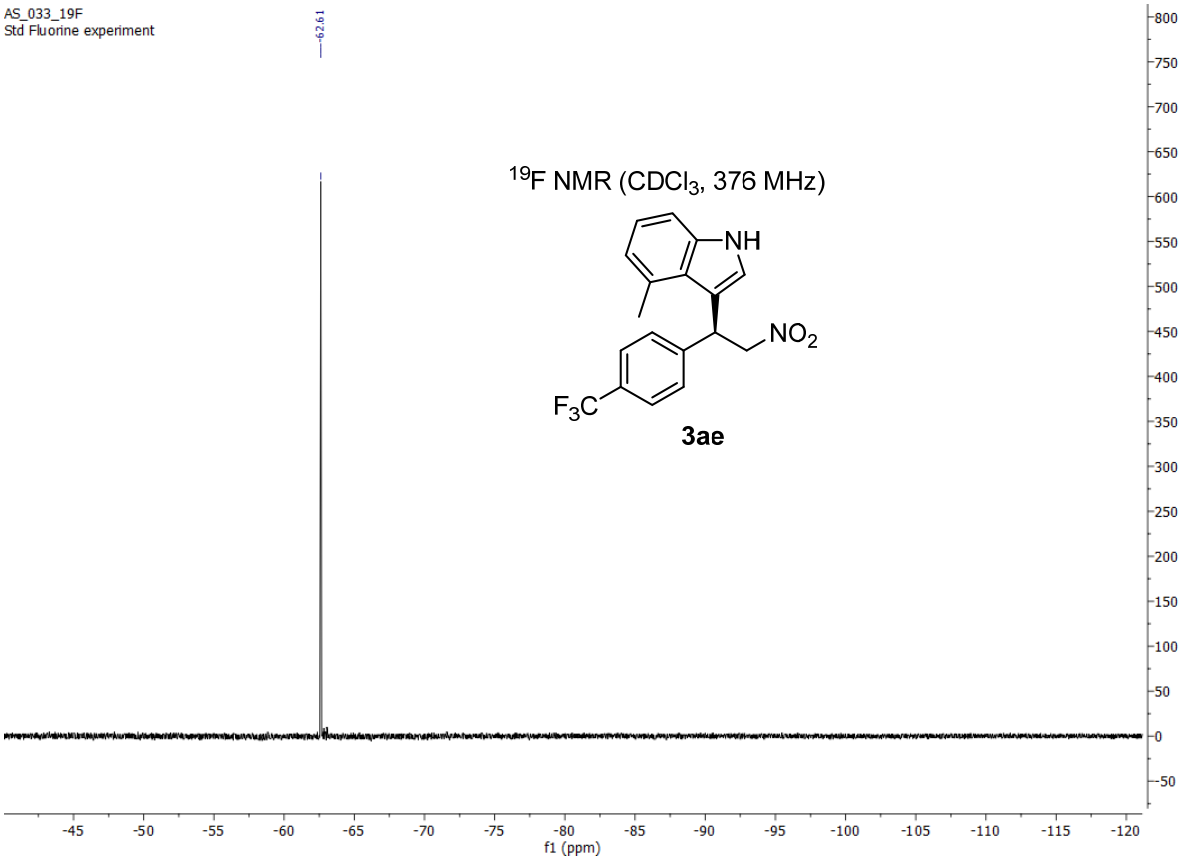
AS_033_19F
Std Fluorine experiment
-62.61
800
750
700
650
600
550
500
450
400
350
300
250
200
150
100
50
0
-50
-45 -50 -55 -60 -65 -70 -75 -80 -85 -90 -95 -100 -105 -110 -115 -120
f1 (ppm)
19F NMR (CDCl3, 376 MHz)
NH
NO2
F3C
3ae

HPLC traces of compounds *rac*-3ae and 3ae

Sample Info : AS_027,0,75 mL/min, 90:10 hex:ipr, 25°C, AD-H

Additional Info : Peak(s) manually integrated

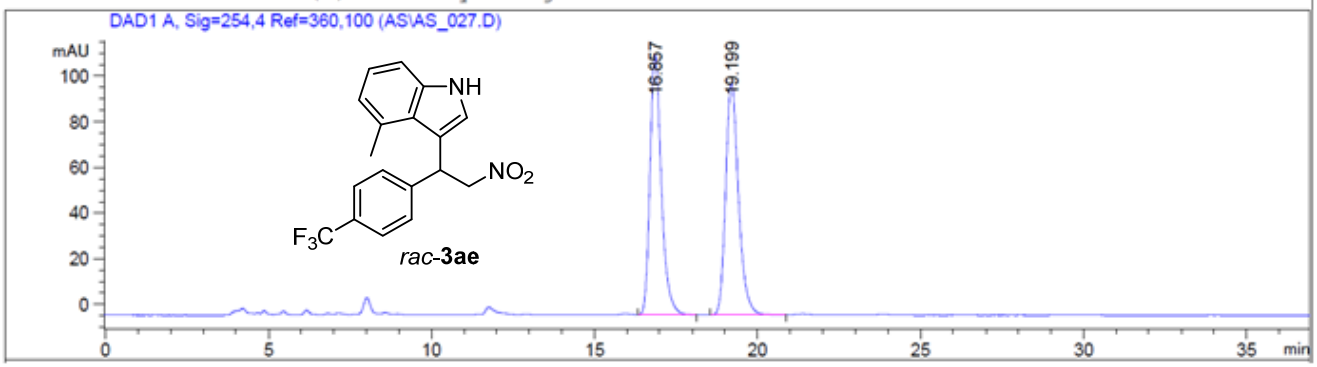

Signal 1: DAD1 A, Sig=254,4 Ref=360,100

Peak #	RetTime [min]	Type	Width [min]	Area [mAU*s]	Height [mAU]	Area %
1	16.857	BB	0.3705	2762.43652	114.07994	49.8492
2	19.199	BB	0.4172	2779.14502	101.58853	50.1508
Totals :				5541.58154	215.66847	

Sample Info : AS_033, 0,75 mL/min, 90:10 hex:ipr, 25°C, AD-H

Additional Info : Peak(s) manually integrated

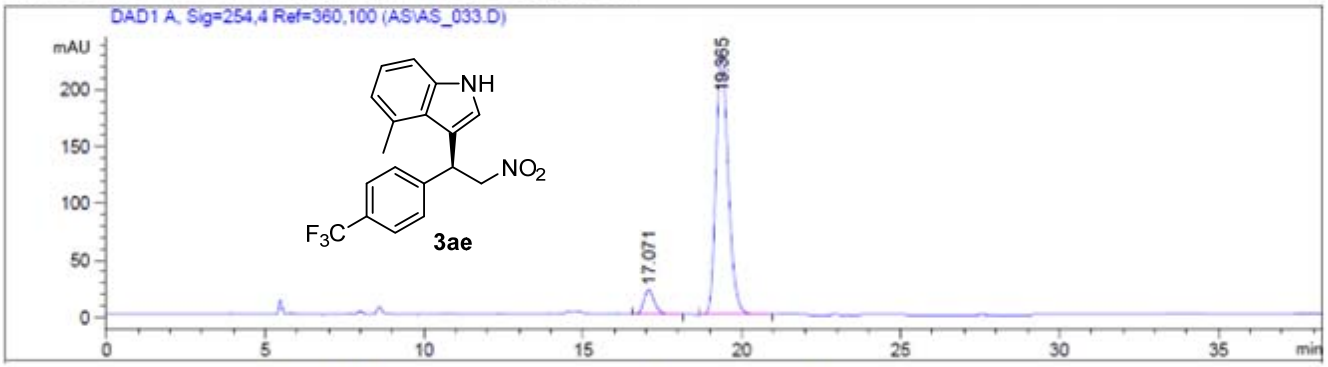

Signal 1: DAD1 A, Sig=254,4 Ref=360,100

Peak #	RetTime [min]	Type	Width [min]	Area [mAU*s]	Height [mAU]	Area %
1	17.071	BB	0.3603	505.72205	21.51124	7.5384
2	19.365	BB	0.4072	6202.91162	232.52612	92.4616
Totals :				6708.63367	254.03736	

(*S*)-3-(2-Nitro-1-phenylethyl)-1*H*-indole (3ba)

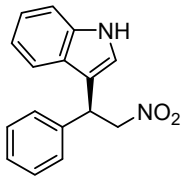

Following the general procedure (48 h reaction time), the title compound was obtained in 75% yield after chromatography on silica gel. The enantiomeric excess of the product was determined by CSP HPLC: ADH column, *n*-hexane/*i*-PrOH 90:10, 0.75 mL/min, t_{maj} = 34.2 min; t_{min} = 31.2 min, 89% ee.

Spectral and optical data are in accordance with literature values.[18,19]

^{1}H NMR ($CDCl_3$, 400 MHz) δ= 8.08 (br s, 1H), 7.45 (d, J = 8.0 Hz, 1H), 7.39 – 7.24 (m, 6H), 7.21 (ddd, J = 8.2, 7.0, 1.2 Hz, 1H), 7.08 (ddd, J = 8.1, 7.1, 1.0 Hz, 1H), 7.03 (dd, J = 2.6, 0.9 Hz, 1H), 5.20 (t, J = 8.4 Hz, 1H), 5.07 (dd, J = 12.4, 7.6 Hz, 1H), 4.95 (dd, J = 12.5, 8.4 Hz, 1H).

^{13}C NMR ($CDCl_3$, 101 MHz) δ= 139.2, 136.5, 128.9, 127.7, 127.6, 126.1, 122.7, 121.6, 120.0, 118.9, 114.4, 111.4, 79.5, 41.5.

$[\alpha]_D^{RT}$ = +26.2 (c =0.5, CH_2Cl_2).

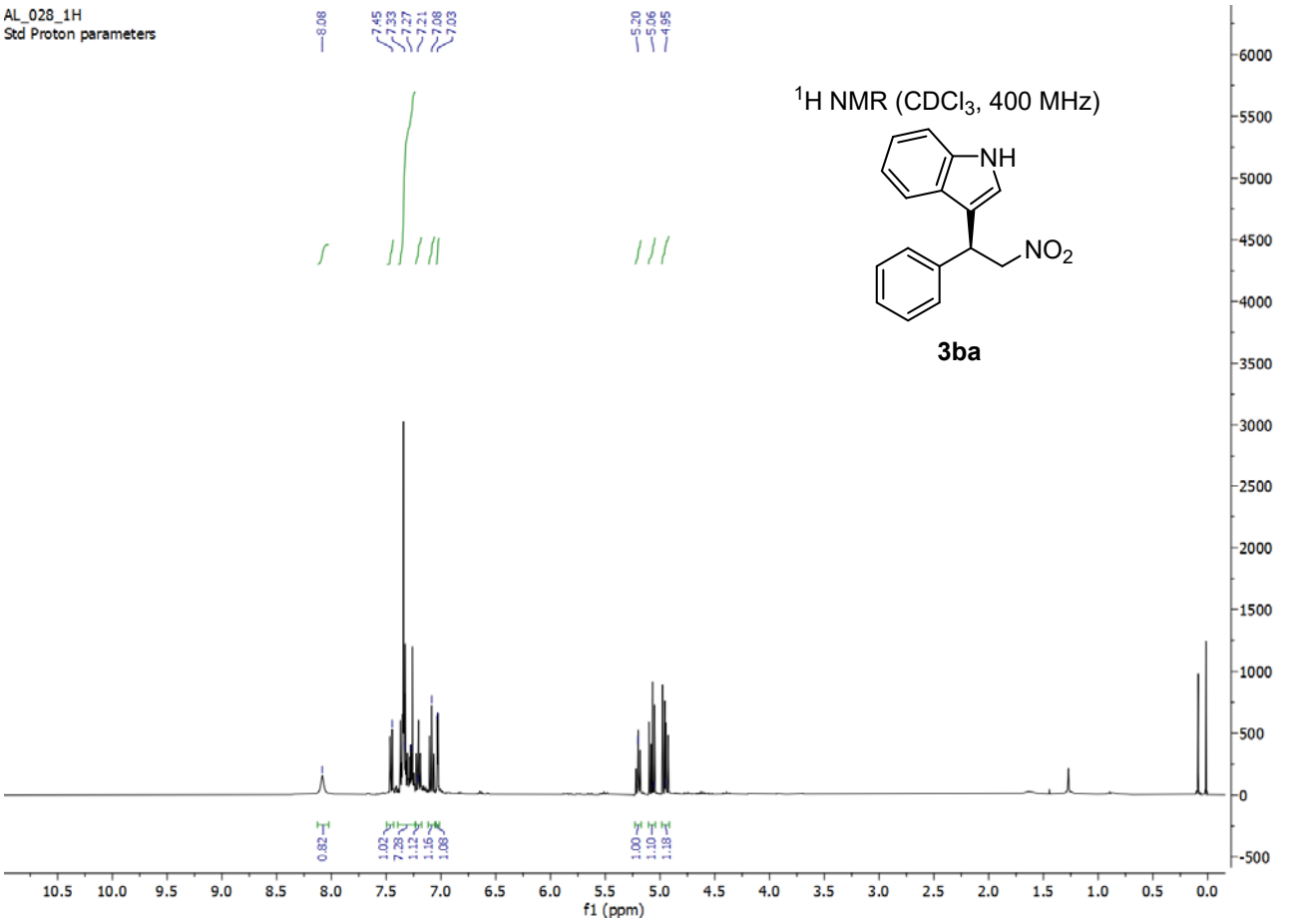

^{1}H NMR ($CDCl_3$, 400 MHz)

3ba

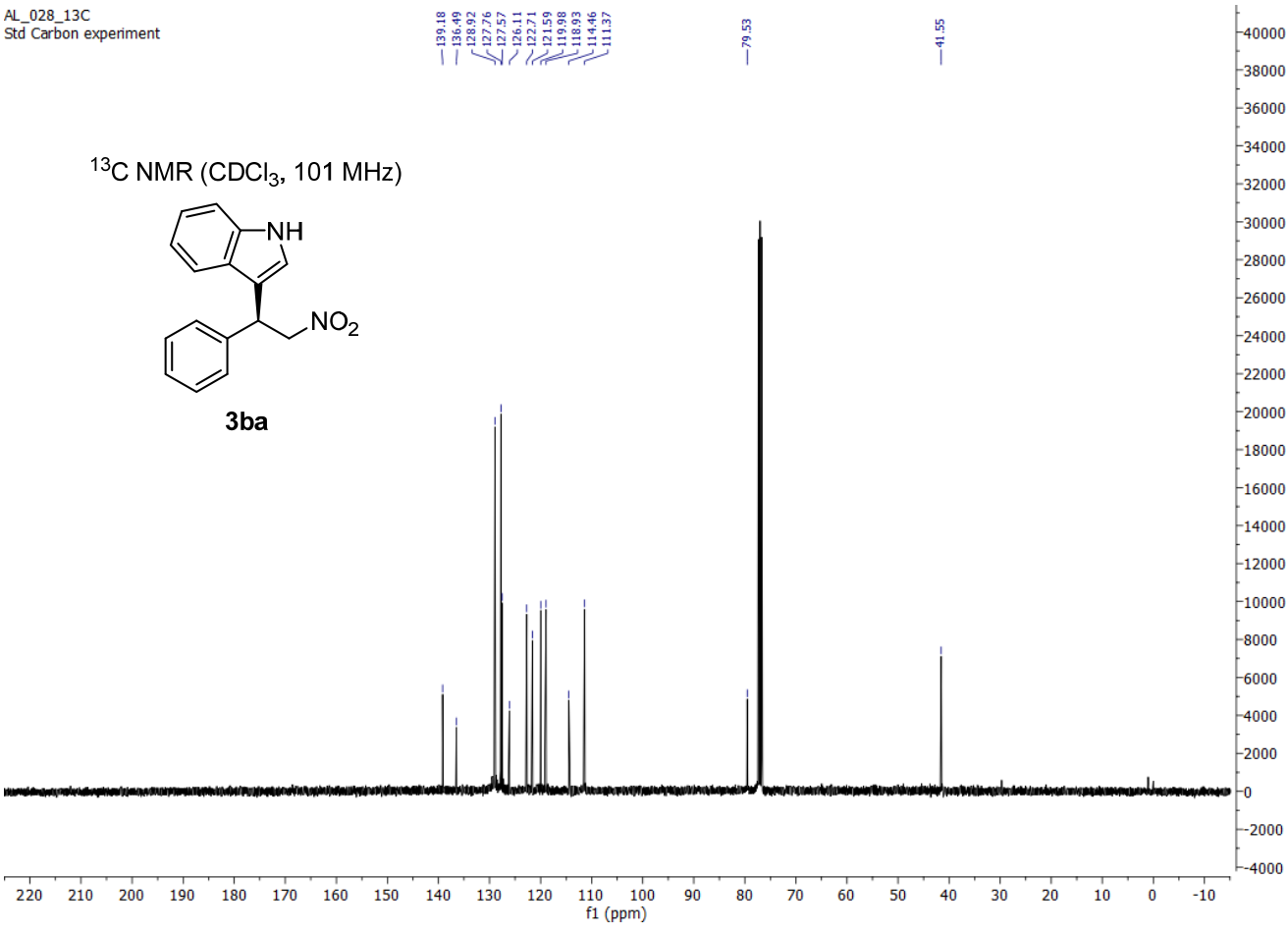

^{13}C NMR ($CDCl_3$, 101 MHz)

3ba

HPLC traces of compounds *rac*-3ba and 3ba

Sample Info : PP_001, 0.75 mL/min, 90:10 hex:ipr, 25°C, AD-H

Additional Info : Peak(s) manually integrated

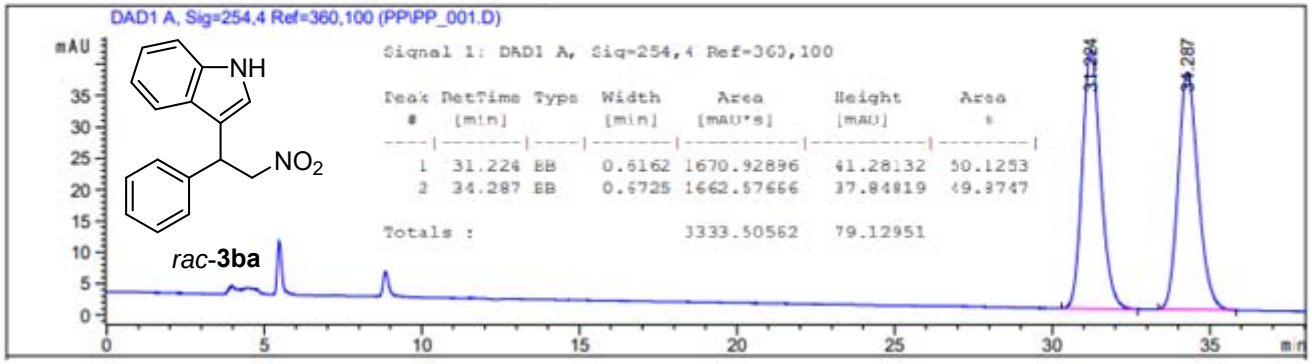

Signal 1: DAD1 A, Sig=254,4 Ref=360,100

Peak #	RetTime [min]	Type	Width [min]	Area [mAU*s]	Height [mAU]	Area %
1	31.224	BB	0.6162	1670.92896	41.28132	50.1253
2	34.287	BB	0.6725	1662.57666	37.84819	49.8747
Totals :				3333.50562	79.12951	

Sample Info : AL_028, 0.75mL/min, 90:10 hex:iPrOH, 25°C, AD-H

Additional Info : Peak(s) manually integrated

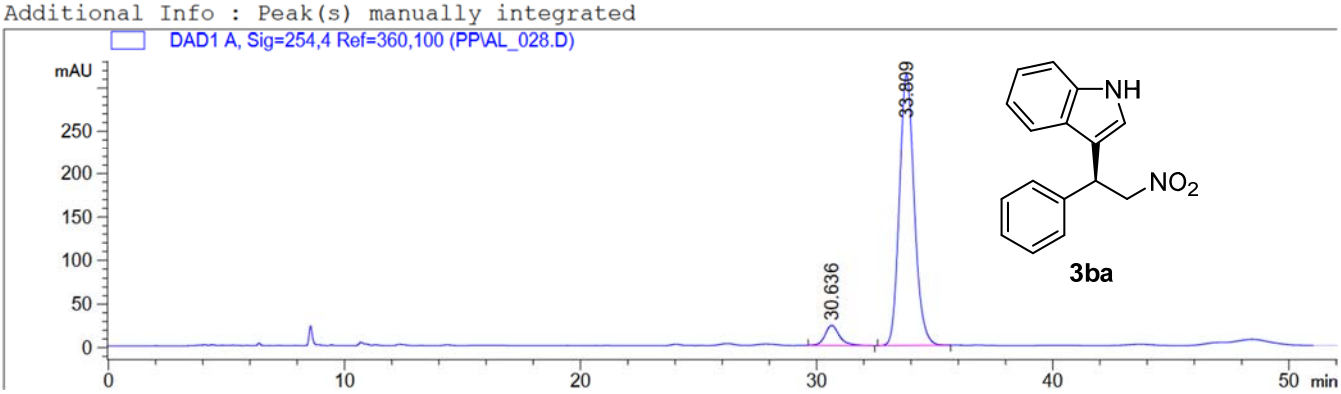

Signal 1: DAD1 A, Sig=254,4 Ref=360,100

Peak #	RetTime [min]	Type	Width [min]	Area [mAU*s]	Height [mAU]	Area %
1	30.626	MM T	0.5904	753.24268	21.26315	5.2211
2	33.809	BB	0.6736	1.36735e4	313.05261	94.7789
Totals :				1.44268e4	334.31576	

(*S*)-3-(2-Nitro-1-(*o*-tolyl)ethyl)-1*H*-indole (3ca)

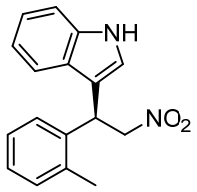

Following the general procedure (48 h reaction time), the title compound was obtained in 50% yield after chromatography on silica gel. The enantiomeric excess of the product was determined by CSP HPLC: ODH column, *n*-hexane/*i*-PrOH 70:30, 0.75 mL/min, t_{maj} = 29.2 min; t_{min} = 25.1 min, 82% ee.

Spectral data are in accordance with the literature.[20]

^{1}H NMR ($CDCl_3$, 400 MHz) δ= 8.07 (br s, 1H), 7.48 (d, J = 8.0 Hz, 1H), 7.36 (d, J = 8.2 Hz, 1H), 7.30 – 7.15 (m, 5H), 7.11 (ddt, J = 7.6, 7.1, 0.7 Hz, 1H), 6.91 (dd, J = 2.5, 0.9 Hz, 1H), 5.44 (t, J = 7.8 Hz, 1H), 5.04 (dd, J = 12.9, 7.6 Hz, 1H), 4.92 (dd, J = 12.8, 8.2 Hz, 1H), 2.44 (s, 3H).

^{13}C NMR ($CDCl_3$, 101 MHz) δ= 137.1, 136.5, 136.3, 131.1, 127.3, 126.4, 126.2, 122.7, 122.5, 120.0, 118.6, 114.3, 111.4, 78.6, 37.2, 19.5.

$[\alpha]_D^{RT}$ = -17.4 (c = 0.5, CH_2Cl_2).

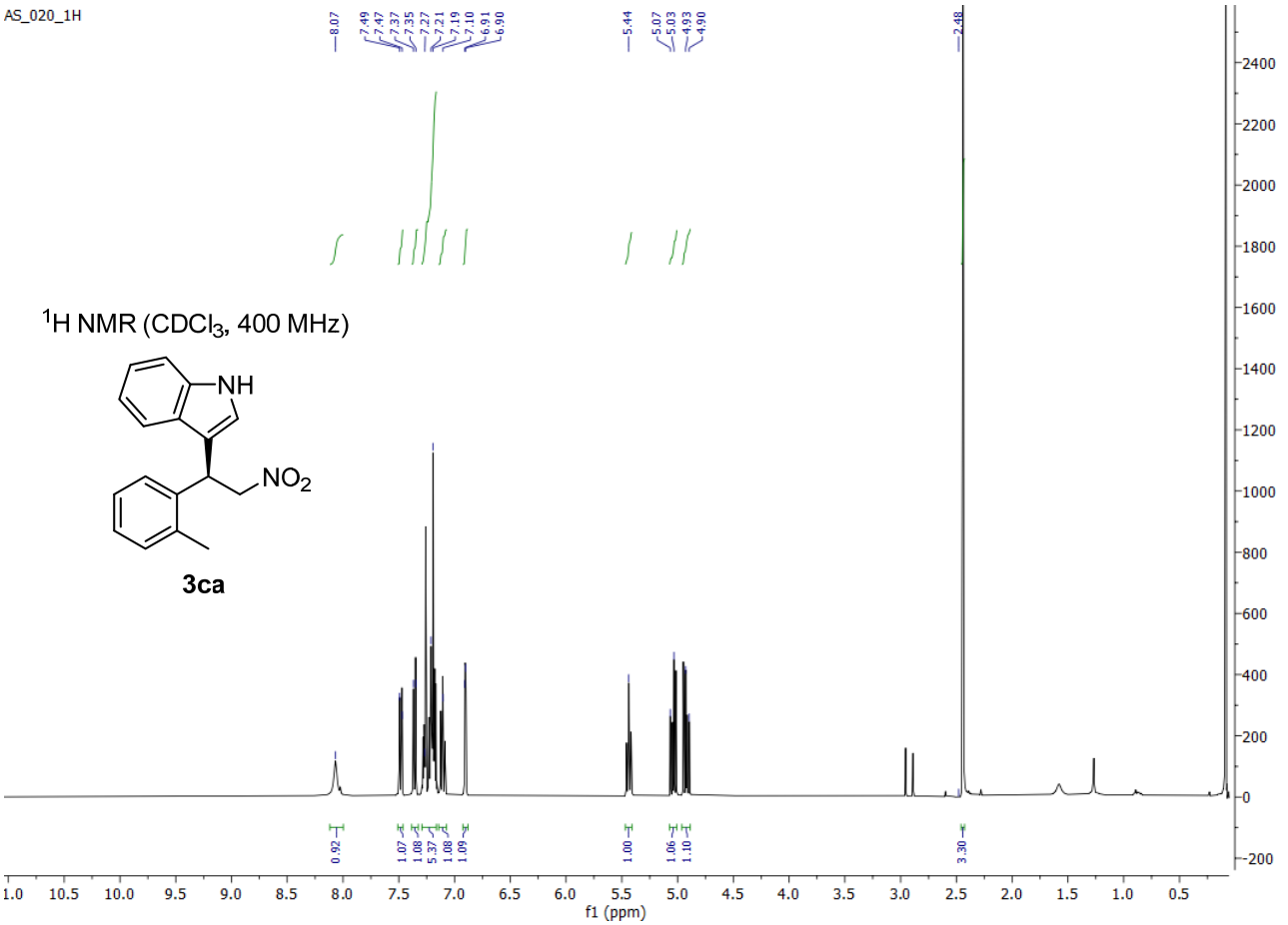

^{1}H NMR ($CDCl_3$, 400 MHz)

3ca

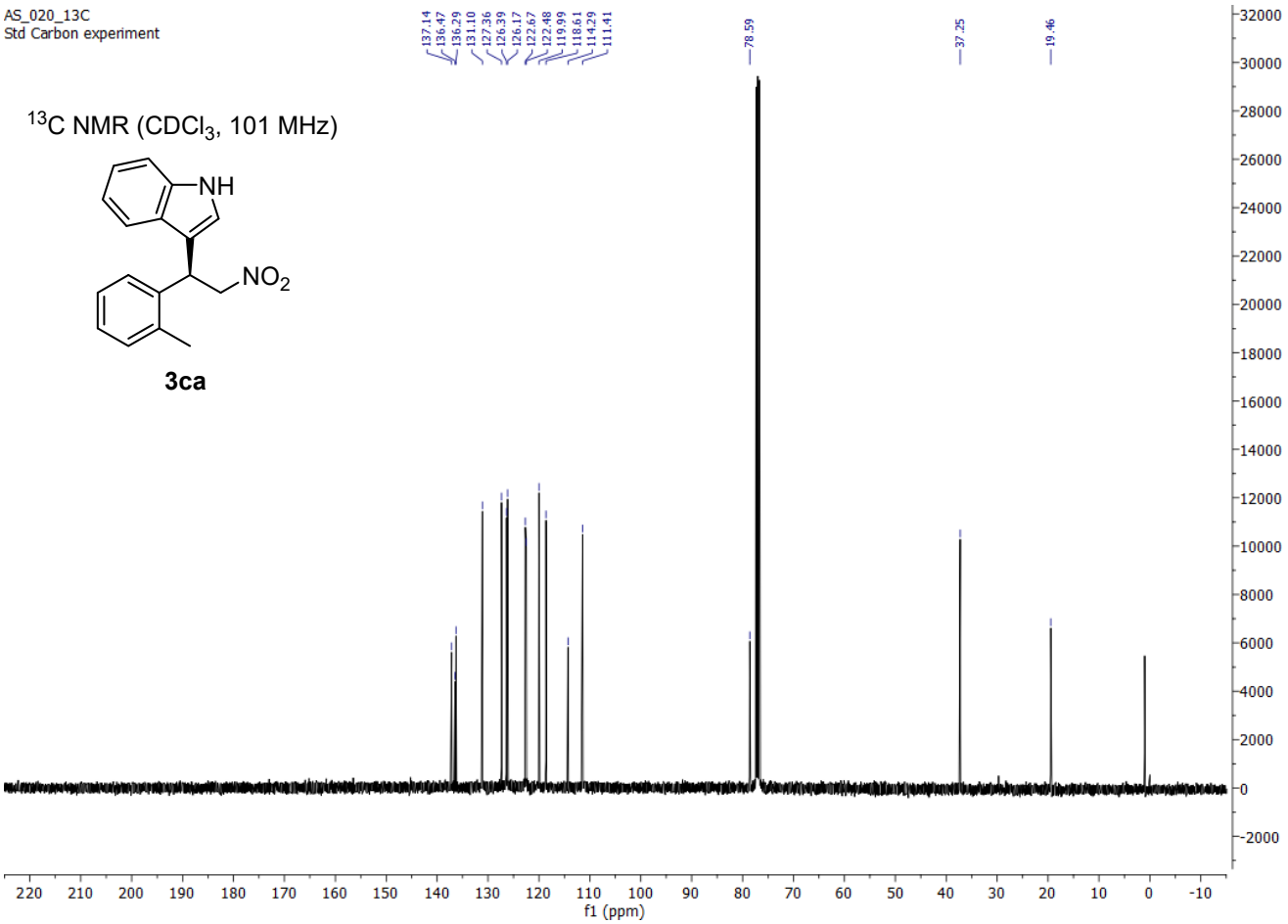

^{13}C NMR ($CDCl_3$, 101 MHz)

3ca

HPLC traces of compounds *rac*-3ca and 3ca

Sample Info : PP_004_2, 0.75 mL/min, 70:30 hex:ipr, 25°C, OD-H

Additional Info : Peak(s) manually integrated

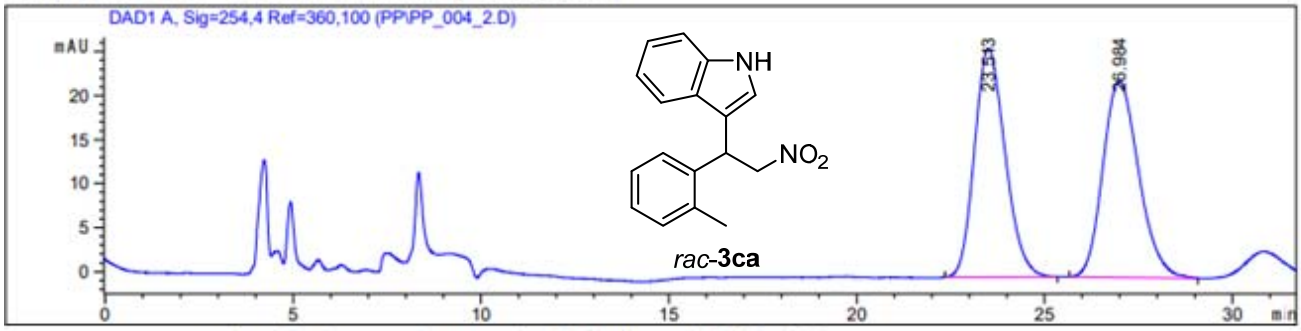

Signal 1: DAD1 A, Sig=254,4 Ref=360,100

Peak #	RetTime [min]	Type	Width [min]	Area [mAU*s]	Height [mAU]	Area %
1	23.513	BB	0.8386	1474.37378	25.96006	49.9174
2	26.984	BB	0.9687	1479.25159	22.27748	50.0826
Totals :				2953.62537	48.23754	

Sample Info : AS_020, 0,75 mL/min, 70:30 hex:ipr, 25°C, OD-H

Additional Info : Peak(s) manually integrated

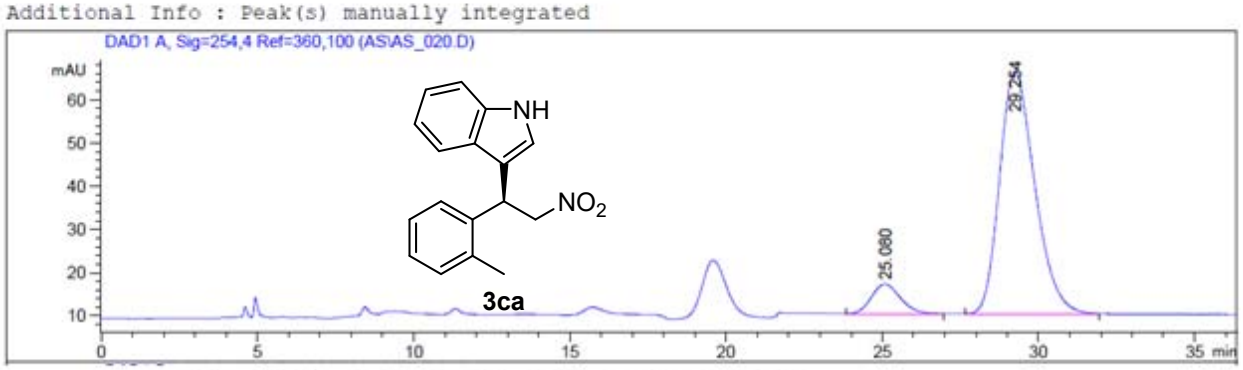

Signal 1: DAD1 A, Sig=254,4 Ref=360,100

Peak #	RetTime [min]	Type	Width [min]	Area [mAU*s]	Height [mAU]	Area %
1	25.080	BB	0.7706	439.09015	6.86101	9.1045
2	29.254	BB	1.1572	4383.71729	55.75819	90.8955
Totals :				4822.80743	62.61919	

(*R*)-3-(1-(2-Bromophenyl)-2-nitroethyl)-1*H*-indole (3da)

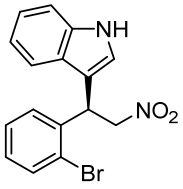

Following the general procedure (48 h reaction time), the title compound was obtained in 78% yield after chromatography on silica gel. The enantiomeric excess of the product was determined by CSP HPLC: ODH column, *n*-hexane/*i*-PrOH 70:30, 0.75 mL/min, t_{maj} = 36.9 min; t_{min} = 21.7 min, 92% ee.

Spectral and optical data are in accordance with the literature.[21]

^{1}H NMR ($CDCl_3$, 400 MHz) δ= 8.11 (br s, 1H), 7.63 (d, J = 7.8 Hz, 1H), 7.44 (d, J = 8.0 Hz, 1H), 7.35 (d, J = 8.2 Hz, 1H), 7.24 – 7.17 (m, 3H), 7.15 – 7.05 (m, 3H), 5.74 (dd, J = 8.8, 7.0 Hz, 1H), 5.03 – 4.91 (m, 2H).

^{13}C NMR ($CDCl_3$, 101 MHz) δ= 138.1, 136.5, 133.5, 129.1, 127.9, 126.2, 124.5, 122.8, 121.9, 120.1, 119.0, 113.4, 111.4, 77.8, 40.6.

$[\alpha]_D^{RT}$ = +101.8 (c = 0.5, CH_2Cl_2).

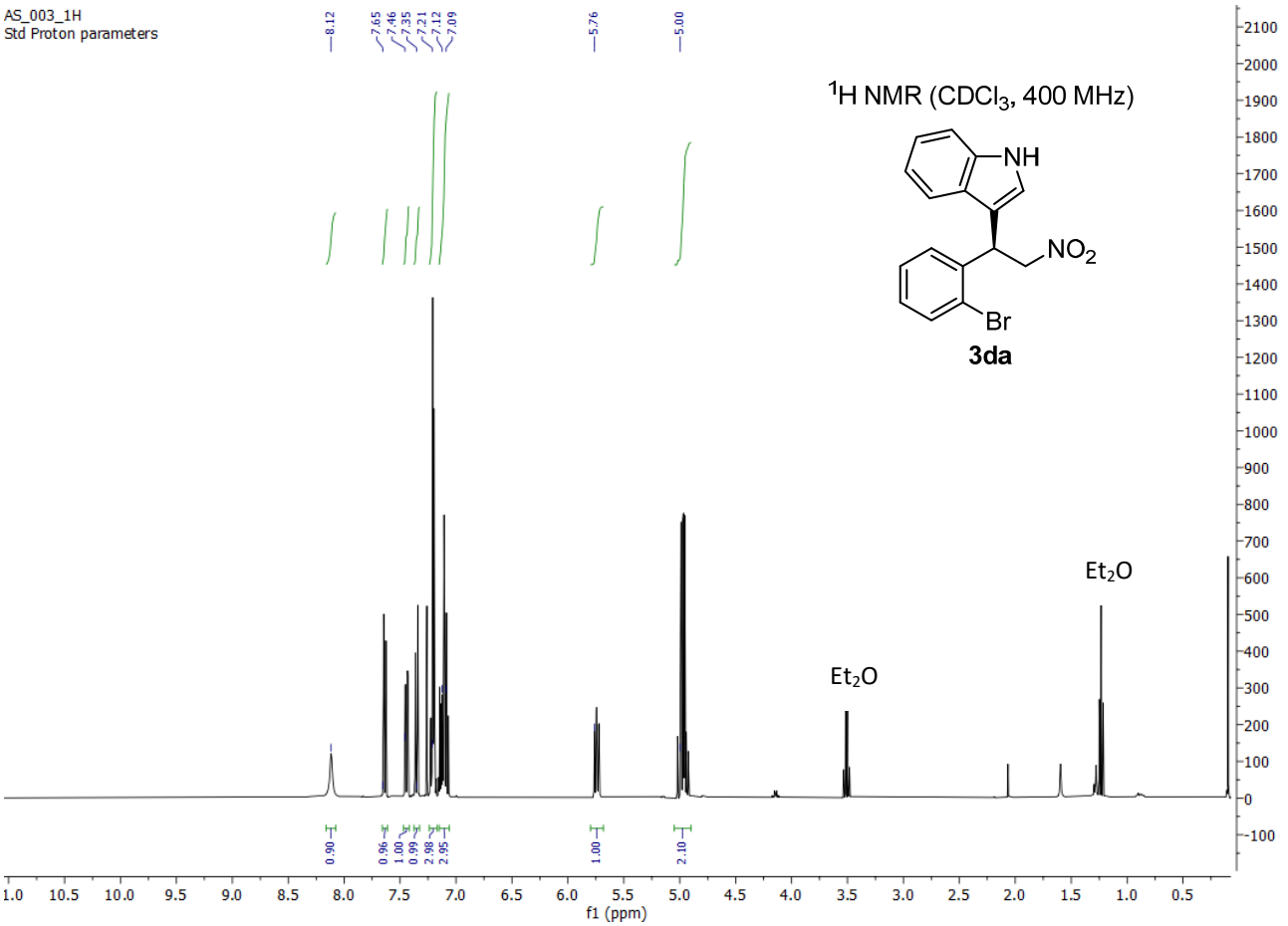
AS_003_1H
Std Proton parameters
8.12
7.65
7.46
7.35
7.21
7.12
7.09
5.76
5.00
^{1}H NMR ($CDCl_3$, 400 MHz)
NH
NO_2
Br
3da
Et_2O
Et_2O
0.90
0.96
1.00
0.99
2.98
2.95
1.00
2.10
f1 (ppm)

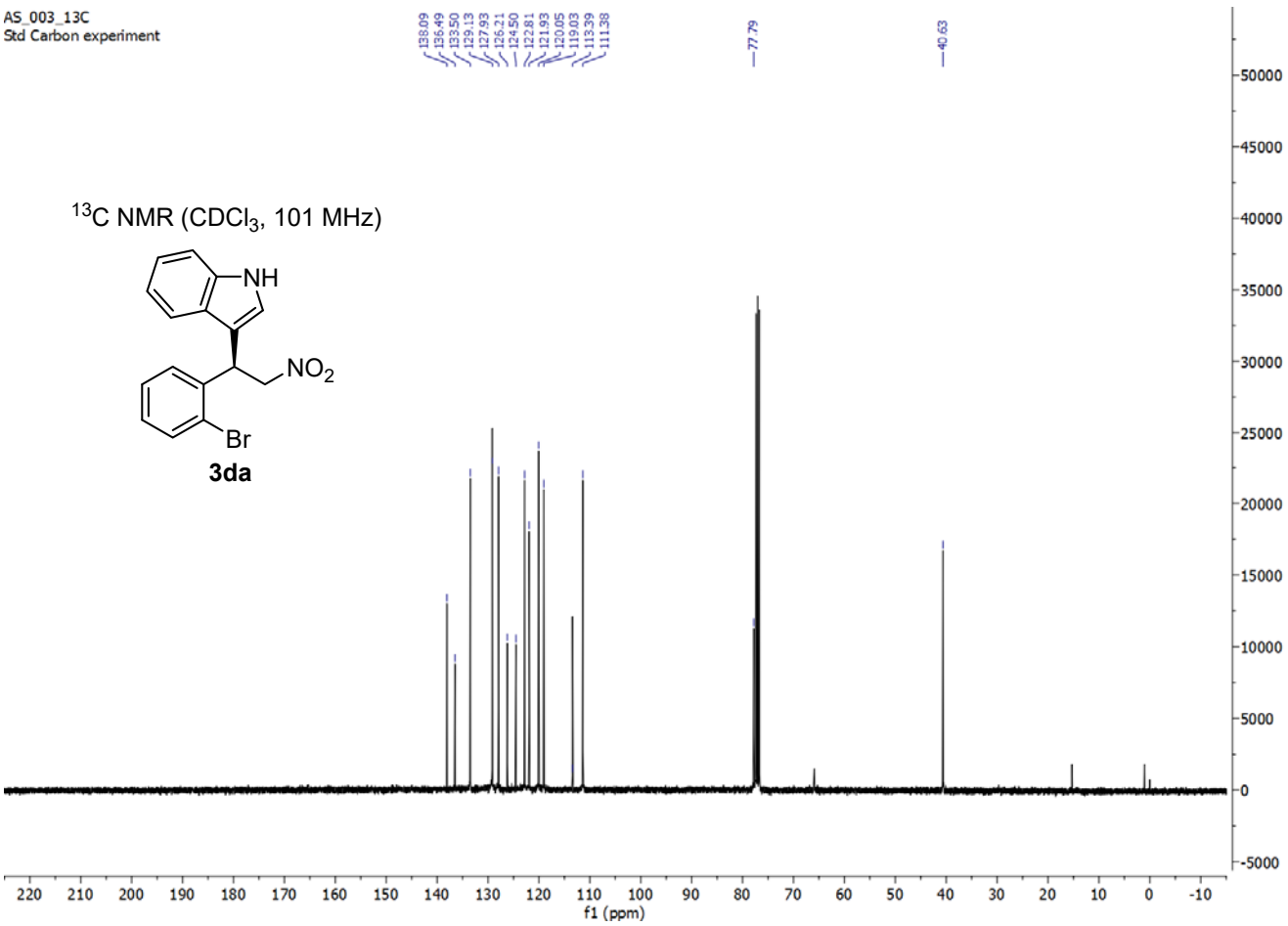
AS_003_13C
Std Carbon experiment
138.09
136.49
133.50
129.13
127.93
126.21
125.50
122.81
121.93
120.05
119.03
113.39
111.38
77.79
40.63
^{13}C NMR ($CDCl_3$, 101 MHz)
NH
NO_2
Br
3da
f1 (ppm)

HPLC traces for compounds *rac*-3da and 3da

Sample Info : AS_AS02, 0.75 mL/min, 70:30 hex:ipr, 25°C, OD-H

Additional Info : Peak(s) manually integrated

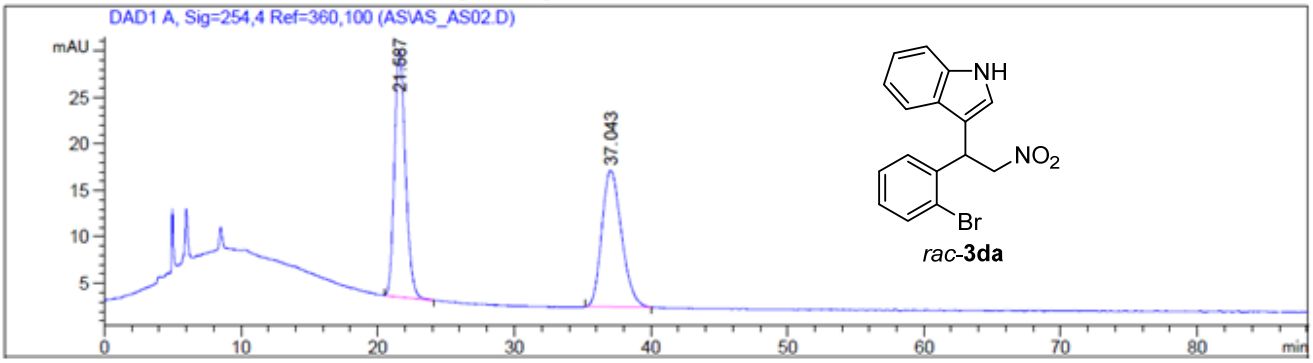

Signal 1: DAD1 A, Sig=254,4 Ref=360,100

Peak #	RetTime [min]	Type	Width [min]	Area [mAU*s]	Height [mAU]	Area %
1	21.587	BB	0.8379	1485.34521	26.50024	50.1947
2	37.043	BB	1.1870	1473.82373	14.65811	49.8053
Totals :				2959.16895	41.15835	

Sample Info : AS_03br, 0,75 mL/min, 70:30 hex:ipr, 25°C, OD-H

Additional Info : Peak(s) manually integrated

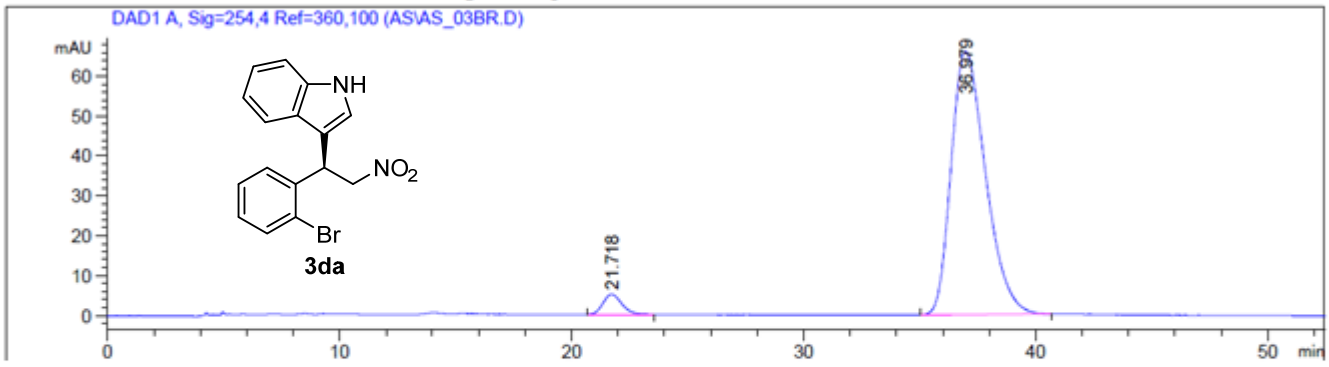

Signal 1: DAD1 A, Sig=254,4 Ref=360,100

Peak #	RetTime [min]	Type	Width [min]	Area [mAU*s]	Height [mAU]	Area %
1	21.718	BB	0.6823	281.12253	5.04351	3.9541
2	36.979	BB	1.4974	6828.51025	66.09357	96.0459
Totals :				7109.63278	71.13708	

(*S*)-3-(2-Nitro-1-(*m*-tolyl)ethyl)-1*H*-indole (3ea)

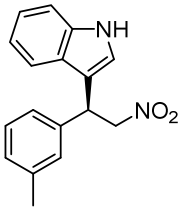

Following the general procedure (72 h reaction time), the title compound was obtained in 76% yield after chromatography on silica gel. The enantiomeric excess of the product was determined by CSP HPLC: ODH column, *n*-hexane/*i*-PrOH 70:30, 0.75 mL/min, t_{maj} = 24.2 min; t_{min} = 21.3 min, 93% ee.

^{1}H NMR ($CDCl_3$, 400 MHz) δ= 8.10 (br s, 1H), 7.50 (d, J = 8.0 Hz, 1H), 7.37 (d, J = 8.2 Hz, 1H), 7.26 – 7.14 (m, 4H), 7.14 – 7.07 (m, 2H), 7.04 (dd, J = 2.5, 0.9 Hz, 1H), 5.18 (t, J = 8.0 Hz, 1H), 5.07 (dd, J = 12.4, 7.7 Hz, 1H), 4.95 (dd, J = 12.4, 8.3 Hz, 1H), 2.34 (s, 3H).

^{13}C NMR ($CDCl_3$, 101 MHz) δ= 139.1, 138.5, 136.5, 128.7, 128.5, 128.3, 126.1, 124.7, 122.6, 121.6, 119.9, 118.9, 114.5, 111.3, 79.6, 41.5, 21.5.

$[\alpha]_D^{RT}$ = +13.4 (c = 0.5, CH_2Cl_2).

HRMS (ESI) m/z: [M - H]+ Calculated for $C_{17}H_{15}N_2O_2$= 279.1134; Found= 279.1149.

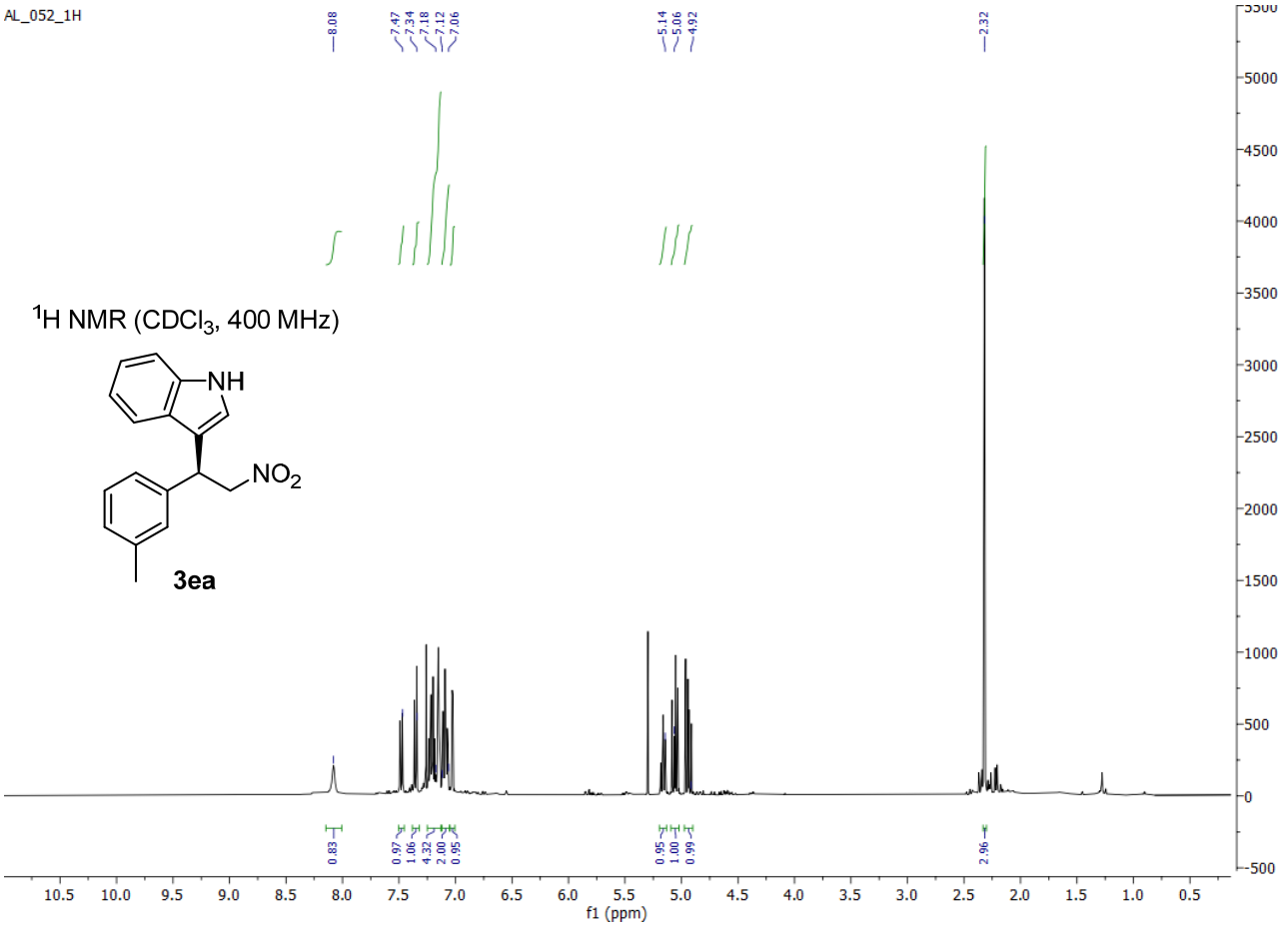

^{1}H NMR ($CDCl_3$, 400 MHz)

3ea

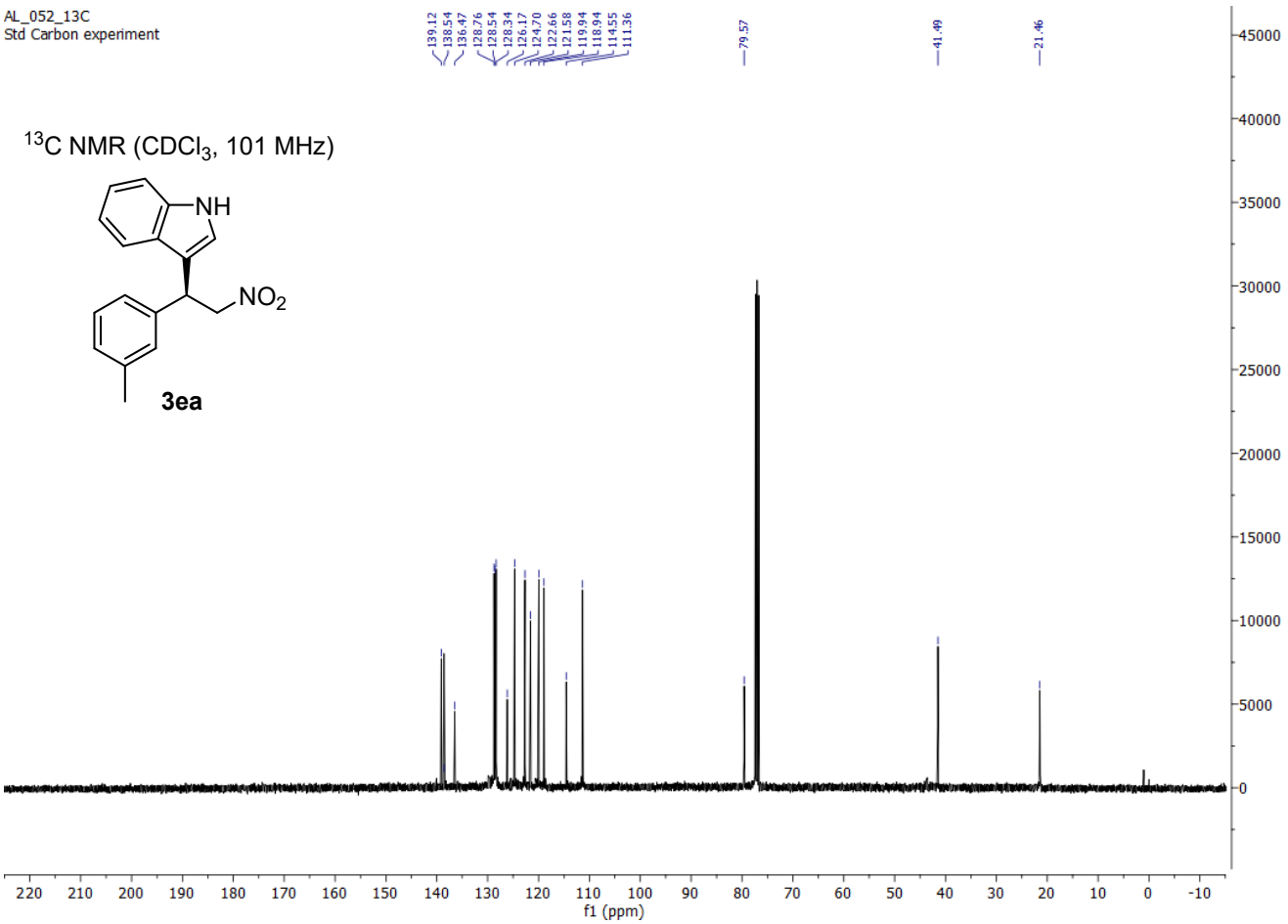

^{13}C NMR ($CDCl_3$, 101 MHz)

3ea

HPLC traces of compounds *rac*-3ea and 3ea

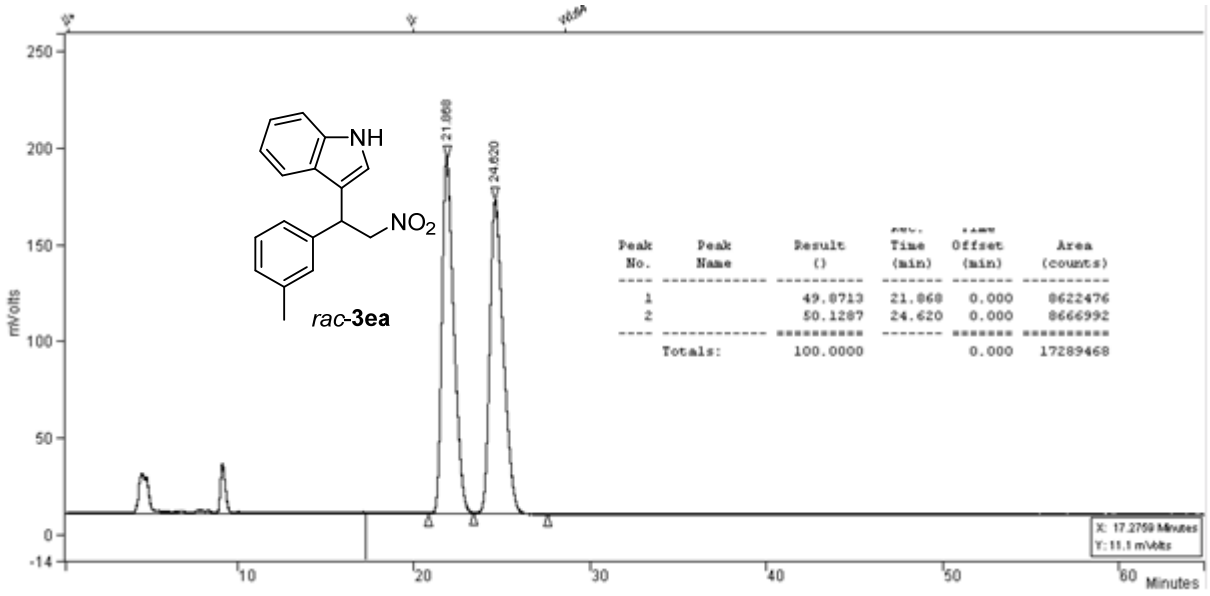

Peak No.	Peak Name	Result ()	Time (min)	Offset (min)	Area (counts)
1		49.8713	21.868	0.000	8622476
2		50.1287	24.620	0.000	8666992
Totals:		100.0000		0.000	17289468

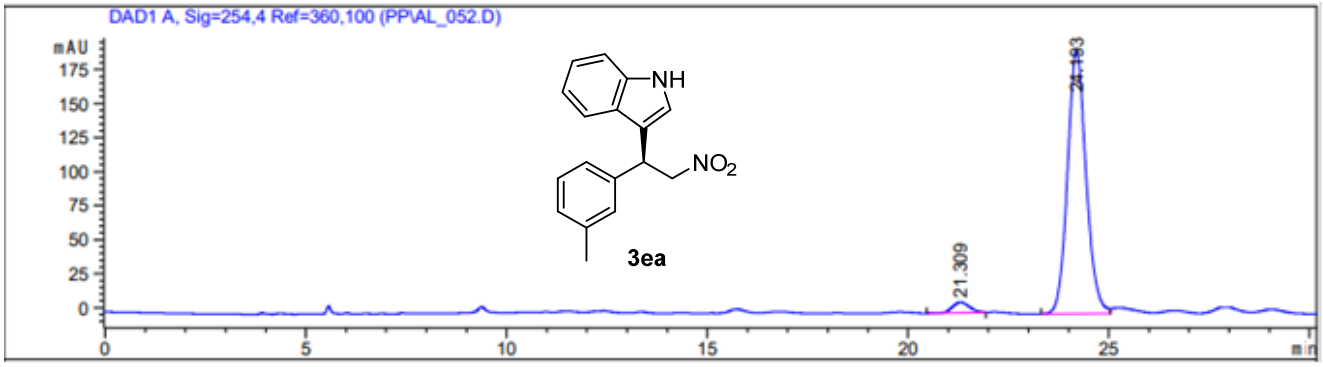

Signal 1: DAD1 A, Sig=254,4 Ref=360,100

Peak #	RetTime [min]	Type	Width [min]	Area [mAU*s]	Height [mAU]	Area %
1	21.309	BB	0.4632	222.49307	7.56245	3.4648
2	24.193	BV	0.4906	6199.02197	193.07726	96.5352
Totals :				6421.51505	200.63971	

(*S*)-3-(2-Nitro-1-(*p*-tolyl)ethyl)-1*H*-indole (3fa)

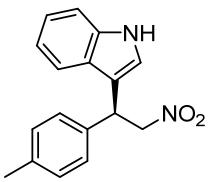

Following the general procedure (48 h reaction time), the title compound was obtained in 72% yield after chromatography on silica gel. The enantiomeric excess of the product was determined by CSP HPLC: ADH column, *n*-hexane/*i*-PrOH 90:10, 0.75 mL/min, t_{maj} = 33.8 min; t_{min} = 29.1 min, 88% ee.

Spectral and optical data are in accordance with the literature.[18]

^{1}H NMR ($CDCl_3$, 400 MHz) δ= 8.06 (s, 1H), 7.46 (d, J = 8.0 Hz, 1H), 7.34 (d, J = 8.2 Hz, 1H), 7.28 – 7.04 (m, 6H), 7.00 (dd, J = 2.6, 0.9 Hz, 1H), 5.16 (t, J = 8.0 Hz, 1H), 5.05 (dd, J = 12.4, 7.6 Hz, 1H), 4.92 (dd, J = 12.3, 8.4 Hz, 1H), 2.32 (s, 3H).

^{13}C NMR ($CDCl_3$, 101 MHz) δ= 137.2, 136.5, 136.1, 129.6, 127.6, 126.1, 122.6, 121.5, 119.9, 118.9, 114.6, 111.4, 79.6, 41.2, 21.0.

$[\alpha]_D^{RT}$ = +10.2 (c = 0.5, CH_2Cl_2).

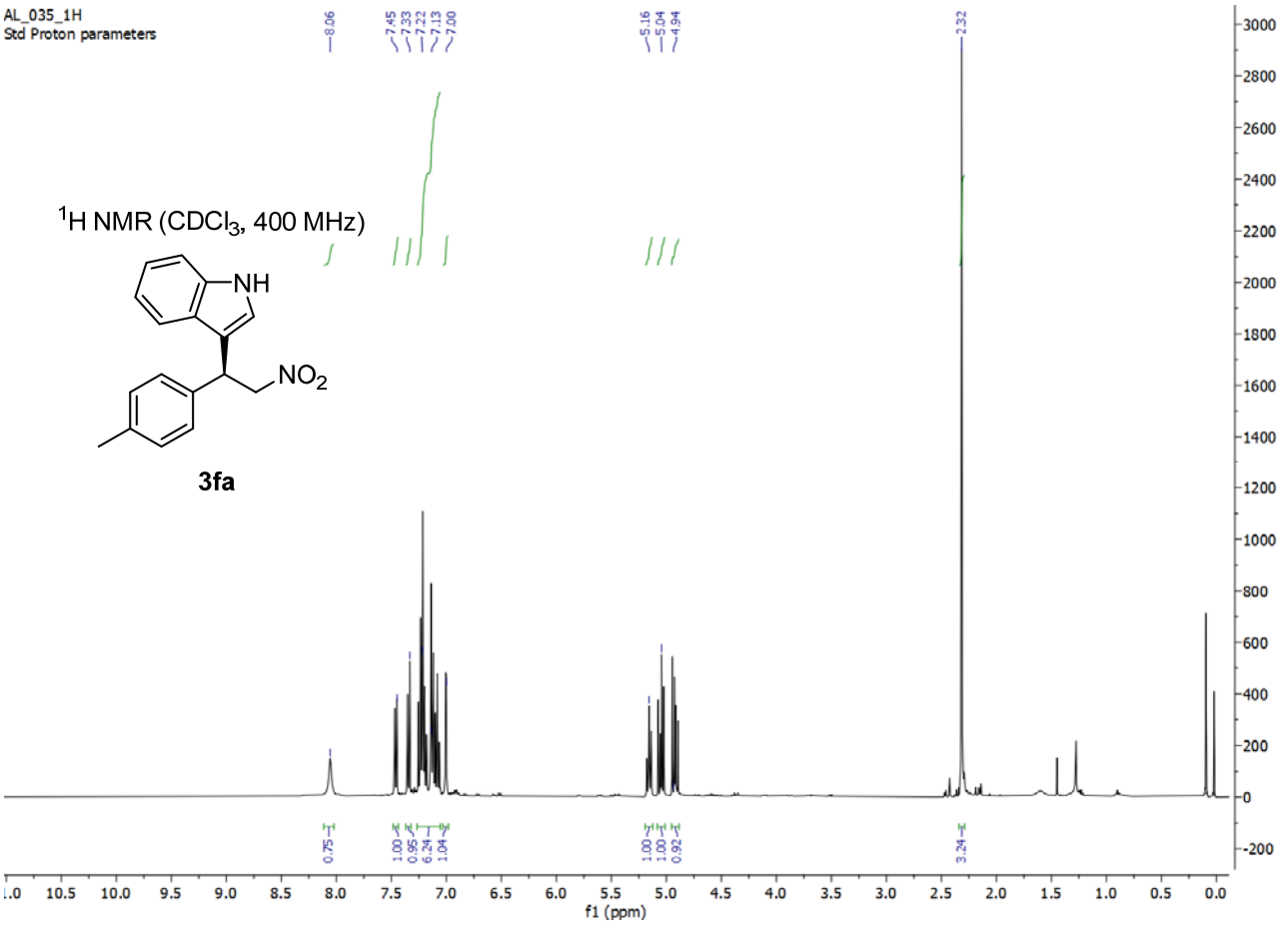

^{1}H NMR ($CDCl_3$, 400 MHz)

3fa

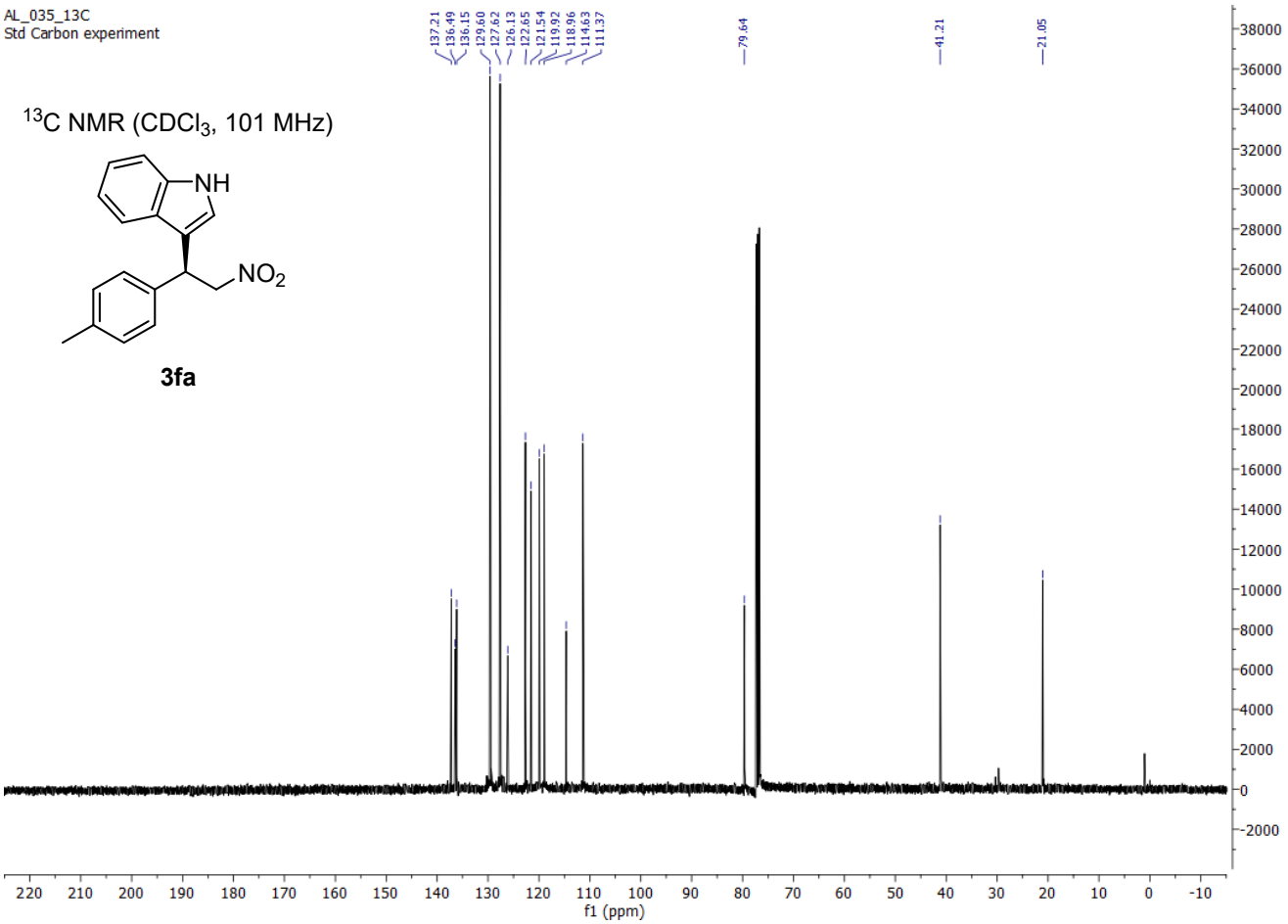

^{13}C NMR ($CDCl_3$, 101 MHz)

3fa

HPLC traces for compounds *rac*-3fa and 3fa

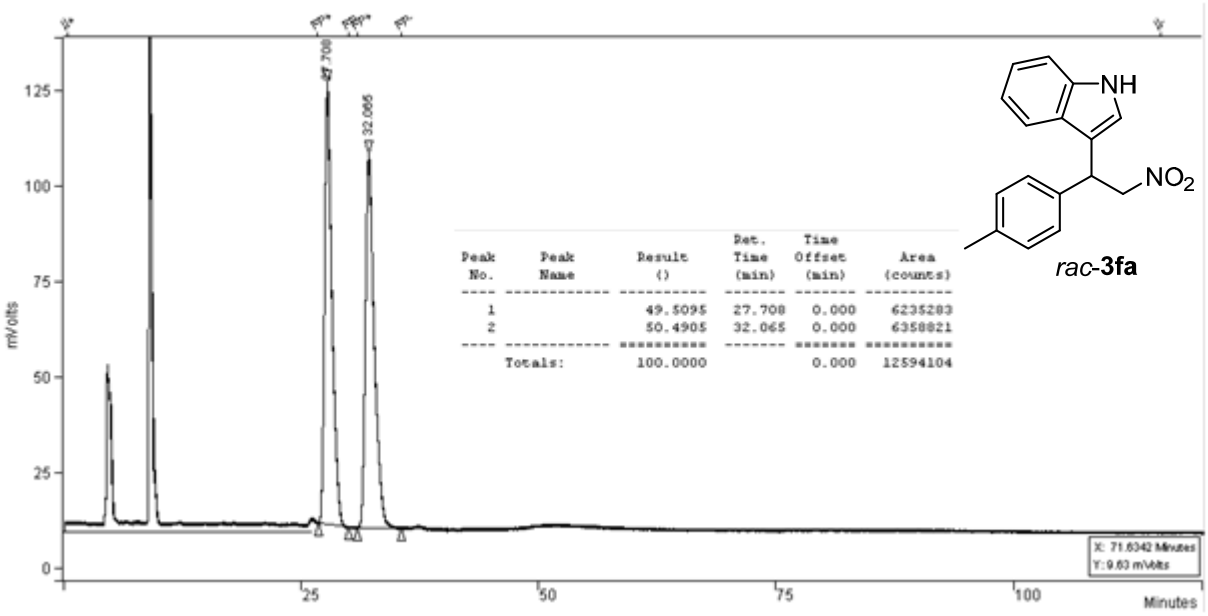

Peak No.	Peak Name	Result ()	Ret. Time (min)	Time Offset (min)	Area (counts)
1		49.5095	27.708	0.000	6235283
2		50.4905	32.065	0.000	6358821
Totals:		100.0000		0.000	12594104

rac-**3fa**

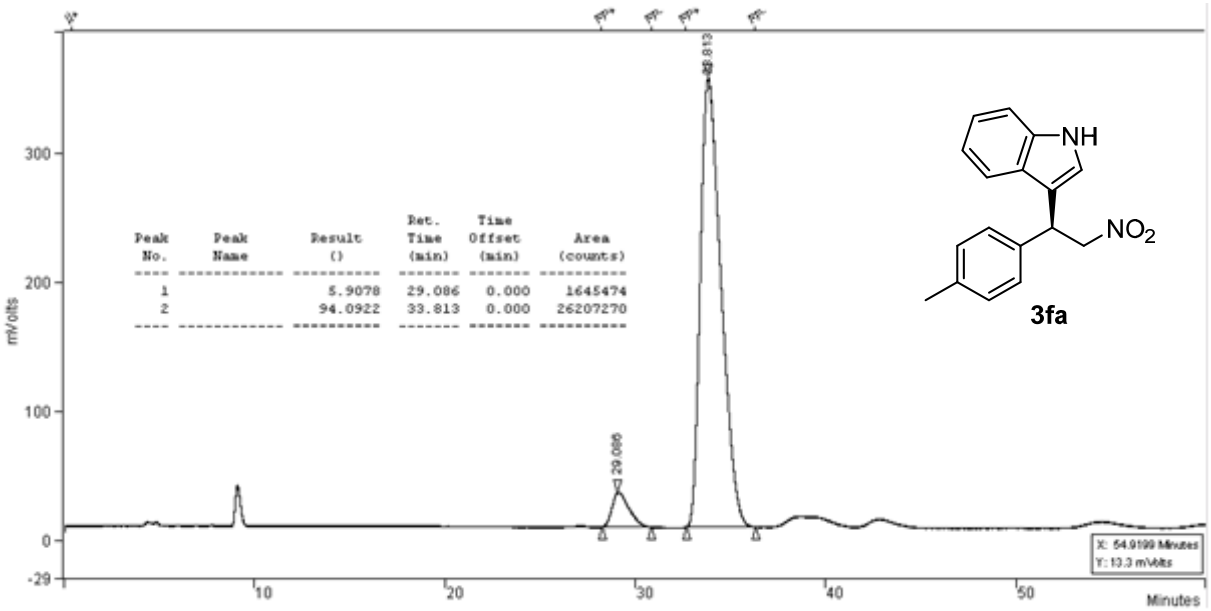

Peak No.	Peak Name	Result ()	Ret. Time (min)	Time Offset (min)	Area (counts)
1		5.9078	29.086	0.000	1645474
2		94.0922	33.813	0.000	26207270

3fa

(*S*)-3-(1-(4-Fluorophenyl)-2-nitroethyl)-1*H*-indole (3ga)

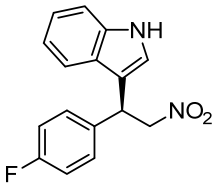

Following the general procedure (48 h reaction time), the title compound was obtained in 88% yield after chromatography on silica gel. The enantiomeric excess of the product was determined by CSP HPLC: ADH column, *n*-hexane/*i*-PrOH 90:10, 0.75 mL/min, t_{maj} = 35.9 min; t_{min} = 29.2 min, 85% ee.

Spectral and optical data are in accordance with the literature.[22]

^{1}H NMR ($CDCl_3$, 400 MHz) δ= 8.12 (br s, 1H), 7.41 (d, J = 8.2 Hz, 1H), 7.36 (d, J = 8.1 Hz, 1H), 7.33 – 7.28 (m, 2H), 7.22 (ddd, J = 8.1, 7.0, 1.2 Hz, 1H), 7.09 (ddd, J = 8.0, 7.0, 1.0 Hz, 1H), 7.05 – 6.98 (m, 3H), 5.18 (t, *J* = 8.0 Hz, 1H), 5.06 (dd, *J* = 12.5, 7.4 Hz, 1H), 4.91 (dd, *J* = 12.5, 8.6 Hz, 1H).

^{13}C NMR ($CDCl_3$, 101 MHz) δ= 162.2 (d, J= 246.2 Hz), 136.5, 134.9 (d, J= 3.3 Hz), 129.3 (d, J= 8.0 Hz), 125.9, 122.8, 121.4, 120.1, 118.8, 115.8 (d, J= 21.4 Hz), 114.3, 111.5, 79.5, 40.9.

^{19}F NMR ($CDCl_3$, 376 MHz) δ= -114.8 (s, 1F).

$[\alpha]_D^{RT}$ = +23.8 (c =0.5, CH_2Cl_2).

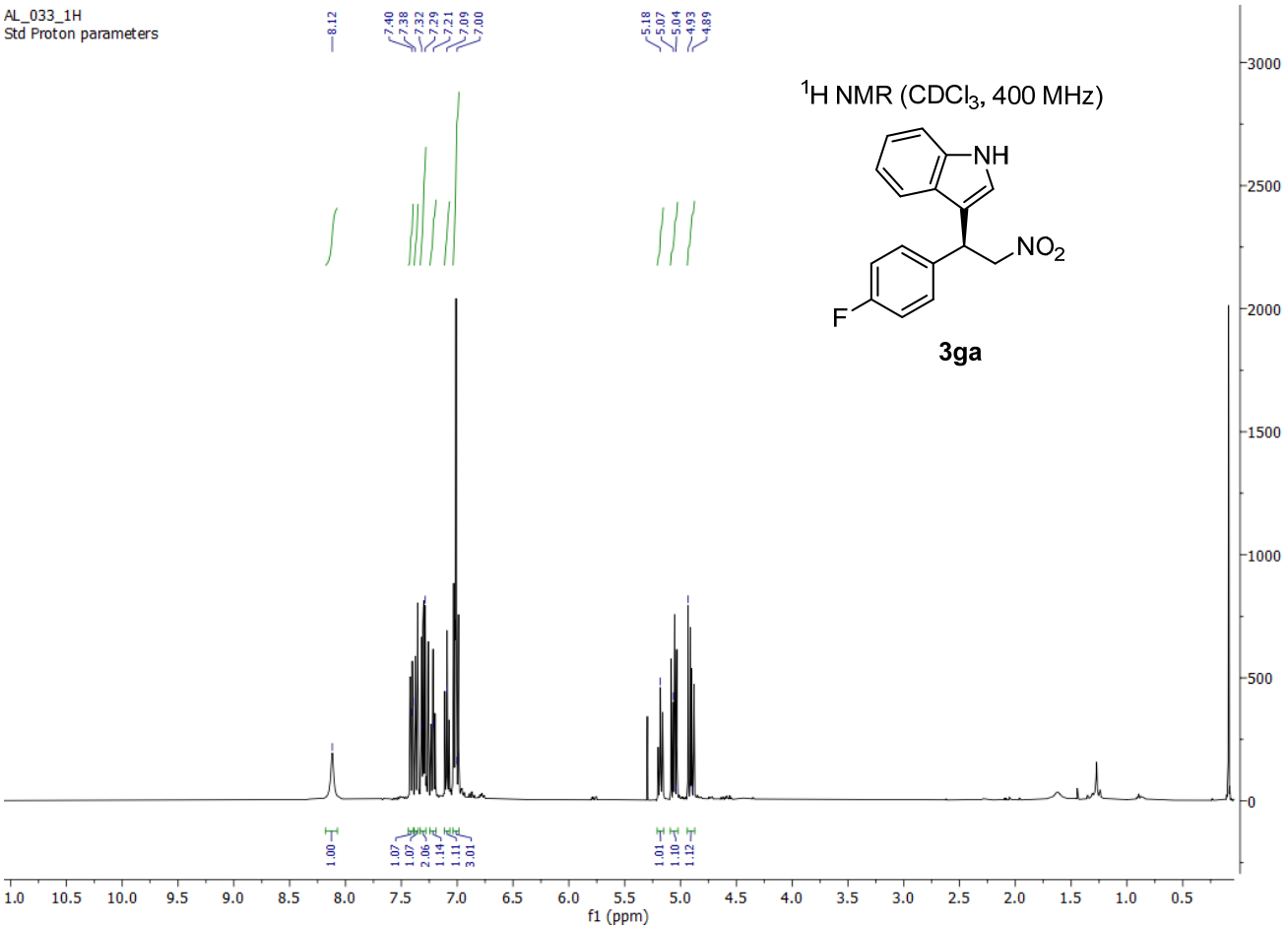

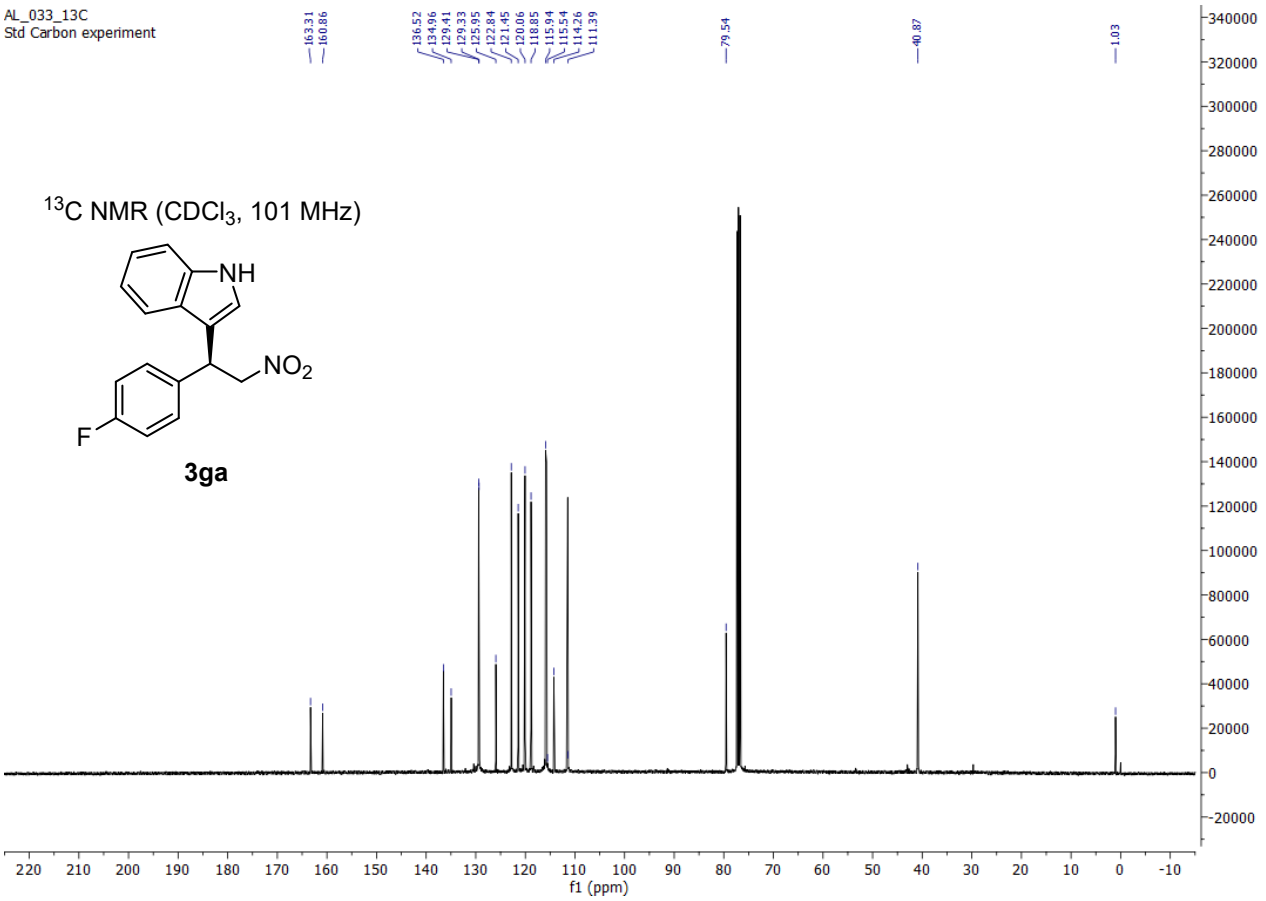
AL_033_13C
Std Carbon experiment
163.31
160.86
136.52
134.96
129.41
129.33
125.95
122.84
121.45
120.06
118.85
115.94
115.54
114.26
111.39
79.54
40.87
1.03
^{13}C NMR ($CDCl_3$, 101 MHz)
NH
NO_2
F
3ga
f1 (ppm)

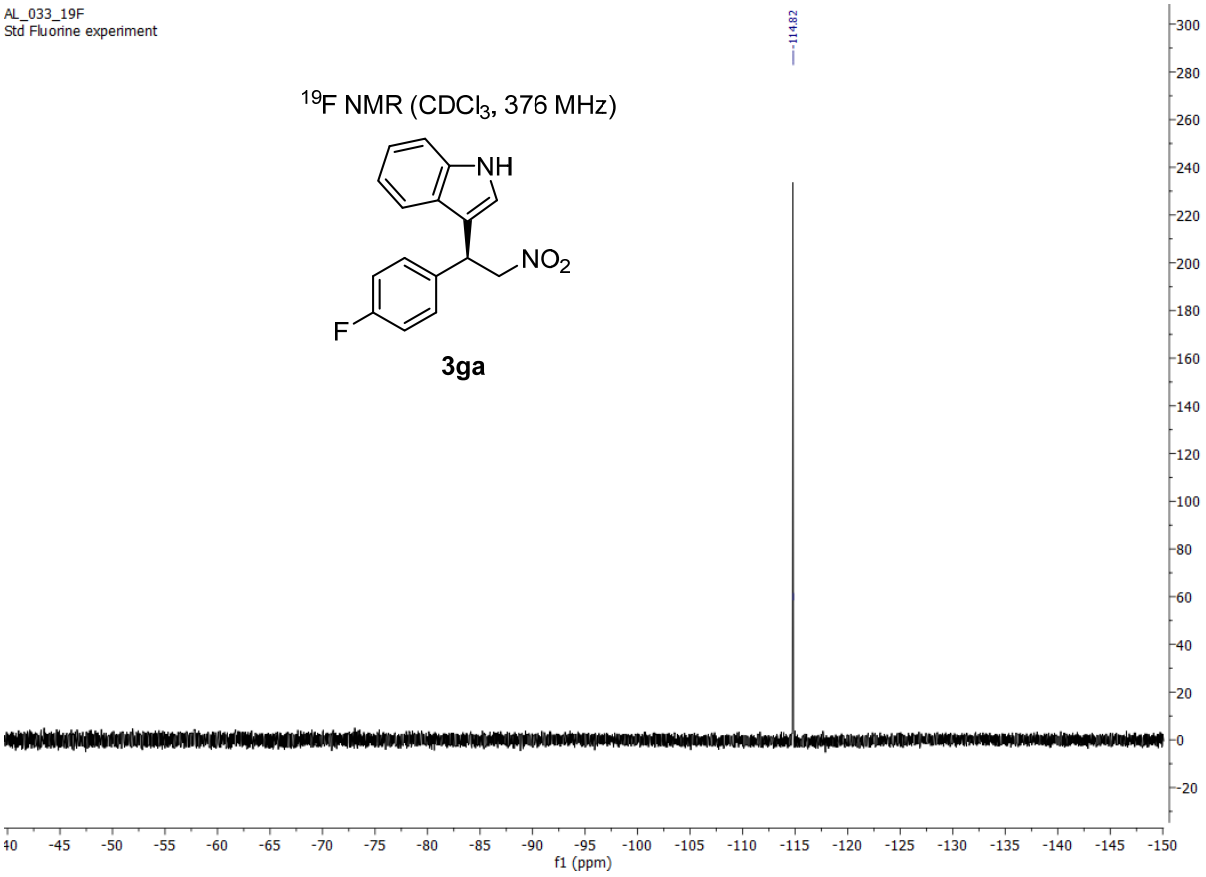
AL_033_19F
Std Fluorine experiment
-114.82
^{19}F NMR ($CDCl_3$, 376 MHz)
NH
NO_2
F
3ga
f1 (ppm)

HPLC traces of compounds *rac*-3ga and 3ga

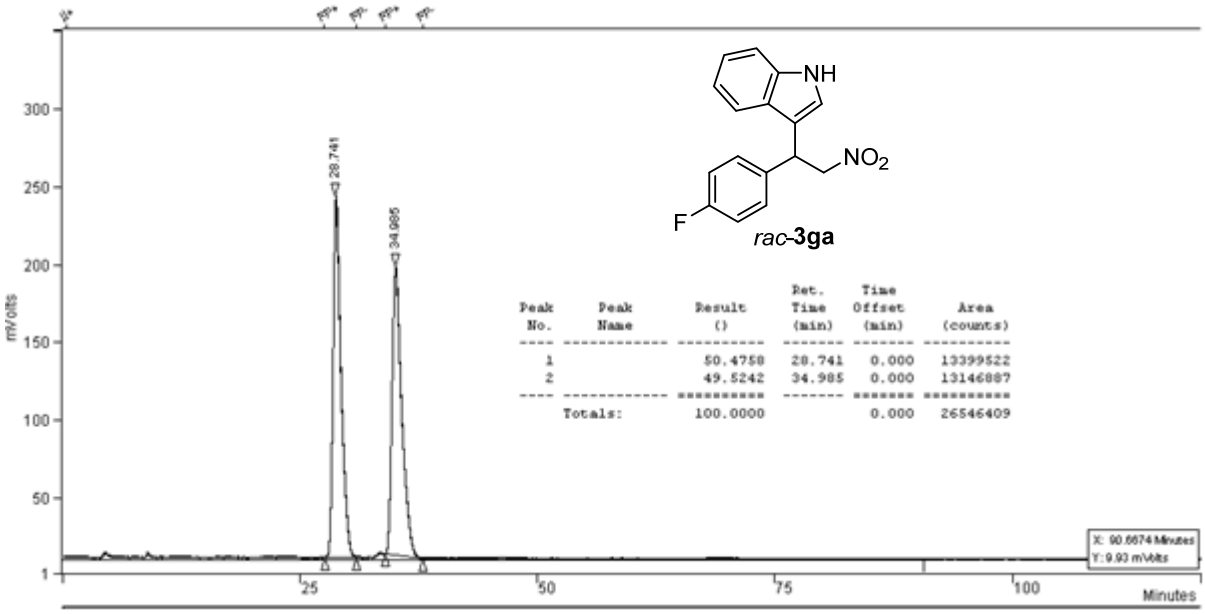

Peak No.	Peak Name	Result ()	Ret. Time (min)	Time Offset (min)	Area (counts)
1		50.4758	28.741	0.000	13399522
2		49.5242	34.985	0.000	13146887
	Totals:	100.0000		0.000	26546409

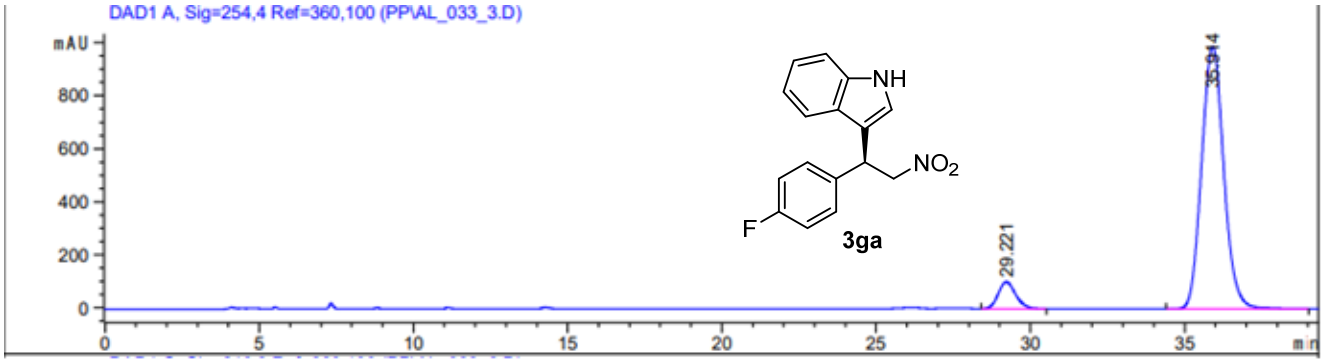

Signal 1: DAD1 A, Sig=254,4 Ref=360,100

Peak #	RetTime [min]	Type	Width [min]	Area [mAU*s]	Height [mAU]	Area %
1	29.221	VB	0.6032	4002.38721	101.68901	7.5007
2	35.914	BBA	0.7860	4.93575e4	989.38409	92.4993
Totals :				5.33598e4	1091.07310	

(*S*)-3-(1-(4-Chlorophenyl)-2-nitroethyl)-1*H*-indole (3ha)

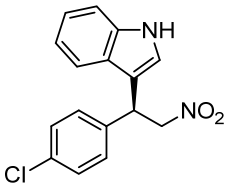

Following the general procedure (48 h reaction time), the title compound was obtained in 52% yield after chromatography on silica gel. The enantiomeric excess of the product was determined by CSP HPLC: ADH column, *n*-hexane/*i*-PrOH 90:10, 0.75 mL/min, t_{maj} = 39.9 min; t_{min} = 30.4 min, 87% ee.

Spectral data are in accordance with the literature.[23]

^{1}H NMR ($CDCl_3$, 400 MHz) δ= 8.12 (br s, 1H), 7.38 (m, 2H), 7.32 – 7.25 (m, 4H), 7.23 – 7.17 (m, 1H), 7.09 (ddd, J = 8.1, 7.1, 1.0 Hz, 1H), 7.02 (dd, J = 2.5, 0.9 Hz, 1H), 5.17 (t, J = 8.4 Hz, 1H), 5.06 (dd, J = 12.5, 7.3 Hz, 1H), 4.91 (dd, J = 12.5, 8.6 Hz, 1H).

^{13}C NMR ($CDCl_3$, 101 MHz) δ= 137.7, 136.5, 133.4, 129.1, 125.9, 122.9, 121.5, 120.1, 118.8, 114.0, 111.4, 79.3, 40.9.

$[\alpha]_D^{RT}$ = +4.4 (c = 0.5, CH_2Cl_2).

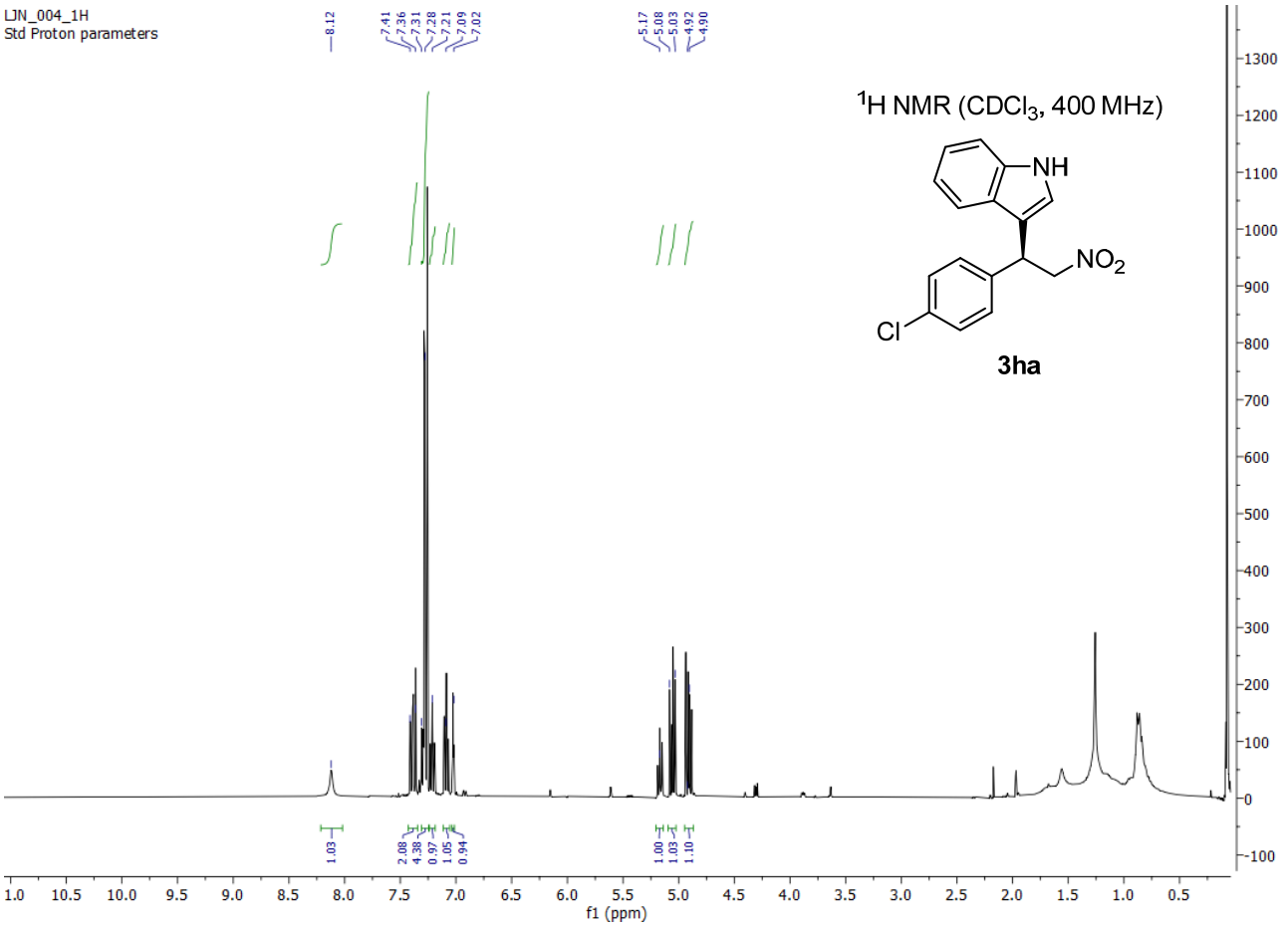

^{1}H NMR ($CDCl_3$, 400 MHz)

3ha

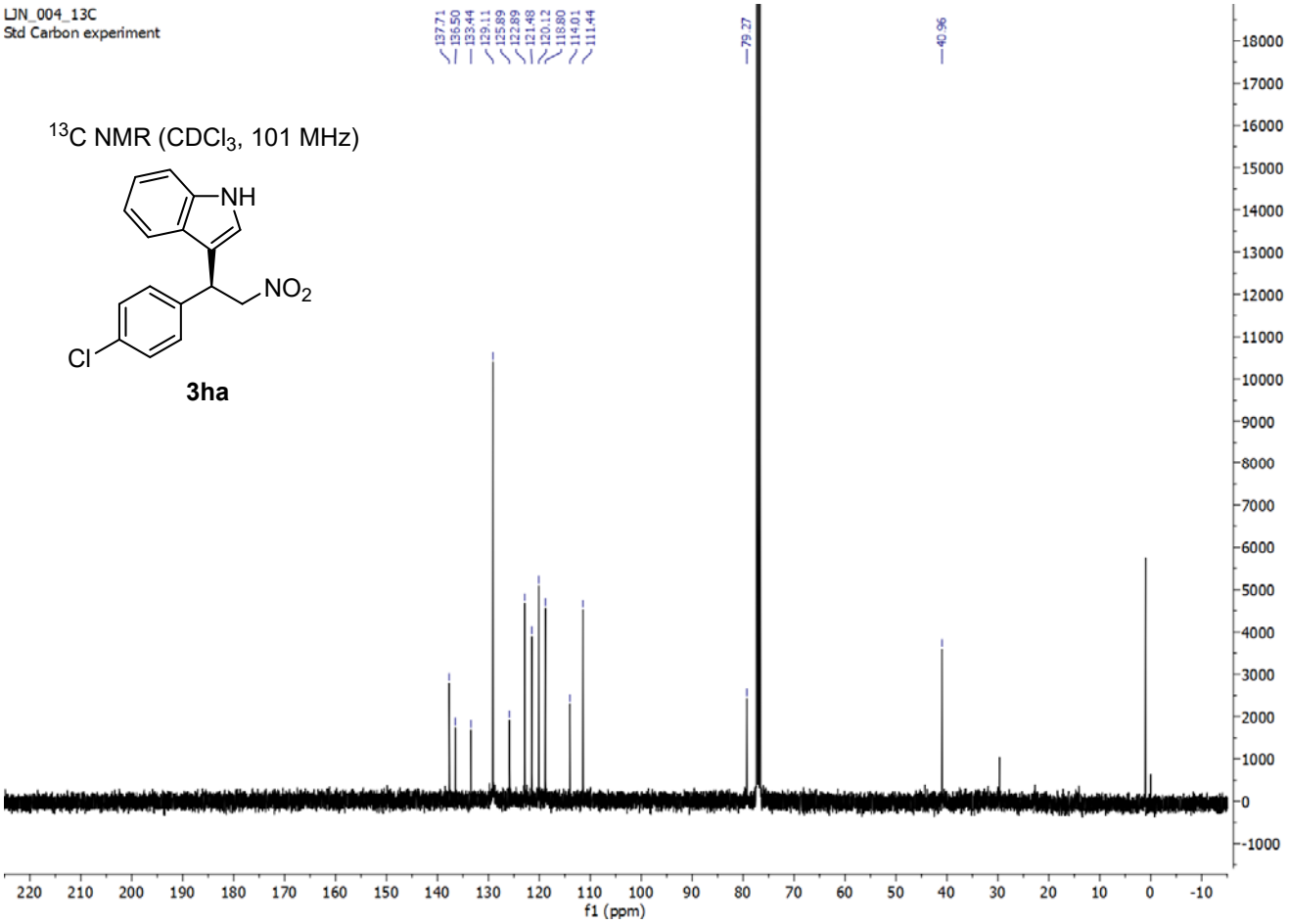

^{13}C NMR ($CDCl_3$, 101 MHz)

3ha

HPLC traces of compounds *rac*-3ha and 3ha

Sample Info : PP_003, 0.75 mL/min, 90:10 hex:ipr, 25°C, AD-H

Additional Info : Peak(s) manually integrated

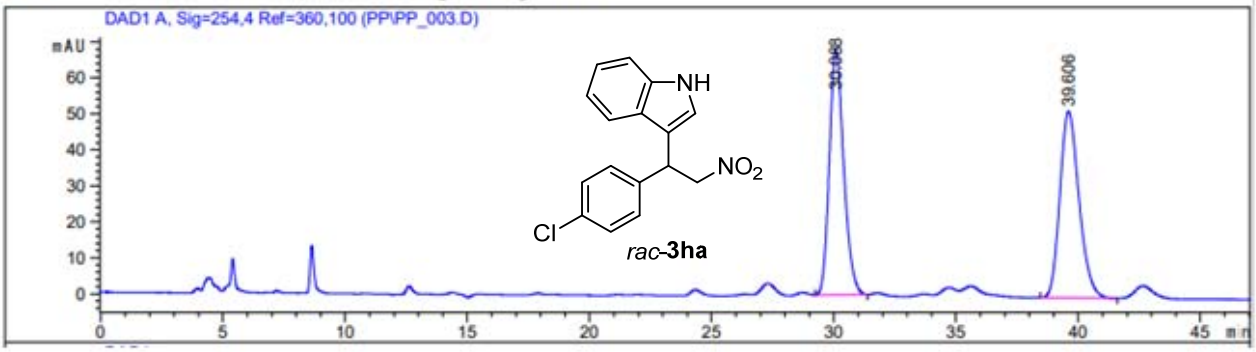

Signal 1: DAD1 A, Sig=254,4 Ref=360,100

Peak #	RetTime [min]	Type	Width [min]	Area [mAU*s]	Height [mAU]	Area %
1	30.088	BB	0.6219	2781.51172	68.19021	49.5568
2	39.606	BB	0.8304	2831.25806	51.90477	50.4432
Totals :				5612.76978	120.09498	

Sample Info : LJN_004, 0.75 mL/min, 90:10 hex:ipr, 25°C, AD-H

Additional Info : Peak(s) manually integrated

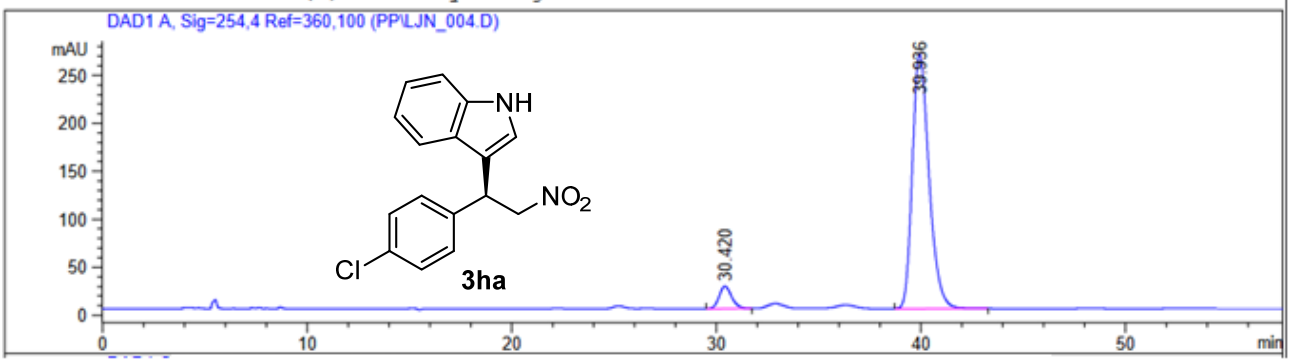

Signal 1: DAD1 A, Sig=254,4 Ref=360,100

Peak #	RetTime [min]	Type	Width [min]	Area [mAU*s]	Height [mAU]	Area %
1	30.420	BB	0.6506	995.71637	23.39368	6.2098
2	39.936	BB	0.8684	1.50390e4	265.69870	93.7902
Totals :				1.60347e4	289.09238	

(*S*)-3-(1-(4-Methoxyphenyl)-2-nitroethyl)-1*H*-indole (3ia)

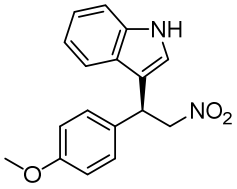

Following the general procedure (96 h reaction time), the title compound was obtained in 43% yield after chromatography on silica gel. The enantiomeric excess of the product was determined by CSP HPLC: ODH column, *n*-hexane/*i*-PrOH 70:30, 0.75 mL/min, t_{maj} = 30.2 min; t_{min} = 37.1 min, 90% ee.

Spectral and optical data are in accordance with the literature.[23]

^{1}H NMR ($CDCl_3$, 400 MHz) δ= 8.08 (br s, 1H), 7.44 (d, J = 7.9 Hz, 1H), 7.36 (d, J = 8.2 Hz, 1H), 7.28 – 7.23 (m, 2H), 7.20 (ddd, J = 8.2, 7.0, 1.2 Hz, 1H), 7.08 (ddd, J = 8.0, 7.0, 1.0 Hz, 1H), 7.02 (dd, J = 2.5, 0.9 Hz, 1H), 6.88 – 6.82 (m, 2H), 5.14 (t, J = 8.1 Hz, 1H), 5.05 (dd, J = 12.3, 7.5 Hz, 1H), 4.90 (dd, J = 12.3, 8.4 Hz, 1H), 3.78 (s, 3H).

^{13}C NMR ($CDCl_3$, 101 MHz) δ= 158.9, 136.5, 131.1, 128.8, 126.1, 122.7, 121.4, 119.9, 119.0, 114.8, 114.3, 111.3, 79.7, 55.2, 40.8.

$[\alpha]_D^{RT}$ = +15.0 (c = 0.5, CH_2Cl_2).

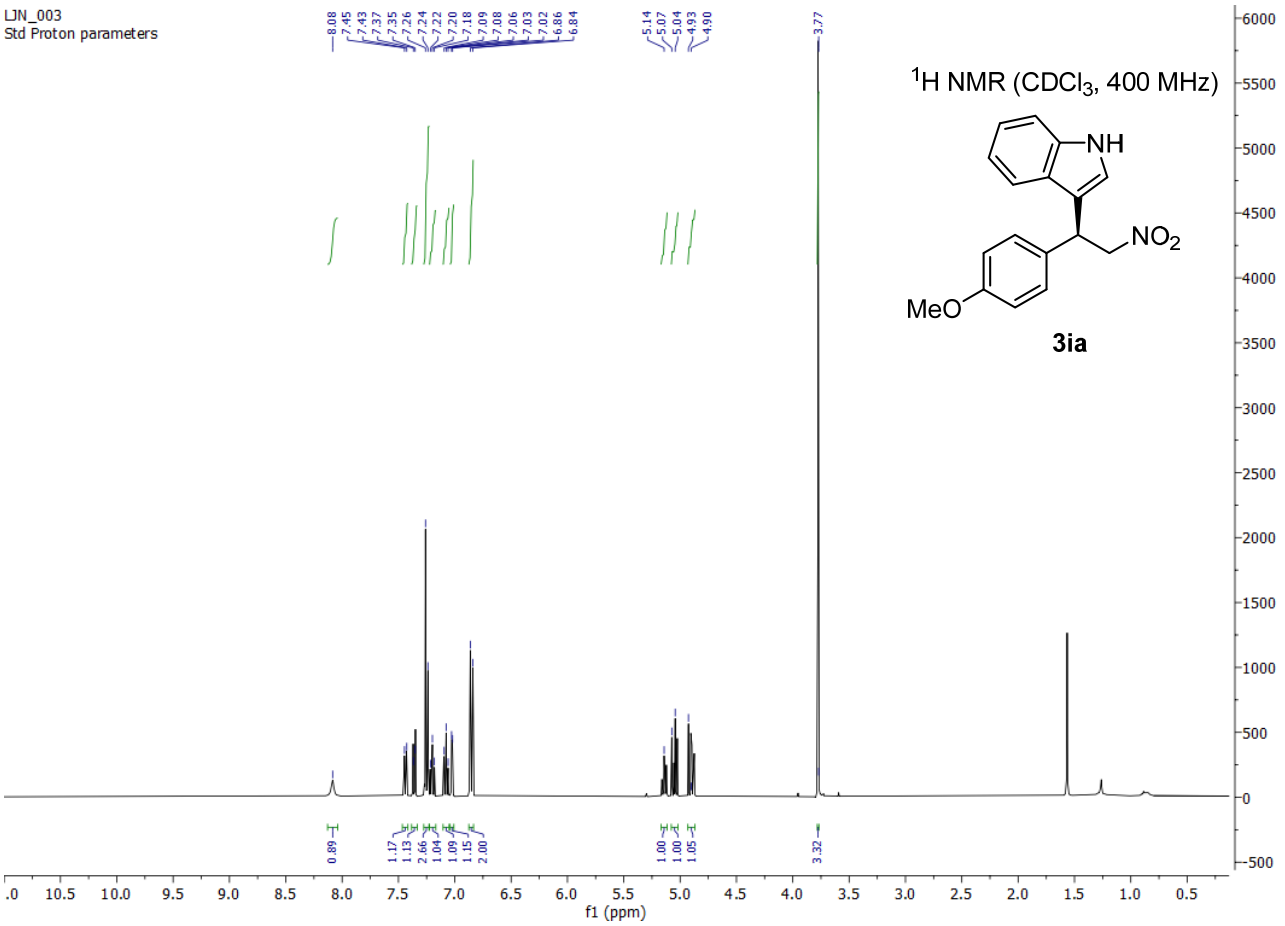

^{1}H NMR ($CDCl_3$, 400 MHz)

3ia

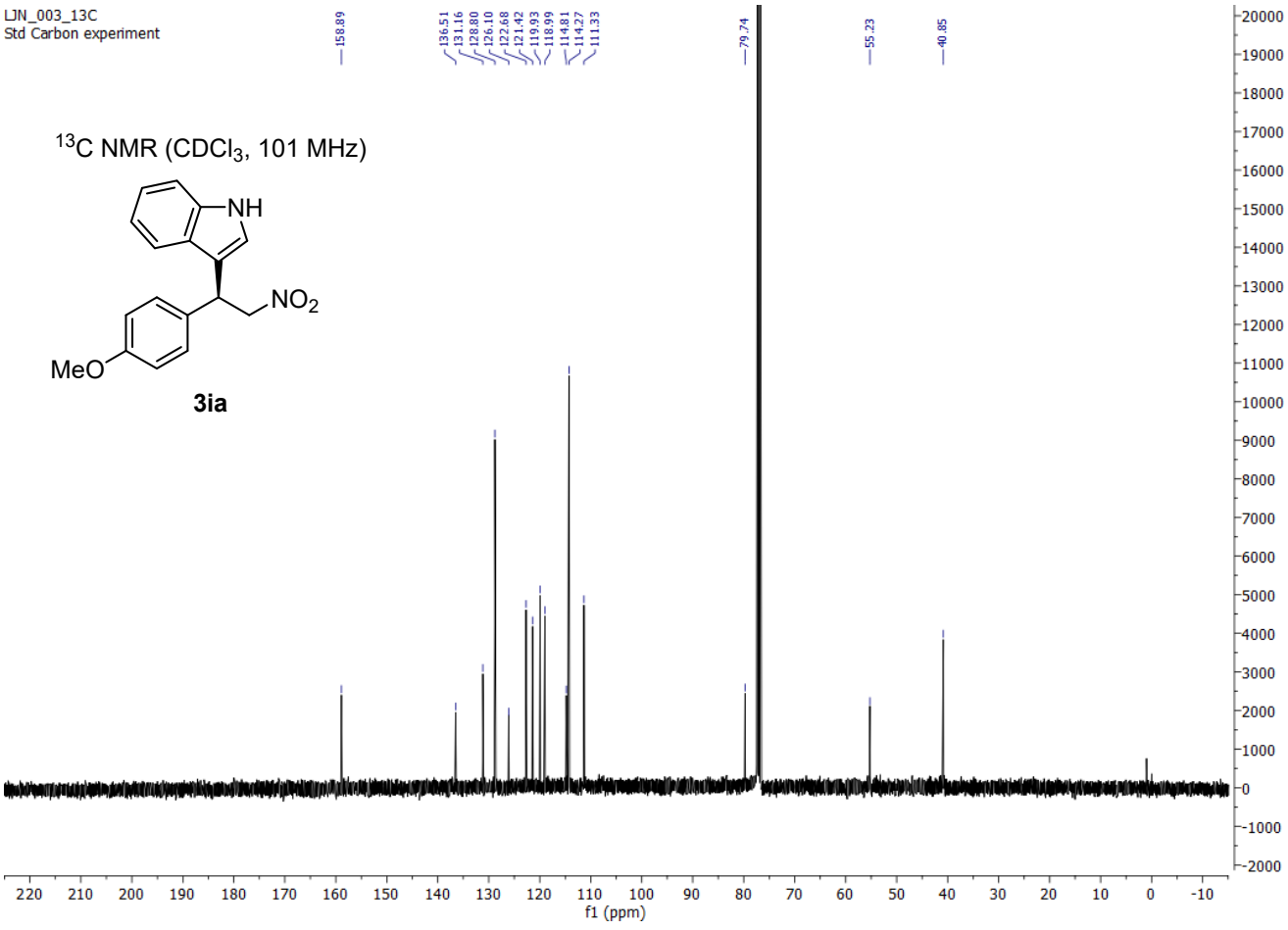

^{13}C NMR ($CDCl_3$, 101 MHz)

3ia

HPLC traces of compounds *rac*-3ia and 3ia

Sample Info : PP_002_4, 0.75 mL/min, 70:30 hex:ipr, 25°C, OD-H

Additional Info : Peak(s) manually integrated

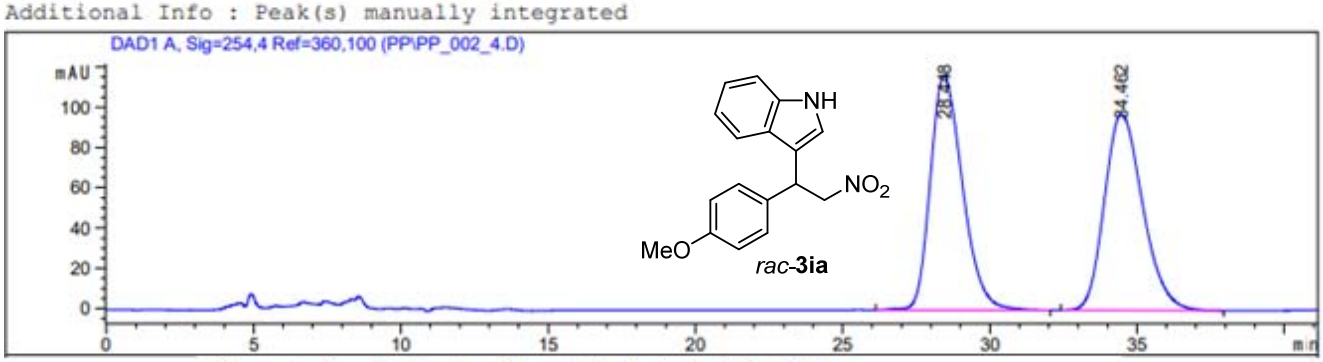

Signal 1: DAD1 A, Sig=254,4 Ref=360,100

Peak #	RetTime [min]	Type	Width [min]	Area [mAU*s]	Height [mAU]	Area %
1	28.448	BB	1.1578	8874.04590	116.62094	50.1747
2	34.462	BB	1.3415	8812.25195	97.03848	49.8253
Totals :				1.76863e4	213.65942	

Sample Info : LJN_003_3 0.75mL/min, 70:30 hex:ipr, 25°C, OD-H

Additional Info : Peak(s) manually integrated

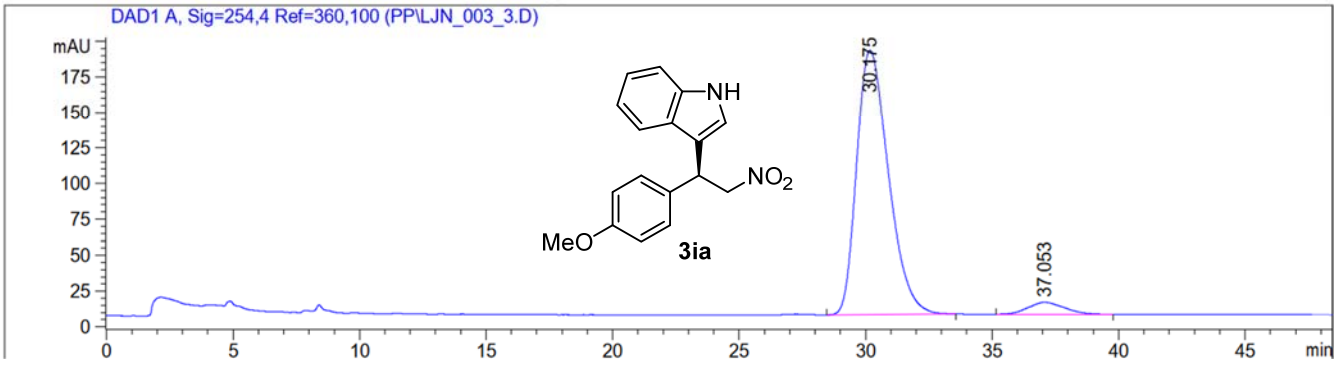

Signal 1: DAD1 A, Sig=254,4 Ref=360,100

Peak #	RetTime [min]	Type	Width [min]	Area [mAU*s]	Height [mAU]	Area %
1	30.175	BB	1.3262	1.61484e4	185.02118	95.0000
2	37.053	BB	1.1774	849.91437	8.50862	5.0000
Totals :				1.69983e4	193.52980	

(*S*)-3-(1-(Furan-2-yl)-2-nitroethyl)-1*H*-indole (3ja)

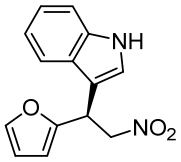

Following the general procedure (48 h reaction time), the title compound was obtained in 65% yield after chromatography on silica gel. The enantiomeric excess of the product was determined by CSP HPLC: ODH column, *n*-hexane/*i*-PrOH 80:20, 0.75 mL/min, t_{maj} = 46.2 min; t_{min} = 31.8 min, 92% ee.

Spectral and optical data are in accordance with literature.[19,24]

^{1}H NMR ($CDCl_3$, 400 MHz) δ= 8.12 (br s, 1H), 7.57 (d, J = 8.0 Hz, 1H), 7.42 – 7.34 (m, 2H), 7.23 (ddd, J = 8.2, 7.0, 1.2 Hz, 1H), 7.17 – 7.11 (m, 2H), 6.32 (dd, J = 3.3, 1.9 Hz, 1H), 6.17 (dt, J = 3.3, 0.9 Hz, 1H), 5.26 (t, J = 8.2 Hz, 1H), 5.06 (dd, J = 12.5, 8.1 Hz, 1H), 4.93 (dd, J = 12.5, 7.4 Hz, 1H).

^{13}C NMR ($CDCl_3$, 101 MHz) δ= 152.2, 142.2, 136.3, 125.7, 122.7, 120.1, 118.7, 111.7, 111.5, 110.5, 107.4, 77.9, 35.7.

$[\alpha]_D^{RT}$ = -35.6 (c = 0.5, CH_2Cl_2).

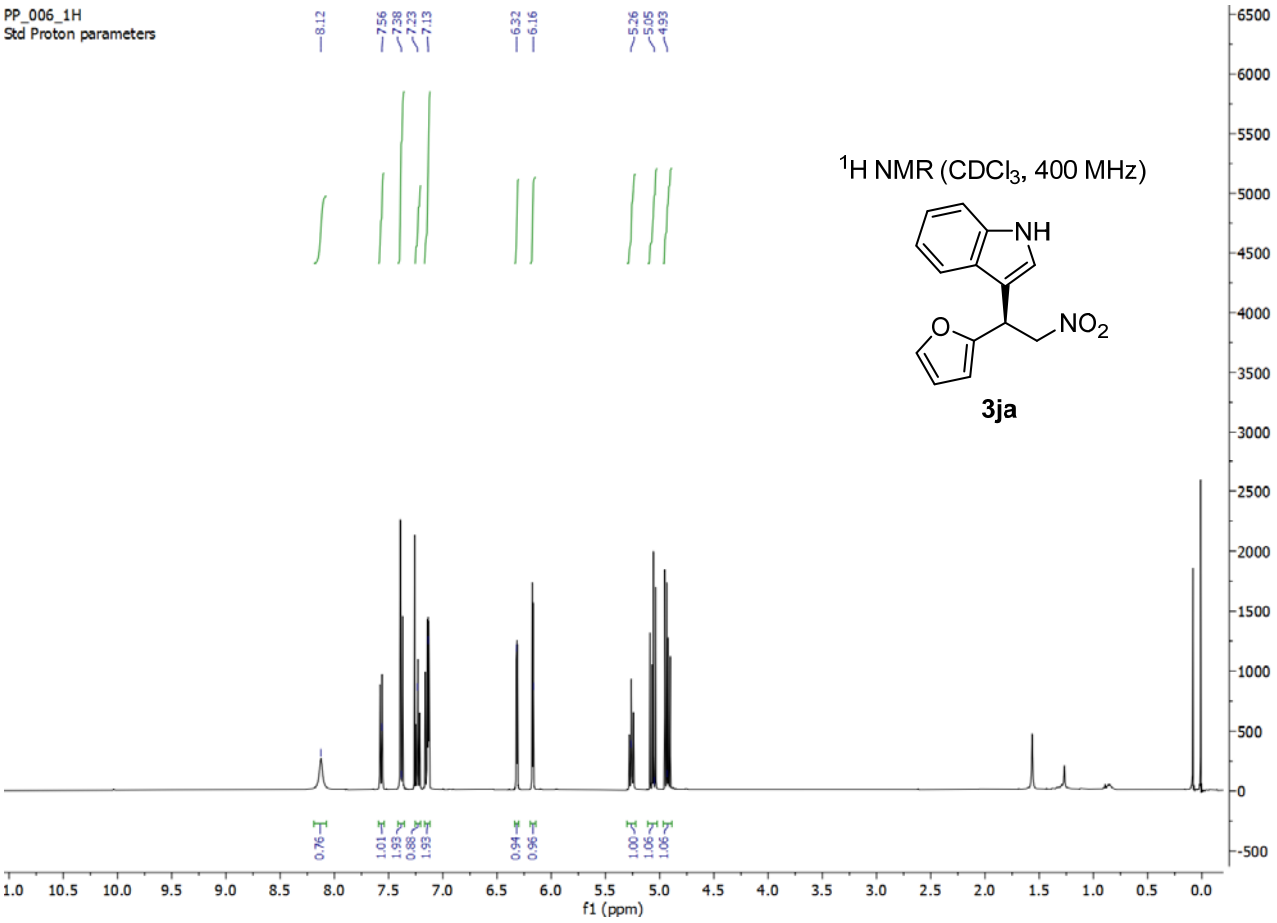

^{1}H NMR ($CDCl_3$, 400 MHz)

3ja

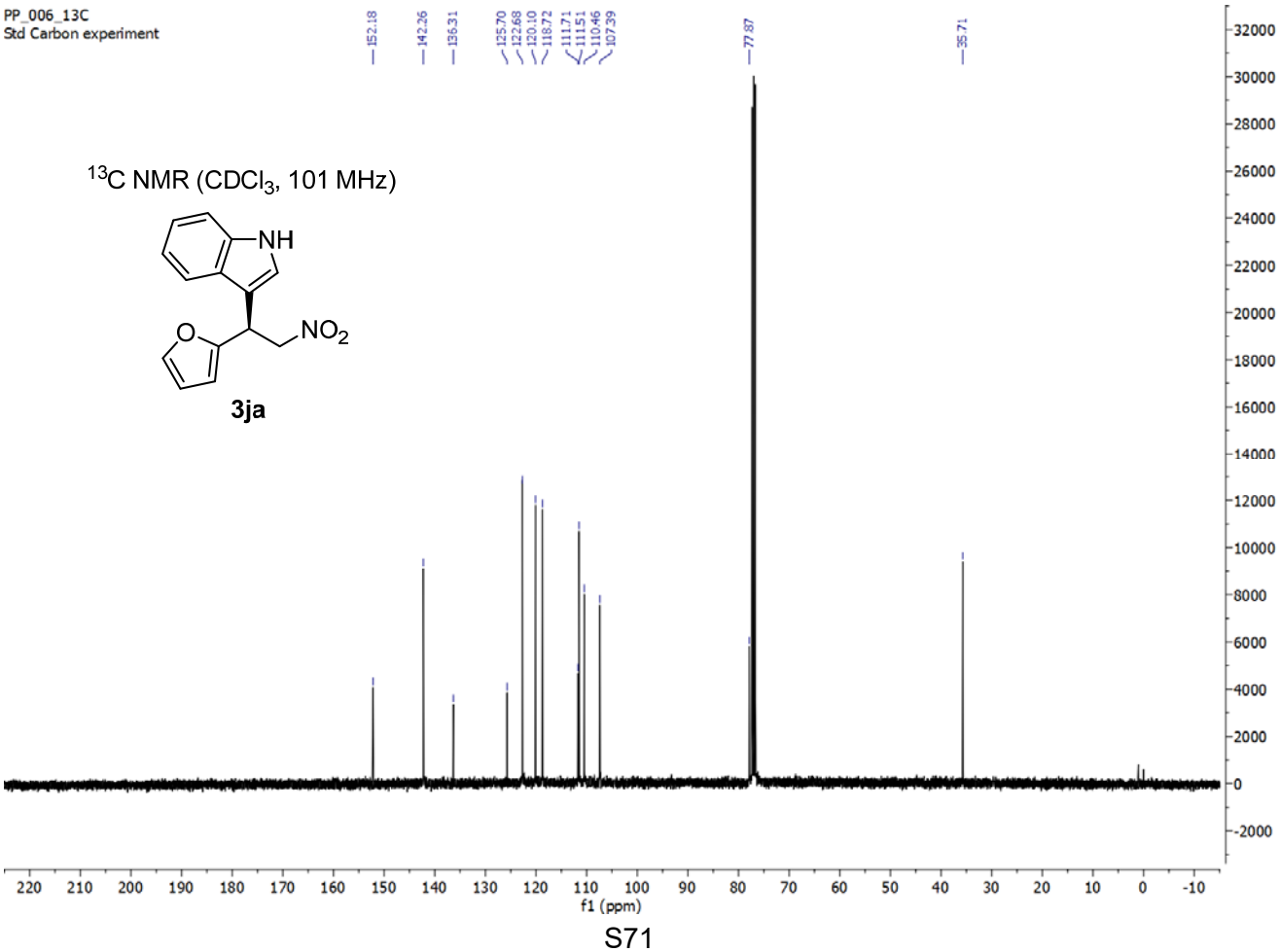

^{13}C NMR ($CDCl_3$, 101 MHz)

3ja

HPLC traces of compounds *rac*-3ja and 3ja

Sample Info : PP_005_3, 0.75 mL/min, 80:20 hex:ipr, 25°C, OD-H

Additional Info : Peak(s) manually integrated

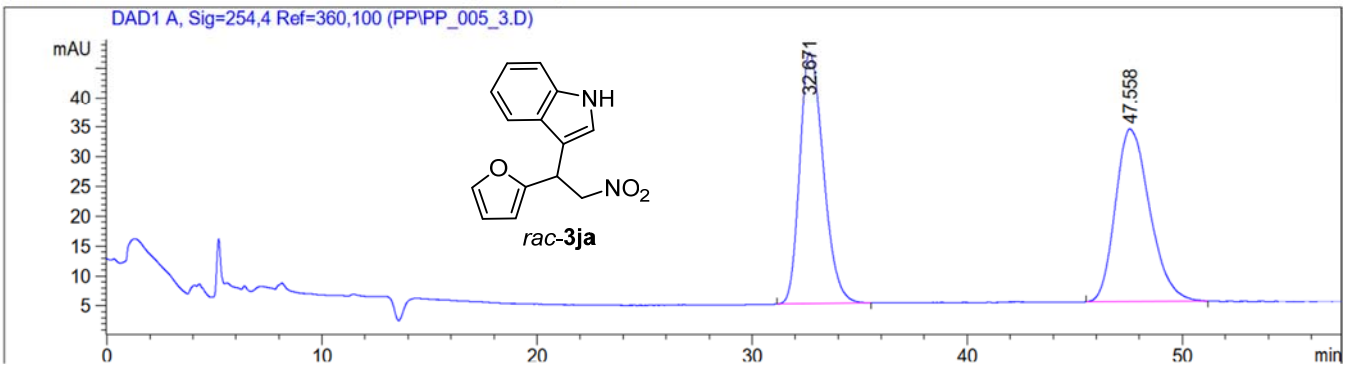

Signal 1: DAD1 A, Sig=254,4 Ref=360,100

Peak #	RetTime [min]	Type	Width [min]	Area [mAU*s]	Height [mAU]	Area %
1	32.671	BB	1.0692	3227.05713	42.24760	50.0279
2	47.558	BB	1.3757	3223.45898	28.98003	49.9721
Totals :				6450.51611	71.22763	

Sample Info : LJN_010_purified 0.75mL/min, 80:20 hex:ipr, 25°C, OD-H

Additional Info : Peak(s) manually integrated

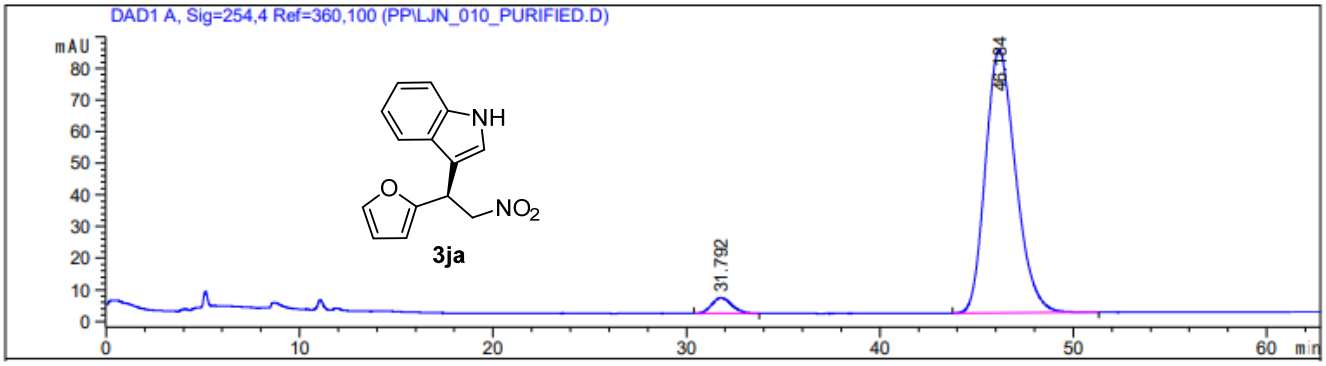

Signal 1: DAD1 A, Sig=254,4 Ref=360,100

Peak #	RetTime [min]	Type	Width [min]	Area [mAU*s]	Height [mAU]	Area %
1	31.792	BB	0.9853	358.86365	4.90655	3.8164
2	46.184	BB	1.6761	9044.43457	83.21251	96.1836
Totals :				9403.29822	88.11905	

(*S*)-3-(2-Nitro-1-(thiophen-2-yl)ethyl)-1*H*-indole (3ka)

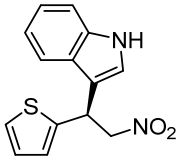

Following the general procedure (48 h reaction time), the title compound was obtained in 58% yield after chromatography on silica gel. The enantiomeric excess of the product was determined by CSP HPLC: ODH column, *n*-hexane/*i*-PrOH 80:20, 1 mL/min, t_{maj} = 41.3 min; t_{min} = 37.4 min, 93% ee.

Spectral and optical data are in accordance with the literature.[18,19]

^{1}H NMR ($CDCl_3$, 400 MHz) δ= 8.13 (br s, 1H), 7.53 (d, J = 8.0 Hz, 1H), 7.38 (d, J = 8.2 Hz, 1H), 7.25 – 7.19 (m, 2H), 7.16 – 7.09 (m, 2H), 7.00 (ddd, J = 3.5, 1.3, 0.9 Hz, 1H), 6.95 (dd, J = 5.1, 3.5 Hz, 1H), 5.47 (t, J = 8.3 Hz, 1H), 5.06 (dd, J = 12.5, 7.5 Hz, 1H), 4.99 (dd, J = 12.5, 8.2 Hz, 1H).

^{13}C NMR ($CDCl_3$, 101 MHz) δ= 142.9, 136.4, 126.9, 125.7, 125.2, 124.9, 122.8, 121.8, 120.1, 118.8, 114.1, 111.5, 80.0, 36.9.

$[\alpha]_D^{RT}$ = +18.6 (c = 0.5, CH_2Cl_2).

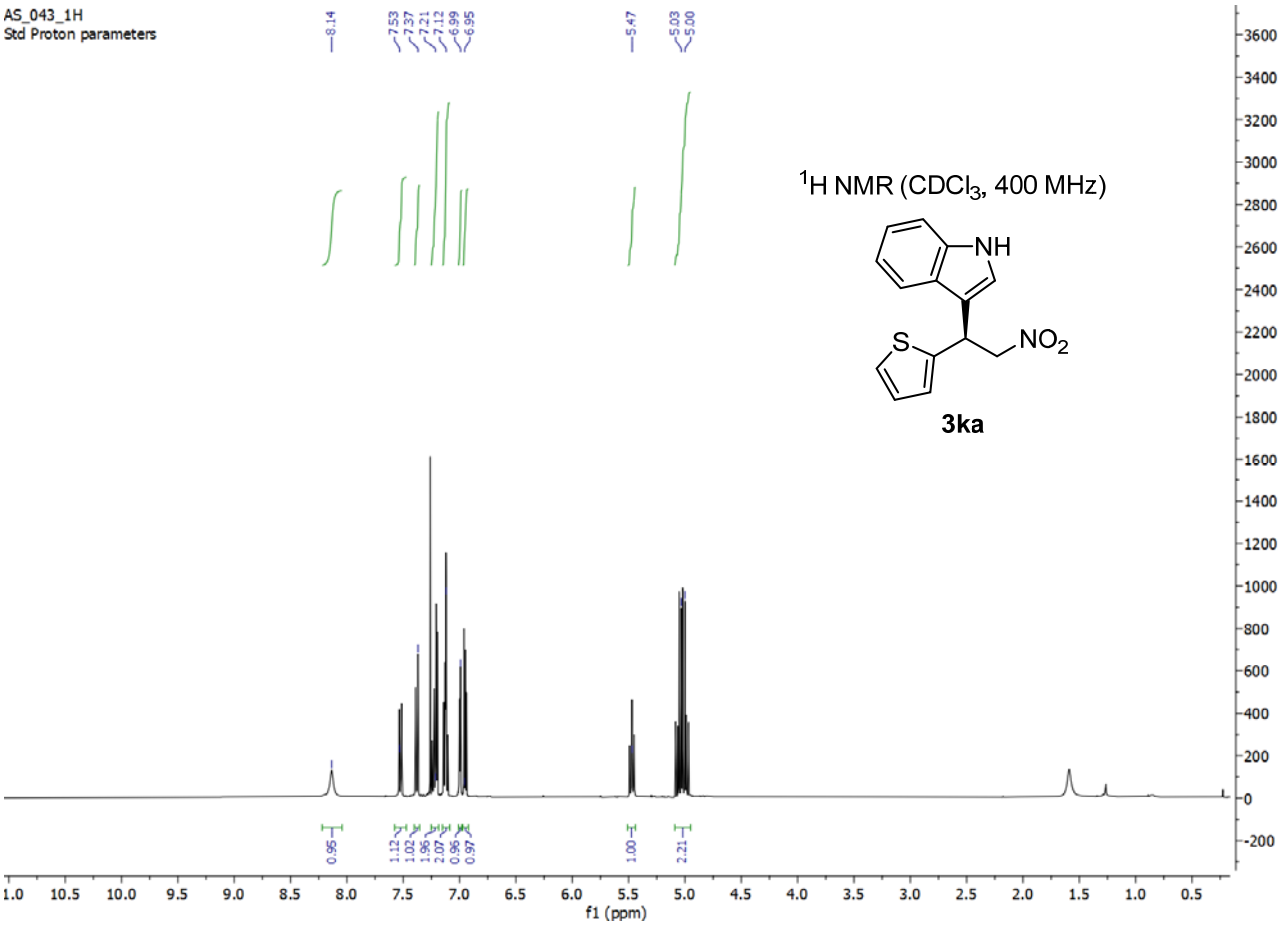

^{1}H NMR ($CDCl_3$, 400 MHz)

3ka

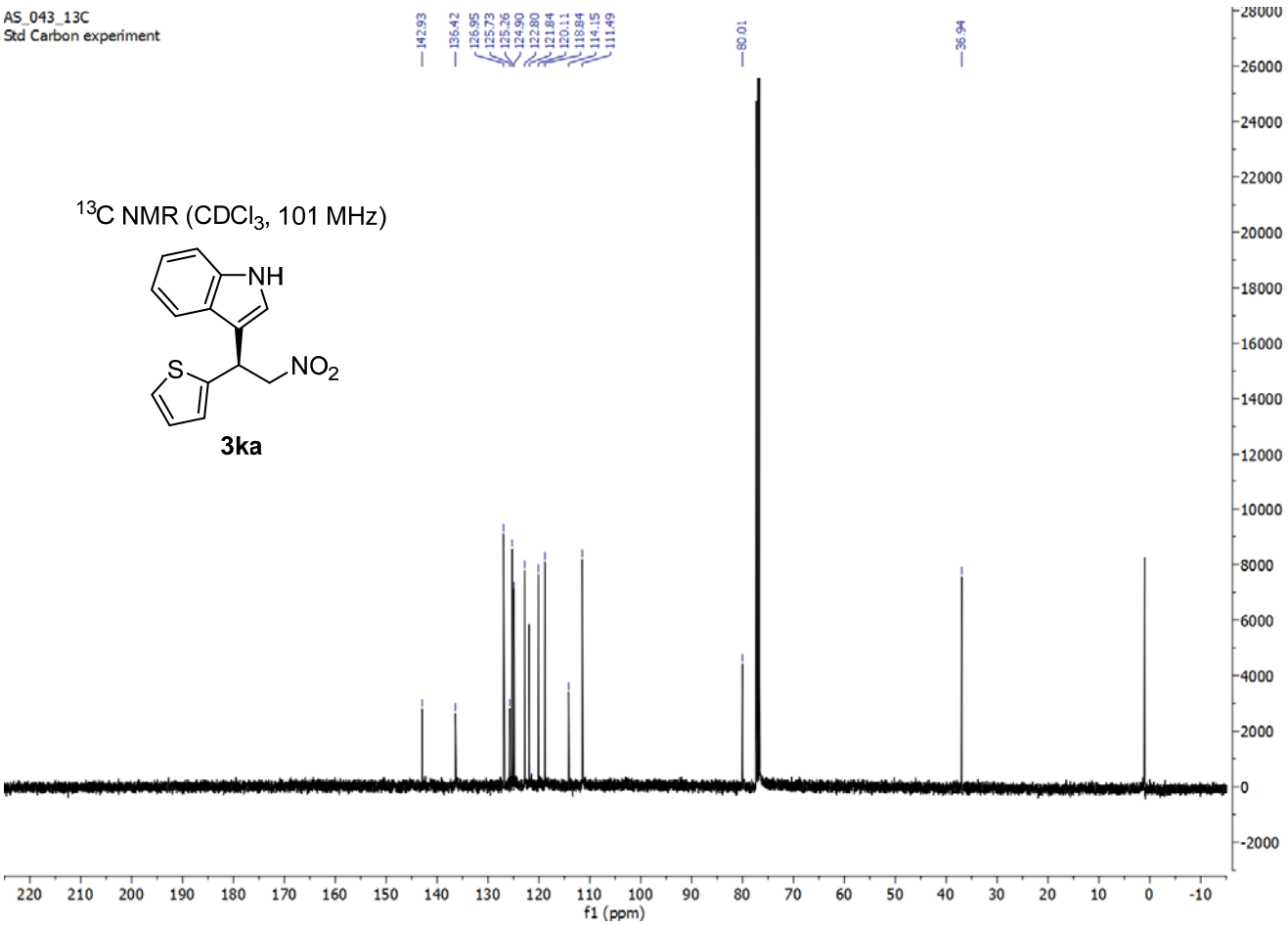

^{13}C NMR ($CDCl_3$, 101 MHz)

3ka

HPLC traces for compounds *rac*-3ka and 3ka

Sample Info : AS_042_80-20, 1,0 mL/min, 80:20 hex:ipr, 25°C, OD-H

Additional Info : Peak(s) manually integrated

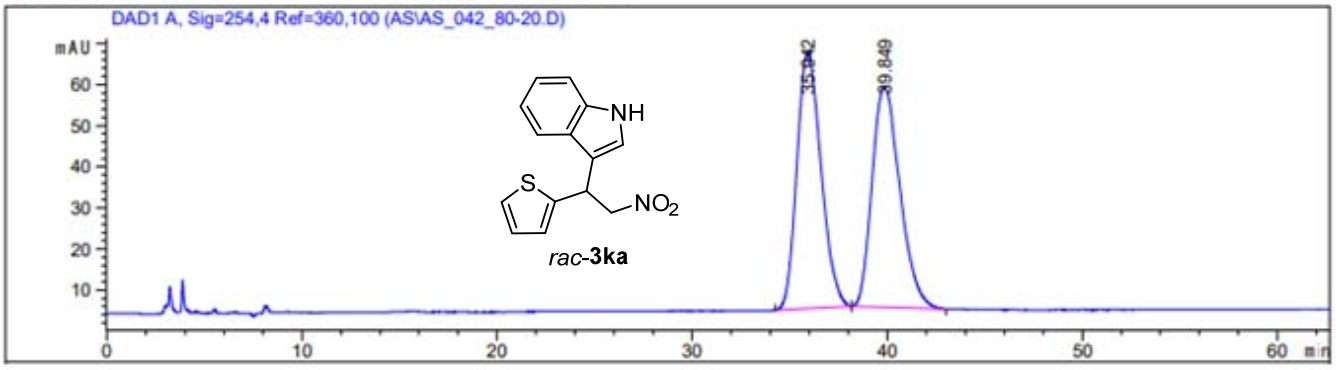

Signal 1: DAD1 A, Sig=254,4 Ref=360,100

Peak #	RetTime [min]	Type	Width [min]	Area [mAU*s]	Height [mAU]	Area %
1	35.942	BB	1.1754	5346.92188	62.54193	50.0859
2	39.849	BB	1.3314	5328.58008	53.71164	49.9141
Totals :				1.06755e4	116.25357	

Sample Info : AS_043_GIUSTO, 1.00 mL/min, 80:20 hex:ipr, 25°C, OD-H

Additional Info : Peak(s) manually integrated

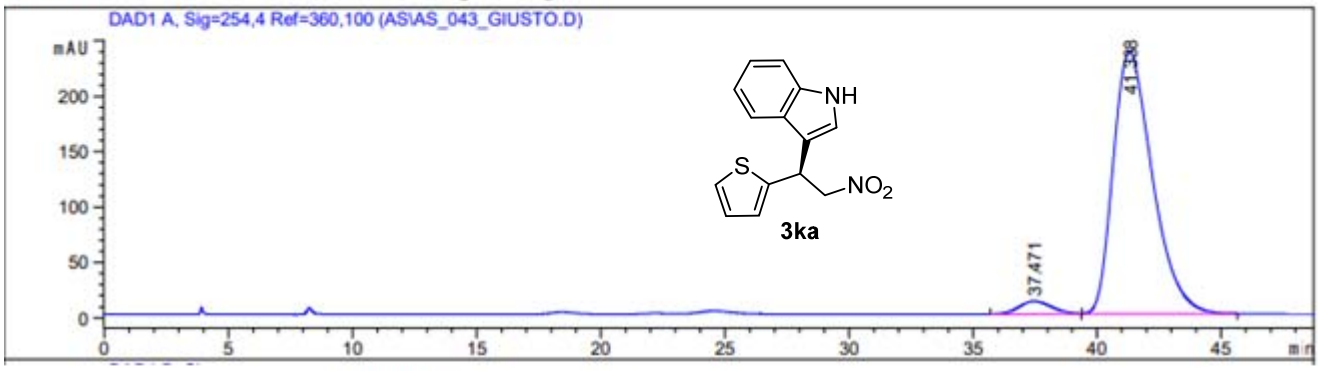

Signal 1: DAD1 A, Sig=254,4 Ref=360,100

Peak #	RetTime [min]	Type	Width [min]	Area [mAU*s]	Height [mAU]	Area %
1	37.471	BB	1.0654	1007.51843	11.33080	3.7425
2	41.338	BB	1.5768	2.59133e4	236.04610	96.2575
Totals :				2.69208e4	247.37690	

References

[1] (a) Xia, X.-F.; Shu, X.-Z.; Ji, K.-G.; Yang, Y.-F.; Shaukat, A.; Liu, X.-Y.; Liang, Y.-M. Platinum-Catalyzed Michael Addition and Cyclization of Tertiary Amines with Nitroolefins by Dehydrogenation of α,β-sp^3 C−H Bonds. *J. Org. Chem.* **2010**, *75*, 2893; (b) Ferraro, A.; Bernardi, L.; Fochi, M. Organocatalytic Enantioselective Transfer Hydrogenation of β-Amino Nitroolefins. *Adv. Synth. Catal.* **2016**, *358*, 1561; (c) Indolone spiral shell thiophane class compound and its salt, preparation method and application. CN107235992, 2017, A.

[2] Approximate value determined by ^{1}H NMR according to: Grasdalen, H.; Larsen, B.; Smidsrød, O. A P.M.R. study of the composition and sequence of urinate residues in alginates. *Carbohydr. Res.* **1979**, *68*, 23.

[3] Skjåk-Bræk, G.; Smidsrød, O.; Larsen, B. Tailoring of alginates by enzymatic modification in vitro. *Int. J. Biol. Macromol.*, **1986**, *8*, 330.

[4] Agulhon, P.; Robitzer, M.; David, L.; Quignard, F. Structural Regime Identification in Ionotropic Alginate Gels: Influence of the Cation Nature and Alginate Structure. *Biomacromol.* **2012**, *13*, 215.

[5] (a) Corma, A.; García, H.; Moussaif, A.; Sabater, M. J.; Zniberb, R.; Redouane, A. Chiral copper(II) bisoxazoline covalently anchored to silica and mesoporous MCM-41 as a heterogeneous catalyst for the enantioselective Friedel–Crafts hydroxyalkylation. *Chem. Commun.* **2002**, 1058; (b) Rosa Silva, A.; Albuquerque, H.; Borges, S.; Siegel, R.; Mafra, L.; Carvalho, A. P.; Pires, J. Strategies for copper bis(oxazoline) immobilization onto porous silica based materials. *Microporous Mesoporous Mater.* **2012**, *158*, 26.

[6] (a) Gong, W.; Chen, Z.; Dong, J.; Liu, Y.; Cui, Y. Chiral Metal-Organic Frameworks. *Chem. Rev.* **2022**, *122*, 9078–9144; (b) Han, X.; Yuan, C.; Hou, B.; Liu, L.; Li, H.; Liu, Y.; Cui, Y. Chiral covalent organic frameworks: design, synthesis and property. *Chem. Soc. Rev.* **2020**, *49*, 6248–6272; (c) Dybtsev, D. N.; Bryliakov, K. P. Asymmetric catalysis using metal-organic frameworks. *Coord. Chem. Rev.* **2021**, *437*, 213845; (d) Sanchez-Fuente, M.; Alonso-Gómez, J. L.; Salonen, L. M.; Mas-Ballesté, R.; Moya, A. Chiral Porous Organic Frameworks: Synthesis, Chiroptical Properties, and Asymmetric Organocatalytic Applications. *Catalysts* **2023**, *13*, 1042. (e) El-Kaderi, H. M.; Hunt, J. R.; Mendoza-Cortés, J. L.; Côté, A. P.; Taylor, R. E.; O'Keeffe, M.; Yaghi, O. M. Designed Synthesis of 3D Covalent Organic Frameworks. *Science* **2007**, *316*, 268.

[7] Pettignano, A.; Bernardi, L.; Fochi, M.; Geraci, L.; Robitzer, M.; Tanchoux, N.; Quignard, F. Alginic acid aerogel: a heterogeneous Brønsted acid promoter for the direct Mannich reaction. *New J. Chem.* **2015**, *39*, 4222.

[8] Shukla, M. S.; Hande, P. E.; Chandra, S. Porous Silica Support for Immobilizing Chiral Metal Catalyst: Unravelling the Activity of Catalyst on Asymmetric Organic Transformations. *ChemistrySelect* **2022**, *7*, e202200549.

[9] (a) Itoh, J.; Fuchibe, K.; Akiyama, T. Chiral Phosphoric Acid Catalyzed Enantioselective Friedel–Crafts Alkylation of Indoles with Nitroalkenes: Cooperative Effect of 3 Å Molecular Sieves. *Angew. Chem. Int. Ed.* **2008**, *47*, 4016; (b) Romanini, S.; Galletti, E.; Caruana, L.; Mazzanti, A.; Himo, F.; Santoro, S.; Fochi, M.; Bernardi, L. Catalytic Asymmetric Reactions of 4-Substituted Indoles with Nitroethene: A Direct Entry to Ergot Alkaloid Structures. *Chem. Eur. J.* **2015**, *21*, 17578, and references cited therein.

[10] Bordwell, F. G.; Drucker, G. E.; Fried, H. E. Acidities of carbon and nitrogen acids: the aromaticity of the cyclopentadienyl anion. *J. Org. Chem.* **1981**, *46*, 632.

[11] Tsubogo, T.; Kano, Y.; Yamashita, Y.; Kobayashi, S. Highly enantioselective Friedel-Crafts-type alkylation reactions of indoles with chalcone derivatives using a chiral barium catalyst. *Chem. Asian J.* **2010**, *5*, 1974.

[12] Agulhon, P.; Markova, V.; Robitzer, M.; Quignard, F.; Mineva, T. Structure of Alginate Gels: Interaction of Diuronate Units with Divalent Cations from Density Functional Calculations. *Biomacromol.* **2012**, *13*, 1899.

[13] (a) Hirata, T.; Yamanaka, M. DFT Study of Chiral-Phosphoric-Acid-Catalyzed Enantioselective Friedel–Crafts Reaction of Indole with Nitroalkene: Bifunctionality and Substituent Effect of Phosphoric Acid. *Chem. Asian J.* **2011**, *6*, 510; (b) Liu, C.; Han, P.; Wu, X.; Tang, M. The mechanism investigation of chiral phosphoric acid-catalyzed Friedel–Crafts reactions – How the chiral phosphoric acid regains the proton. *Comput. Theor. Chem.* **2014**, *1050*, 39; (c) Méndez, I.; Rodríguez, R.; Polo, V.; Passarelli, V.; Lahoz, F. J.; García-Orduña, P.; Carmona, D. Temperature Dual Enantioselective Control in a Rhodium-Catalyzed Michael-Type Friedel–Crafts Reaction: A Mechanistic Explanation. *Chem. Eur. J.* **2016**, *22*, 11064.

[14] Hu, C.; Lu, W.; Mata, A.; Nishinari, K.; Fang, Y. Ions-induced gelation of alginate: Mechanisms and applications. *Int. J. Biol. Macromol.* **2021**, *177*, 578.

[15] (a) Valentin, R.; Molvinger, K.; Viton, C.; Domard, A.; Quignard, F. From Hydrocolloids to High Specific Surface Area Porous Supports for Catalysis. *Biomacromol.* **2005**, *6*, 2785; (b) Verrier, C.; Oudeyer, S.; Dez, I.; Levacher, V. Metal or ammonium alginates as Lewis base catalysts for the 1,2-addition of silyl nucleophiles to carbonyl compounds. *Tetrahedron Lett.* **2012**, *53*, 1958; (c) Häring, M.; Tautz, M.; Alegre-Requena, J. V.; Saldías, C.; Díaz Díaz, D. Non-enzyme entrapping biohydrogels in catalysis. *Tetrahedron Lett.* **2018**, *59*, 3293; (d) Kühbeck, D.; Mayr, J.; Häring, M.; Hofmann, M.; Quignard, F.; Díaz Díaz, D. Evaluation of the nitroaldol reaction in the presence of metal ion-crosslinked alginates. *New J. Chem.* **2015**, *39*, 2306, and references therein.

[16] (a) Quignard, F.; Valentin, R.; Di Renzo, F. Aerogel materials from marine polysaccharides. *New J. Chem.* **2008**, *32*, 1300; (b) Pettignano, A. Duarte-Rodrigues, A.; Quignard, F.; Tanchoux, N. *Alginate and Carrageenan Based Aerogels: Processing and Morphology* in *Biobased Aerogels: Polysaccharide and Protein-based Materials* (Eds. Thomas, S.; Pothan, L. A.; Mavelil-Sam, R.), Green Chemistry Series No. 58, RSC **2018**, Ch. 5, pp. 54-66.

[17] Ross, A. B.; Hall, C.; Anastasakis, K.; Westwood, A.; Jones, J. M.; Crewe, R. J. Influence of cation on the pyrolysis and oxidation of alginates. *J. Anal. Appl. Pyrolysis* **2011**, *91*, 344.

[18] Itoh, J.; Fuchibe, K.; Akiyama, T. Chiral Phosphoric Acid Catalyzed Enantioselective Friedel–Crafts Alkylation of Indoles with Nitroalkenes: Cooperative Effect of 3 Å Molecular Sieves. *Angew. Chem. Int. Ed.* **2008**, *47*, 4016.

[19] Herrera, R. P.; Sgarzani, V.; Bernardi, L.; Ricci, A. Catalytic enantioselective Friedel-Crafts alkylation of indoles with nitroalkenes by using a simple thiourea organocatalyst. *Angew. Chem. Int. Ed.* **2005**, *44*, 6576.

[20] Jagdamba, S.; Snehlata, Y.; Madhulika, S.; Pratibha, R.; Bhartendu Pati, T.; Anu, M.; Jaya, S. Oxidative organophotoredox catalysis: a regioselective synthesis of 2-nitro substituted imidazopyridines and 3-substituted indoles, initiated by visible light. *New J. Chem.* **2016**, *40*, 9694.

[21] Wu, J.; Li, X.; Wu, F.; Wan, B. A New Type of Bis(sulfonamide)-Diamine Ligand for a $Cu(OTf)_2$-Catalyzed Asymmetric Friedel–Crafts Alkylation Reaction of Indoles with Nitroalkenes. *Org. Lett.* **2011**, *13*, 4834.

[22] Jiang, H.; Zhang, J.; Xie, J.; Liu, P.; Xue, M. Water-soluble (salicyladimine)$_2$Cu complex as an efficient and renewable catalyst for Michael addition of indoles to nitroolefins in water. *Synth. Commun.* **2017**, *47*, 211.

[23] Li, C.; Pan, Y.; Feng, Y.; He, Y.-M.; Liu, Y.; Fan, Q.-H. Asymmetric Ruthenium-Catalyzed Hydrogenation of Terpyridine-Type N-Heteroarenes: Direct Access to Chiral Tridentate Nitrogen Ligands. *Org. Lett.* **2020**, *22*, 6452.

[24] Li, W. Chiral Bis(Oxazolinyl)thiophenes for Enantioselective Cu(II)-Catalyzed Friedel–Crafts Alkylation of Indole Derivatives with Nitroalkenes. *Catal. Lett.* **2014**, *144*, 943.